UNIVERSITÀ DEGLI STUDI DI MILANO

Dottorato di Ricerca in Scienze della Terra
Ciclo XXVIII

# Time-dependent methods to evaluate the effects of urban sprawl on groundwater quality

Ph.D. Thesis

**Stefania Stevenazzi**
Matricola R10226

*Tutors*
**Prof. Marco Masetti**
**Dott. Alessandro Sorichetta**

**Academic Year**
**2014-2015**

*Coordinator*
**Prof.ssa Elisabetta Erba**

# Contents

# Chapter 1

# Introduction

## 1.1 Urban sprawl

Urban sprawl is perceived as a specific physical formation of urban growth characterized by an excessive increase in urban land uses, decreasing urban densities, and a spatially dispersed distribution of households and economic functions.

Urban sprawl seems to be a process with similar characteristics worldwide and similar economic and social root causes. However, the physical result may vary in different countries, with significant dissimilarities in terms of land-use patterns, densities and urban design (Siedentop and Fina, 2012). Classically, it is a US phenomenon associated with the rapid low-densities outward expansion of US cities, in the early part of the 20$^{th}$ century. In Europe, cities have traditionally been much more compact, developing a dense historical core. However, since the 1950s, urban sprawl has become a common phenomenon even in Europe, with no apparent slowing in these trends (EEA, 2006; Kasanko et al., 2006).

Urban sprawl generally follows periods of rapid urbanization associated with population growth and with the excessive migration of people from rural to urban areas. Drivers of urban sprawl have to be found in socio-economic causes (EEA, 2006; Pendall, 1999), such as:

a) global economic growth, which has impacts on the spatial distribution of population and employment;
b) improved transportation links and enhanced personal mobility, which makes possible to live farther away from the city center or the workplace;
c) low price of agricultural land, compared to already urbanized land or the city core;
d) preference of living in rural areas, including city suburbs, looking for a better quality of life, being closer to nature and farther from inner city cores, where a poor environment, social problems and safety issues are usually located;
e) land-use planning policies at both local and regional scales, which control the spatial pattern of urban growth.

Urban sprawl impacts the regional environment, the social structure, and the economy (Barnes et al., 2001; EEA, 2006). In particular, the main environmental impacts in Europe are (EEA, 2006): (a) the consumption of numerous natural resources (and energy); (b) the reduction of the capacity of soil to act as a filter for contamination sources; (c) the decrease of permeable superficial surfaces which influence the quantity of groundwater recharge; (d) the alteration of surface and groundwater interactions; (e) the increase in the emission of pollutants in the atmosphere (e.g., $CO_2$, $NO_2$); (f) the increasing incidences of river and coastal flooding.

The areas with the most visible impacts of urban sprawl are in countries or regions with high population density and economic activity (Belgium, the Netherlands, southern and western Germany, northern Italy, the Paris region) and/or rapid growth (Ireland, Portugal, eastern Germany, the Madrid region). Historical trends, since the mid-1950s, show that European cities have expanded on average by 78 % whereas the population has grown by only 33 % (EEA, 2006). In particular, over the past 20 years, the extent of build-up areas in many eastern and western countries has increased by 20 % while the population has increased by only 6 % (EEA, 2006). This kind of urban development is referred to as "sprawl without growth", where population growth is no more related to urban areas expansion or land-use change (Siedentop and Fina, 2012).
In a global perspective, over half of the world's population now lives in urban areas, up from 30 % in 1950. The coming decades will bring further profound changes to the size and spatial distribution of the global population such that the world's population in 2050 is projected to be 66 % urban (UN, 2015). In this scenario, Europe, with 73 % of its population living in urban areas in 2010, is expected to be over 80 % urban by 2050.
In Italy, the percentage of population residing in urban areas was 54 % in 1950, 67 % in 2000 and would be 78 % in 2050, with an increasing of around 2 % every 10 years between 2000 and 2050 (UN, 2015).

The Po Plain in northern Italy is one of the most populated regions in Europe with a "sprawl without growth" pattern: an initial phase of urban area expansion from the 1950s to the 1970s followed by an urban sprawl in the subsequent decades. This pattern qualifies the Po Plain as a representative "pilot area" to identify the interplay of urbanization and environmental, social and economic impacts after the rapid urban increase.

## 1.2 Urban groundwater

With over half the world's population now living in towns and cities, serious questions should be raised about the sustainability of urban water supplies. Groundwater is a particular concern as it represents over 95 % of the world's available fresh water reserves and supplies over 1.5 billion city dwellers (Foster et al., 2010).
Compared with surface waters (lakes, reservoirs and rivers) groundwater tends to be relatively well protected from pollutant sources and, only in extreme cases, is influenced to any great extent by drought and climate change. A particular benefit of aquifers is that groundwater supplies can be introduced in stages, just one borehole at a time, to meet increasing private, municipal, and industrial demand with minimal upfront expenditure. On the downside, an ''out of sight, out of mind'' mentality has led to an increasing neglect of urban groundwater in many parts of the world (Howard, 2015) and its vital function in the urban water cycle is frequently overlooked and undervalued.
The science of urban groundwater is comparatively young (mid-80s). Nevertheless, considerable scientific progress has been made on a number of key urban groundwater issues (e.g., Jin et al., 2004; Vázquez-Suñé et al., 2005; Nas and Berktay, 2010; or see Howard, 2015 for further reviews). Much of this work has involved issues relating to quantity (urban water balance and sources of recharge) and water quality (pollution sources and a wide range of contaminating chemicals).

Regarding water quantity, there is strong evidence that the loss of direct aquifer recharge in urban areas due to the vast expanse of impermeable surface is more than compensated by new sources of aquifer recharge (Howard, 2015): leaking sewer pipes, leaking water mains, septic tank discharge, over-irrigation of parks and gardens, infiltration of stormwater runoff.
Furthermore, Wiles and Sharp (2008) have demonstrated that the ‘‘impervious cover’’ (a term that describes buildings and pavements, including roads, driveways, parking lots, and sidewalks) is not impermeable. Even new pavements contain fractures and joints that are available as preferential pathways for infiltration of precipitation. Decreases in direct recharge from the low-permeability matrix of asphalt and concrete pavements can be offset by an increase in localized recharge through fractures and joints.
The effects of urbanization on groundwater levels depend also on well abstractions for drinking purposes or industrial activities. Consequences of groundwater level changes may be (Foster and Chilton, 2003): reversal of groundwater flow directions, phenomena of subsidence in cities located on some types of aquifer, numerous costly impacts on urban buildings and infrastructure after the cessation of the abstraction.
This fact involves another critical issue, which is related to groundwater quality. In fact, sewer pipe lines, water mains or septic tanks create preferential paths where pollutants can infiltrate and contaminate the aquifers. Fig. 1.1 shows the numerous urban sources of water pollution and the main contaminants.

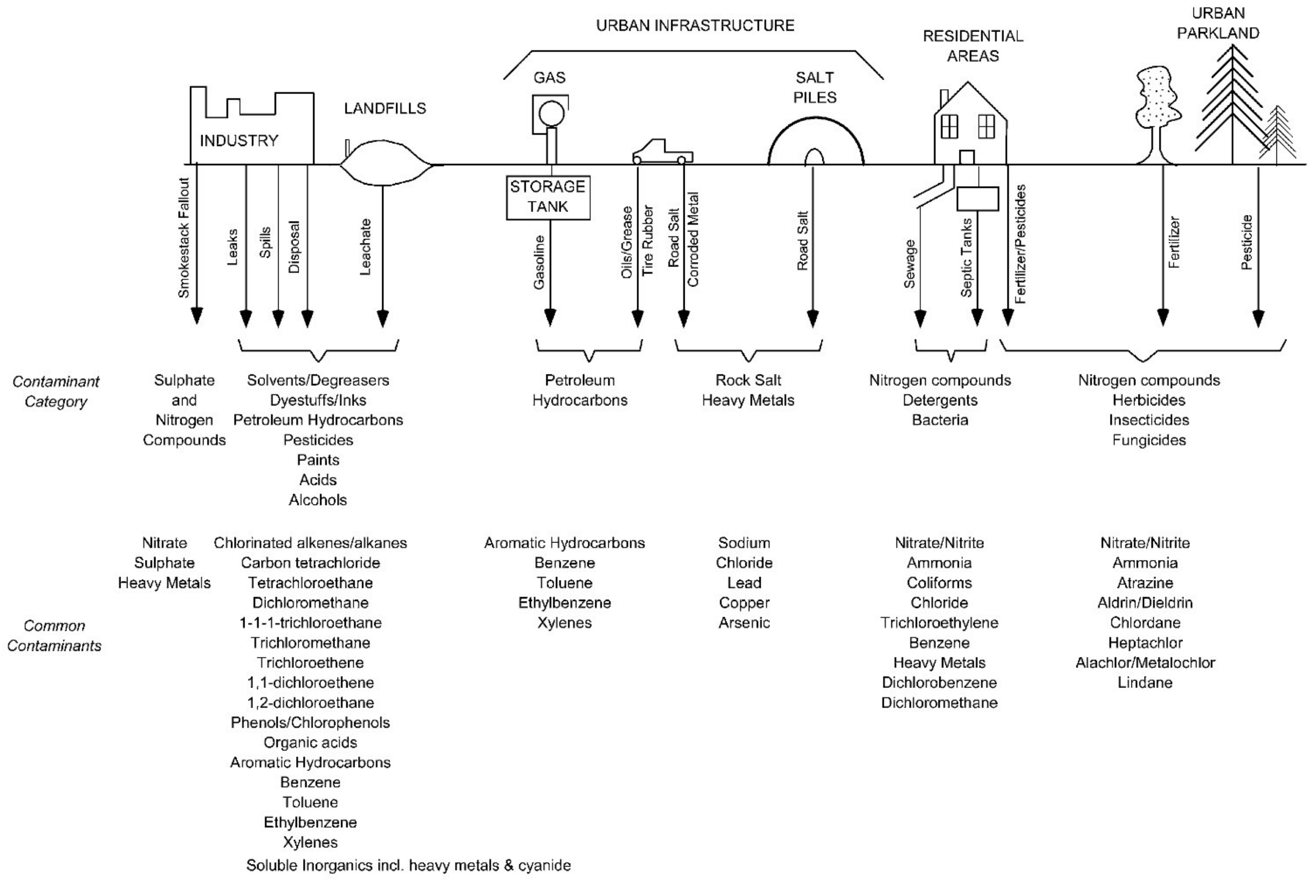


**Fig. 1.1 - Sources of groundwater contamination in urban areas (from Howard, 1997).**

Infiltration of urban runoff which mobilizes contaminants from the pavement and direct contamination from the sewage system is common in many cities (Eiswirth and Hötzl, 1997; Vázquez-Suñé et al., 2005). Contaminants typically include different compounds of nitrogen (Jin et al., 2004), detergents, medical compounds and their metabolites, pharmaceutical and endocrine disruptors (Gibson et al., 2010) or personal-care products, among others. Moreover, traditionally point-source phenomenon, like PCE and TCE, are increasingly destined to be considered as indicators of a widespread source of contamination, from multi-source diffuse type-urban pollution of groundwater (Balderacchi et al., 2014). Unfortunately, quantification of these processes and estimation of sewage losses at the city scale remain difficult.

Apart from the direct sources, there are also indirect ones. Mixing sewage water (high organic load) with chlorinated supply water may lead to further pollution by toxic chlorinated and recalcitrant compounds (Vázquez-Suñé et al., 2005). Moreover, changes in groundwater chemistry may also change the chemical conditions under which the pollutants were immobilized, thus mobilizing toxic compounds (typically, heavy metals).

On the other hand, significant improvements in water quality often occur as a consequence of organic matter oxidation. Much research has been done on understanding degradation processes (Eiswirth and Hötzl, 1997). However, no safe predictions can yet be made. This is especially severe because organic pollutant degradation is the limiting factor for groundwater exploitation in many cities.

Among the various contaminants, a particular focus is necessary on nitrate, which is one of the most abundant contaminant in groundwater. In fact, it is highly soluble in water, can easily leach through soil, and can persist in shallow groundwater for decades (Nolan, 1999). It has also potential human health and environmental impacts, such as causing an infant disease called methemoglobinemia (WHO, 2011), or expediting eutrophication and decreasing dissolved oxygen levels in surficial waters (Vitousek et al., 1997). Nitrate occurs naturally from mineral sources and animal wastes, and anthropogenically as a by-product of agriculture activities and urban wastes: fertilizers, feedlots, dairy and poultry farmings, sewage systems and septic tank drainages (Madison and Burnett, 1985; Howard, 1997; Jin et al., 2004; Wick et al., 2012).

Thus, deterioration of groundwater quality is due to urbanization and industrialization in and around cities, and intensification of production from agricultural lands (Foster and Chilton, 2003). The former is related to leakages of old sewer systems or septic tanks that increase the amount of contaminant loads (e.g., nitrate). The latter is related to the intense use of both organic and inorganic fertilizers, over the past 20-50 years. Natural attenuation of nitrate (mainly denitrification, through bacteria activity) is proved to be effective in groundwater (Korom, 1992). Nevertheless, in the vadose zone, the generally aerobic conditions imply that denitrification cannot be widely active, despite the presence of some potentially denitrifying bacteria, but it may be more significant in the zone of water-table fluctuation (Foster and Chilton, 2003).

Determining areas where groundwater is at risk of nitrate contamination and which factors mainly influence nitrate presence in groundwater represents an important step in managing and protecting this resource and human health. During the 1990s, aquifer pollution vulnerability assessment and mapping became increasingly utilized as a screening tool for protecting groundwater quality (Foster et al., 2013), and the approach has subsequently been adopted in various shapes and forms by most countries throughout the world (e.g., NRC, 1993; Vrba and Zaporozec, 1994; Nolan et al., 2002; Arthur et al., 2005).

However, in order to be considered effective tools to be used in environmental planning and management, groundwater vulnerability maps must be scientifically sound, meaningful and reliable (Focazio et al., 2002). To this regard, the use of statistical methods to assess groundwater vulnerability represents a reasonable compromise, among model complexity and costs, in order to produce scientifically defensible end-products (Focazio et al., 2002). Among the various statistical methods (ranging from descriptive statistics to regression and conditional probability analyses), the Weights of Evidence method (Bonham-Carter, 1994) has proven to be a reliable method to assess groundwater vulnerability to nitrate contamination (e.g., Masetti et al., 2008; Sorichetta, 2011). These recent studies have also shown that, in some areas of the Po Plain, nitrate occurrence in groundwater is strongly related to urban sources (using population density as a proxy) more than to agricultural activities.

## 1.3 Groundwater and legislation

As groundwater resources have become more vulnerable in recent years, it is necessary to urgently close the gap between the information required for land use planning to efficiently safeguard groundwater quality and techniques required to accurately assess groundwater vulnerability.

In fact, for the protection of groundwater quality in the European Union, the Water Framework Directive (WFD, 2000/60/EC) and the Groundwater Directive (GWD, 2006/118/EC) require member states to achieve good chemical status of their groundwater bodies by the year 2015 (art. 4, WFD). To achieve this, these directives ask member states to delineate groundwater bodies and assess their current chemical status. To detect possible threats of future groundwater quality, the GWD requires the identification of areas where groundwater suffers increasing trends in contaminant concentration, highlighting the need to carefully manage such areas even if the concentration is below the regulatory limit (Fig. 1.2). If upward trends are found, these should be reversed when the concentration of the pollutant reaches 75 % of the threshold value. The GWD also lays down requirements on the implementation of measures necessary to reverse any significant and sustained upward trend. In the context of the WFD and GWD, it is necessary to (1) assess the current groundwater quality status, (2) detect changes or trends, (3) assess the threat of deterioration and (4) predict future changes in groundwater quality by extrapolating present day trends and possibly predict trend reversal in response to legislation.

The WFD requires the realization of groundwater quality monitoring networks, which had already been installed in several European countries, such as Denmark, the Netherlands, the UK, and Italy. These networks have since produced time series of monitoring data, which have been used to detect and quantify changes in groundwater quality (e.g., Worral et al., 2002; Cinnirella et al., 2005; Capri et al., 2009) and to extrapolate trends in groundwater contamination (e.g., Stuart et al., 2007; Visser et al., 2009).

Annex I of the GWD contains Europe-wide environmental quality standards for two types of pollutants: nitrates and pesticides. The Annex I set these standards according to the regulations being in force at that time; in particular the nitrate standard was established based on epidemiological studies (WHO, 2011) and the pesticides standard took into account the detection limit of the analytical equipment available at the beginning of the ‘90s.

The guideline value for nitrate, for potable purposes, is 50 mg/L (WHO, 2011).

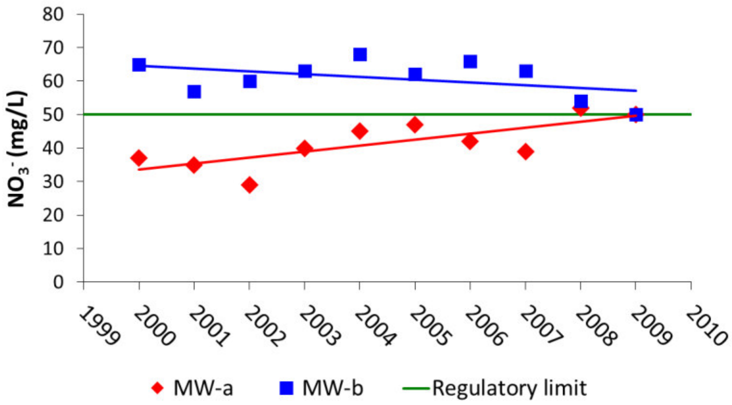


**Fig. 1.2 - Example of nitrate concentration monitoring. MW-a (*red diamonds*) shows concentrations below the regulatory limit (*solid green line*), but an increasing concentration trend. MW-b (*blue squares*) shows concentrations higher than the regulatory limit, but a decreasing concentration trend.**

## 1.4 Remote sensing, urban areas and groundwater

Satellite remote sensing are an effective solution for mapping settlements and monitoring urbanization at a range of spatial and temporal scales. Various techniques and algorithms have been developed in order to extract information starting from remotely sensed multiple data sets, such as SAR and optical images (Gamba, 2005): multi-sensor imagery/information/data fusion techniques suited for urban areas; multi-resolution/scale-space techniques for characterizing urban areas; multi-temporal issues for urban area monitoring.

As examples, these techniques have been applied to recognize spatial extent and patterns of urban sprawl (Barnes et al., 2001), identify impervious surface areas (Elvidge et al., 2007), or extract built-up areas (De Vecchi et al., 2015; Shimoni et al., 2015). Moreover, satellite remote sensing have been widely used for identifying the relationship between land use development and population growth (Kasanko et al., 2008) and forecasting the population distribution in urban and rural areas (Linard et al., 2013).

In groundwater issues, satellite data have been typically used to qualitatively assess the availability of groundwater resources, such as mapping of groundwater potential, or indirect estimation of groundwater potential and recharge (e.g., Tweed et al., 2007; Jasmin and Mallikarjuna, 2011; Frappart et al., 2011; Wang et al., 2014). Only a limited number of studies used satellite data to quantitatively assess groundwater quality (Werz and Hötzl, 2007). Instead, remote sensing data have been used in various studies for the impact assessment of urbanization on groundwater quantity and quality (e.g., Barber et al., 1996; Jat et al., 2009; Martin Del Campo et al., 2014). However, most of these studies uses aerial images or optical satellite images (e.g., LANDSAT Missions) and their derived products (i.e, land use / land cover datasets, such as the CORINE Land Cover inventory in Europe) to identify and delineate urban areas and their changes.

The present study explores the use of an innovative dataset to delineate urban areas with satellite scatterometer data, which allows identifying manmade infrastructures or buildings and zones where different rates of urban growth occurred. Radar backscatter data acquired by the SeaWinds scatterometer aboard the QuikSCAT satellite together with the Dense Sampling Method (QSCAT-DSM; Nghiem et al., 2009) have been used to identify and map urban extent and surface features at a posting scale of about 1 $km^2$.

The main advantages of QSCAT-DSM are (Nghiem et al., 2009): (a) worldwide coverage continuously in the decade of the 2000’s, (b) delineation of urban and suburban contours both in metropolitan and rural areas, (c) identification of urban development both fast and expansive or slow and restrained.

These aspects ensure that QSCAT-DSM data can be potentially applied in natural hazard issues related to the development of urban areas, which require a continuous data collection or a complete coverage of the study area.

## 1.5 Purpose of this study

Urban transformations and the intensification of agriculture since the 1950s have resulted in a deterioration of groundwater quality in many European countries, such as Italy. As suggested by the European Directives, for the protection of groundwater quality, it is necessary to (1) assess the current groundwater quality status, (2) detect changes or trends in groundwater quality, (3) assess the threat of deterioration and (4) predict future changes in groundwater quality.

Following this path, the study allowed to:

- develop a time-dependent method to assess groundwater vulnerability, which could take into account both the current groundwater quality status and its changes, through the spatial statistical technique Weights of Evidence;
- evaluate different variables that express urban changes in the decade of 2000s, such as population density, land use / land cover from aerial images and satellite remote sensing data;
- demonstrate the reliability of satellite remote sensing (QuikSCAT-DSM) data for evaluating urban changes without a temporal or spatial gap, and its usefulness in the assessment of groundwater vulnerability;
- develop a predictive spatio-temporal model, to evaluate the impacts of urban growth, until 2020, on groundwater resources, as urbanization accelerates across the world.

## References

Arthur J.D., Baker A.E., Cichon J.R., Wood A.R., Rudin A., 2005. Florida Aquifer Vulnerability Assessment (FAVA): Contamination potential of Florida's principal aquifer systems. Division of Resource Assessment and Management, Florida Geological Survey

Balderacchi M., Filippini M., Gemitzi A., Klöve B., Petitta M., Trevisan M., Wachniew P., Witczak S., Gargini A., 2014. Does groundwater protection in Europe require new EU-wide environmental quality standards? Frontiers in Chemistry, vol. 2, n. 32

Barber C., Otto C.J., Bates L.E., 1996. Evaluation of the relationship between land-use change and groundwater quality in a water supply catchment using GIS technology: the Gwelup wellfield Western Australia. Hydrogeology Journal, vol. 4, n. 1, pp. 6-19

Barnes K.B., Morgan J.M. III, Roberge M.C., Lowe S., 2001. Sprawl development: its patterns, consequences, and measurement. Towson University, Towson

Bonham-Carter G.F., 1994. Geographic Information Systems for Geoscientists-Modelling with GIS. Pergamon Press

Capri E., Civita M., Corniello A., Cusimano G., De Maio M., Ducci D., Fait G., Fiorucci A., Hauser S., Pisciotta A., Pranzini G., Trevisan M., Delgado Huertas A., Ferrari F., Frullini R., Nisi B., Offi M., Vaselli O., Vassallo M., 2009. Assessment of nitrate contamination risk: The Italian experience. Journal of Geochemical Exploration, vol. 102, n. 2, pp. 71-86, doi: 10.1016/j.gexplo.2009.02.006

Cinnirella S., Buttafuoco G., Pirrone N., 2005. Stochastic analysis to assess the spatial distribution of groundwater nitrate concentrations in the Po catchment (Italy). Environmental Pollution, vol. 133, n. 3, pp. 569-580, doi: 10.1016/j.envpol.2004.06.020

De Vecchi D., Harb M., Dell’Acqua F., 2015. A PCS-based hybrid approach for built-up area extraction from LANDSAT 5, 7 and 8 datasets, in: IEEE Geoscience and Remote Sensing Symposium, Milan, Italy, pp. 1152-1154. ISBN: 978-1-4799-7928-8

EEA – European Environment Agency, 2006. Urban sprawl in Europe: The ignored challenge (EEA Report No. 10/2006). Office for Official Publications of the European Communities, Luxembourg, 56 pp., ISSN: 1725-9177

Eiswirth M., Hötzl H., 1997. The impact of leaking sewers on urban groundwater. In: Chilton et al. (ed.) Groundwater in the urban area: problems processes and management. 27th Cong. Int. Assoc. Hydrogeologists (IAH), 21–27 September 1997, Nottingham, pp. 399–404

Elvidge C.D., Tuttle B.T., Sutton P.C., Baugh K.E., Howard A.T., Milesi C., Bhaduri B., Nemani R., 2007. Global Distribution and Density of Constructed Impervious Surfaces. Sensors, vol. 7, pp. 1962-1979

European Community, 2000. Directive 2000/60/EC of the European Parliament and of the Council of 23 October 2000 establishing a framework for Community action in the field of water policy, (Water Framework Directive). OJ L 327, 22 December 2000, pp. 1-73

European Community, 2006. Directive 2006/118/EC on the protection of groundwater against pollution and deterioration, (Groundwater Directive). OJ L 372, 27 December 2006, pp. 19-31

Focazio M.J., Reilly T.E., Rupert M.G., Helsel D.R., 2002. Assessing Ground-Water Vulnerability to Contamination: Providing Scientifically Defensible Information for Decision Makers. U.S. Geological Survey Circular 1224. ISBN: 0-607-89025-8

Foster S.S.D., Chilton P.J., 2003. Groundwater: the processes and global significance of aquifer degradation. Philosophical Transactions of the Royal Society B, vol. 358, n. 1440, pp. 1957-1972

Foster S., Hirata R., Garduno H., Tovey C., 2010. Urban groundwater use policy—balancing benefits and risks, GW-MATE strategic overview series No. 3. World Bank, Washington, D.C. http://www.worldbank.org/gwmate

Foster S., Hirata R., Andreo B., 2013. The aquifer pollution vulnerability concept: aid or impediment in promoting groundwater protection? Hydrogeology Journal, vol. 21, pp. 1389-1392

Frappart F., Papa F., Güntner A., Werth S., Santos da Silva J., Tomasella J., Seyler F., Prigent C., Rossow W.B., Calmant S., Bonnet M.-P., 2011. Satellite-based estimates of groundwater storage variations in large drainage basins with extensive floodplains. Remote Sensing of Environment, vol. 115, n. 6, pp. 1588-1594, doi 10.1016/j.rse.2011.02.003

Gamba P., Dell'Acqua F., Dasarathy B.V., 2005. Urban remote sensing using multiple data sets: Past, present, and future. Information Fusion, vol. 6, pp. 319-326, doi 10.1016/j.inffus.2005.02.007

Gibson R., Durán-Álvarez J.C., León Estrada K., Chávez A., Jiménez Cisneros B., 2010. Accumulation and leaching potential of some pharmaceuticals and potential endocrine disruptors in soils irrigated with wastewater in the Tula Valley, Mexico. Chemosphere, vol. 81, n. 11, pp. 1437-1445

Howard K.W.F., 1997. Impacts of urban development on groundwater. In: Eyles N. (ed.), Environmental geology of urban areas. Geotext, vol. 3, pp. 93-104. Special publication of the Geological Association of Canada

Howard K.W.F., 2015. Sustainable cities and the groundwater governance challenge. Environmental Earth Sciences, vol. 73, n. 6, pp. 2543-2554, doi 10.1007/s12665-014-3370-y

Jasmin I., Mallikarjuna P., 2011. Review: Satellite-based remote sensing and geographic information systems and their application in the assessment of groundwater potential, with particular reference to India. Hydrogeology Journal, vol. 19, n. 4, pp. 729-740, doi 10.1007/s10040-011-0712-7

Jat M.K., Khare D., Garg P.K., 2009. Urbanization and its impact on groundwater: a remote sensing and GIS-based assessment approach. Environmentalist, vol. 29, n. 1, pp. 17-32, doi: 10.1007/s10669-008-9176-2

Jin Z., Chen Y., Wang F., Ogura N., 2004. Detection of nitrate sources in urban groundwater by isotopic and chemical indicators, Hangzhou City, China. Environmental Geology, vol. 45, n. 7, pp. 1017-1024

Korom S.F., 1992. Natural denitrification in the saturated zone: a review. Water Resources Research, vol. 28, pp. 1657-1668

Kasanko M., Barredo J.I., Lavalle C., McCormick N., Demicheli L., Sagris V., Brezger A., 2006. Are European cities becoming dispersed? A comparative analysis of 15 European urban areas. Landscape and Urban Planning, vol. 77, n. 1-2, pp. 111-130, doi 10.1016/j.landurbplan.2005.02.003

Linard C., Tatem A.J., Gilbert M., 2013. Modelling spatial patterns of urban growth in Africa. Applied Geography, vol. 44: 23-32, ISSN: 0143-6228, doi 10.1016/j.apgeog.2013.07.009

Madison R.J., Burnett J.O., 1985. Overview of the occurrence of nitrate in groundwater of the United States. U.S. Geological Survey Water Supply Paper, vol. 2275, pp. 93-105

Masetti M., Poli S., Sterlacchini S., Beretta G.P., Facchi A., 2008. Spatial and statistical assessment of factors influencing nitrate contamination in groundwater. Journal of Environmental Management, vol. 86, n. 1, pp. 272-281, doi 10.1016/j.jenvman.2006.12.023

Martín Del Campo M.A., Esteller M.V., Expósito J.L., Hirata R., 2014. Impacts of urbanization on groundwater hydrodynamics and hydrochemistry of the Toluca Valley aquifer (Mexico). Environmental Monitoring and Assessment, vol. 186, n. 5, pp. 2979-2999, doi 10.1007/s10661-013-3595-3

Nas B., Berktay A., 2010. Groundwater quality mapping in urban groundwater using GIS. Environmental Monitoring and Assessment, vol. 160, n. 1, pp. 215-227, doi 10.1007/s10661-008-0689-4

Nghiem S.V., Balk D., Rodriguez E., Neumann G., Sorichetta A., Small C., Elvidge C.D., 2009. Observations of urban and suburban environments with global satellite scatterometer data. ISPRS – Journal of Photogrammetry and Remote Sensing, vol. 64, n. 4, pp. 367-380, doi 10.1016/j.isprsjprs.2009.01.004

Nolan B.T., 1999. Nitrate behavior in groundwater of southeastern USA. Journal of Environmental Quality, vol. 28, n. 5, pp. 1518-1527

Nolan B.T., Hitt K.J., Ruddy B.C., 2002. Probability of nitrate contamination of recently recharged groundwaters in the conterminous United States. Environmental Science and Technology, vol. 36, n. 10, pp. 2138-2145, doi 10.1021/es0113854

NRC - National Research Council, 1993. Ground water vulnerability assessment: Predictive relative contamination potential under conditions of uncertainty. National Academy Press, Washington DC, ISBN: 978-0-309-04799-9

Pendall R., 1999. Do land-use controls cause sprawl? Environment and Planning B: Planning and Design, vol. 26, n. 4, pp. 555-571

Shimoni M., Lopez J., Forget Y., Wolff E., Michellier C., Grippa T., Linard C., Gilbert M., 2015. An urban expansion model for Africa cities using fused multi temporal optical and SAR data, in: IEEE Geoscience and Remote Sensing Symposium, Milan, Italy, pp. 1159-1162. ISBN: 978-1-4799-7928-8

Siedentop S., Fina S., 2012. Who sprawls most? Exploring the patterns of urban growth across 26 European countries. Environment and Planning A, vol. 44, n. 11, pp. 2765-2784

Sorichetta A., 2011. Groundwater vulnerability assessment using statistical methods. Università degli Studi di Milano, Academic year 2010, 141 pp. http://hdl.handle.net/2434/152913

Stuart M.E., Chilton P.J., Kinniburgh D.G., Cooper D.M., 2007. Screening for long-term trends in groundwater nitrate monitoring data. Quarterly Journal of Engineering Geology and Hydrogeology, vol. 40, n. 4, pp. 361-376, doi 10.1144/1470-9236/07-040

United Nations, Department of Economic and Social Affairs, Population Division, 2015. World Urbanization Prospects: The 2014 Revision, ST/ESA/SER.A/366

Tweed S., Leblanc M., Webb J.A., Lubczynski M.W., 2007. Remote sensing and GIS for mapping groundwater recharge and discharge areas in salinity prone catchments, southeastern Australia. Hydrogeology Journal, vol. 15, n. 1, pp. 75-96, doi 10.1007/s10040-006-0129-x

Vázquez-Suñé E., Sánchez-Vila X., Carrera J., 2005. Introductory review of specific factors influencing urban groundwater, an emerging branch of hydrogeology, with reference to Barcelona, Spain. Hydrogeology Journal, vol. 13, n. 3, pp. 522-533

Visser A., Dubus I., Broers H.P., Brouyère S., Korcz M., Orban P., Goderniaux P., Batlle-Aguilar J., Surdyk N., Amraoui N., Job H., Pinault J.L., Bierkens M., 2009. Comparison of methods for the detection and extrapolation of trends in groundwater quality. Journal of Environmental Monitoring, vol. 11, pp. 2030-2043, doi 10.1039/b905926a

Vitousek P.M., Aber J.D., Howarth R.W., Likens G.E., Matson P.A., Schindler D.W., Schlesinger W.H., Tilman D.G., 1997. Human alteration of the global nitrogen cycle: Sources and consequences. Ecological Applications, vol. 7, n. 3, pp. 737-750

Vrba J., Zaporozec A., 1994. Guidebook on mapping groundwater vulnerability. International Association of Hydrogeologists, International Contributions to Hydrogeology, Publication No. 16. Verlag Heinz Heise, Hannover

Wang H., Guan H., Gutiérrez-Jurado H.A., Simmons C.T., 2014. Examination of water budget using satellite products over Australia. Journal of Hydrology, vol. 511, pp. 546-554, doi 10.1016/j.jhydrol.2014.01.076

Werz H., Hötzl H., 2007. Groundwater risk intensity mapping in semi-arid regions using optical remote sensing data as an additional tool. Hydrogeology Journal, vol. 15, n. 6, pp. 1031-1049, doi 10.1007/s10040-007-0202-0

WHO - World Health Organization, 2011. Nitrate and nitrite in drinking-water. Background document for preparation of WHO Guidelines for drinking-water quality. Geneva, World Health Organization (WHO/HSE/AMR/07.01/16/Rev/1)

Wick K., Heumesser C., Schmid E., 2012. Groundwater nitrate contamination: Factors and indicators. Journal of Environmental Management, vol. 111, pp. 178-186, doi 10.1016/j.jenvman.2012.06.030

Wiles T.J., Sharp J.M. Jr, 2008. The secondary permeability of impervious cover. Environmental and Engineering Geoscience, vol. 14, n. 4, pp. 251-265, doi: 10.2113/gseegeosci.14.4.251

Worrall F., Besien T., Kolpin D.W., 2002. Groundwater vulnerability: interactions of chemical and site properties. Science of the Total Environment, vol. 299, n. 1-3, pp. 131-143, doi 10.1016/S0048-9697(02)00270-X

# Chapter 2

# Study area

## 2.1 Geographical setting

The Po Plain is the largest plain in Italy and, because of its position and climate conditions, it is also the most intensively cultivated and industrialized area in the country. Stretching over an area of 47,000 km², it covers 15 % of the Italian territory. The Po Plain is constrained between the Alps to the north and west, and the Apennines to the south. The Po River flows through the middle of the plain from west to east, flowing into the Adriatic Sea.

The study area is located within the Po Plain area of Lombardy Region, and covers an area of 13,400 km², where urban, industrial, livestock and agricultural activities are extensively and heterogeneously present.
This region is surrounded by important rivers influencing groundwater flow in the unconfined aquifer: Po River along the south; Ticino and Sesia rivers and another small sector of the Po River along the west; and Mincio River along the east (Fig. 2.1). It is also constrained by mountain chains forming the boundary of the plain: Lombardy Prealps along the north and Appennines along the southwest.

## 2.2 Hydrogeological setting

This area has a complex hydrogeological setting consisting of multiple aquifers with various properties and interactions. The Lombardy plain subsoil is characterized by Plio-Pleistocene sediments whose upper unit forms the shallow unconfined aquifers (Fig. 2.2). Sediments are mainly gravels and sands, although the presence of finer sediments increases from the north to the south where shallow aquifers are mainly constituted by fine sands and are partially confined. These aquifers have high transmissivity, ranging from $10^{-2}$ to $10^{-4}$ m²/s and medium-high hydraulic conductivity, ranging from $10^{-4}$ to $10^{-6}$ m/s, while its thickness ranges from 40 to 80 m (Regione Lombardia and ENI, 2002).
According to the classification based on the study conducted by the Regione Lombardia and ENI (2002), four major hydrogeological units, each one delimitated at the bottom by a regional unconformity stratigraphic surface, can be identified in the study area. Such four hydrogeological units are denominated Group A, Group B, Group C, and Group D from the shallower to the deeper one. Other classifications derived from previous studies are shown in Fig. 2.3 (e.g., Martinis and Mazzarella, 1971; Francani and Pozzi, 1981; Avanzini et al., 1995).
In the subsoil, the boundary between fresh and brackish water identifies the bottom of the aquifers useful for drinkable and agricultural/industrial purposes.

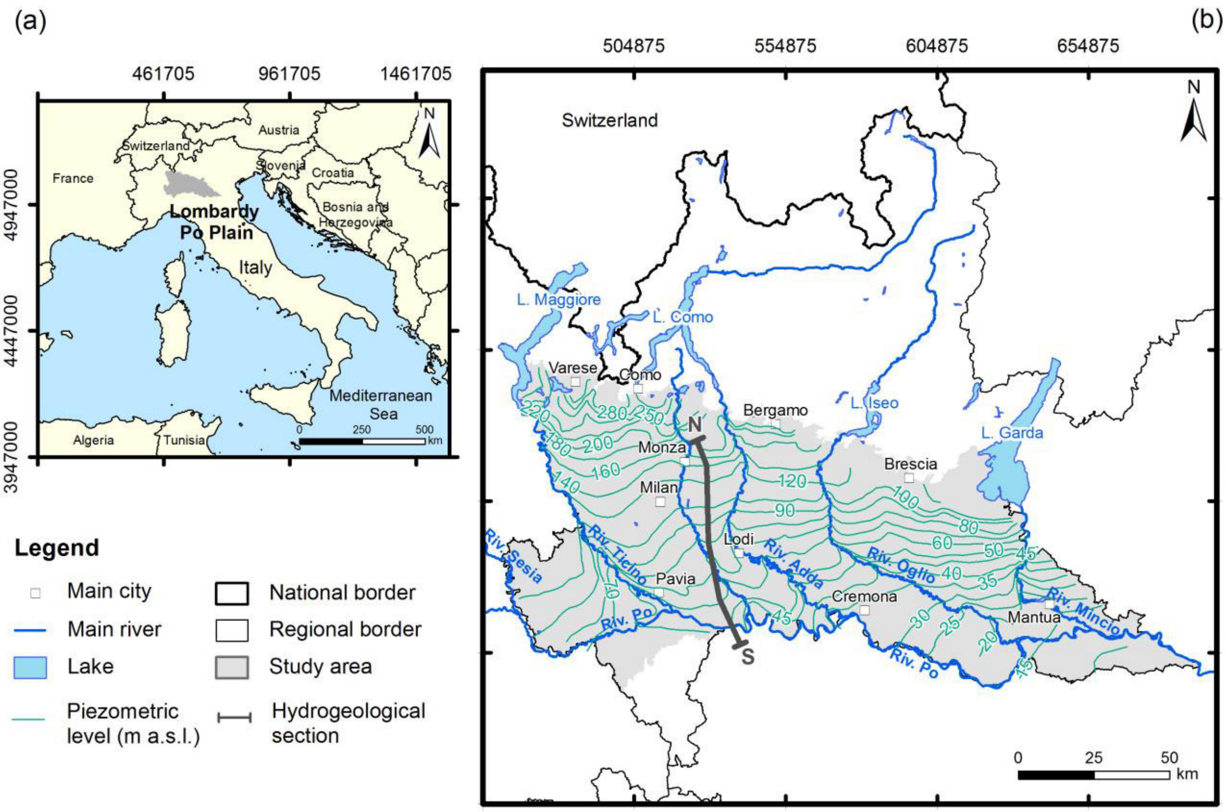


**Fig. 2.1 - (a) Location of the study area. (b) Study area within the Lombardy Region, main rivers and lakes and piezometric levels of the shallow aquifer. *Dark grey line* shows the location of the hydrogeological scheme in Fig. 2.2. Coordinates refer to WGS 1984 – UTM Zone 32N projection.**

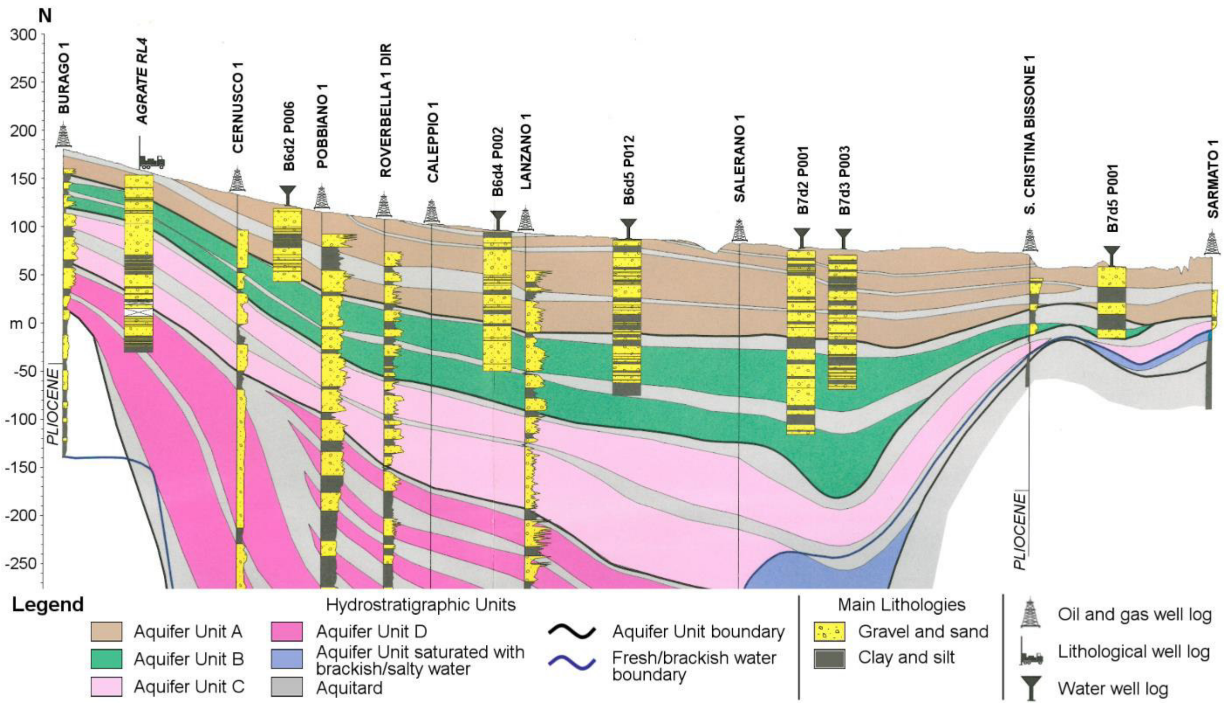


**Fig. 2.2 - Hydrogeological scheme along the N-S section marked by the dark grey line on the map in Fig. 2.1b (modified from Regione Lombardia and ENI, 2002).**

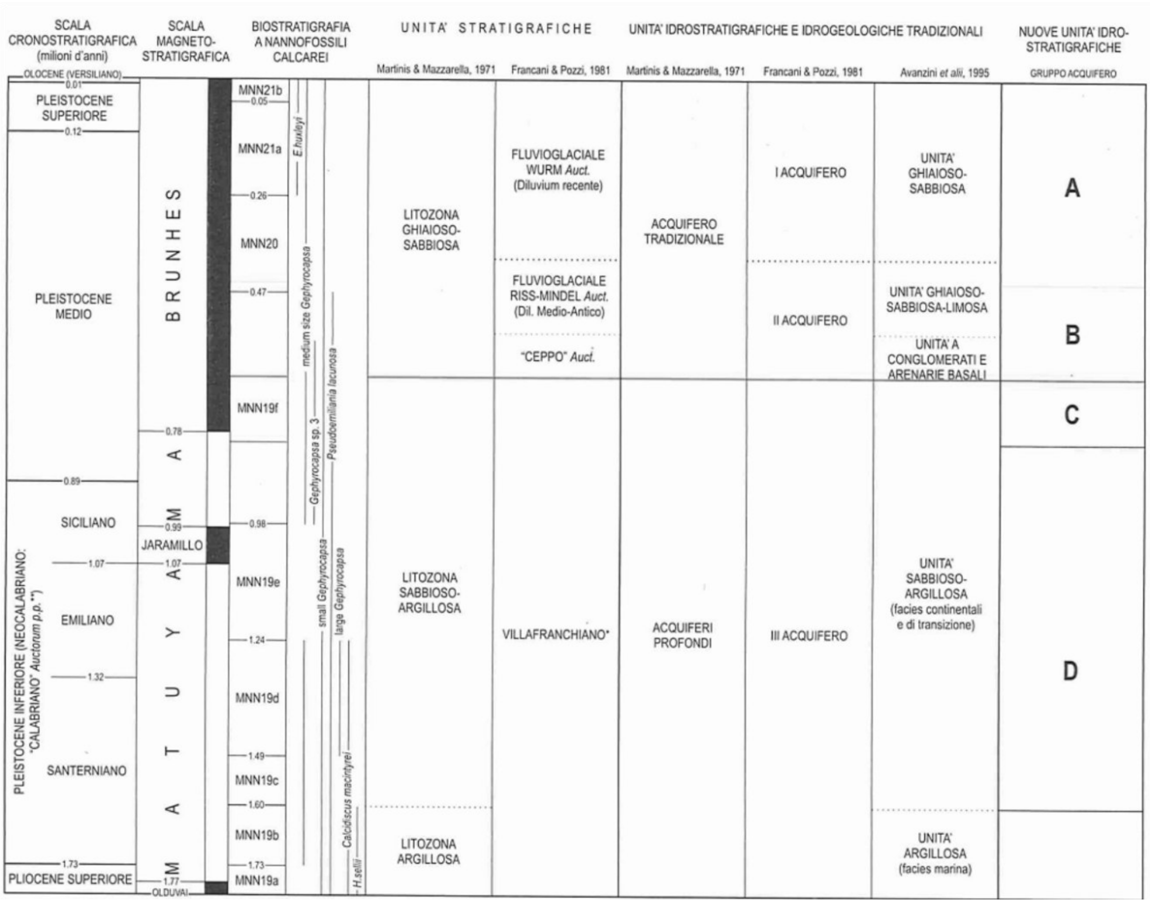


**Fig. 2.3 - Stratigraphic relationships among the hydrogeological units identified in different studies (from Regione Lombardia and ENI, 2002).**

- **Group A**

The Group A (Middle-to-Late Pleistocene) identifies aquifers mainly constituted by medium-to-very-thick layers of polygenic coarse gravel and pebbles, from gray to yellowish-grey, in a medium-to-coarse sandy matrix. Few yellow layers constituted by medium-to-very-coarse – often pebbly – sand are interbedded. The sedimentary environment of Group A is a high-energy alluvial plain (braided system), with an origin of the sediments located in the north area (Alps). The Group A has a thickness of 20 to 40 meters (uncommonly can reach 70 m) and is characterized by high values of hydraulic conductivity (ranging from $10^{-4}$ to $10^{-3}$ m/s) and transmissivity (usually higher than $10^{-2}$ m²/s).

- **Group B**

The Group B (Middle Pleistocene) is constituted by continental sediments of high-energy fluvial environments (braided systems), with origins generally from north to south, from the Alpine belt. The Group B identifies aquifers mainly constituted by gravel and medium-coarse sand in a sandy matrix. Limited to the lower part of the aquifer, very few silty-clay and silty layers, of thickness ranging from few decimeters to few meters, are interbedded. The Group B has almost the same average thickness (40-50 meters) of the Group A but, due to the higher presence of clay and silt, it is characterized by lower values of hydraulic conductivity (ranging from $10^{-5}$ to $10^{-4}$ m/s) and transmissivity (ranging from $10^{-3}$ to $10^{-2}$ m²/s).

- **Group C**

The Group C (Early-Middle Pleistocene) is constituted by sediments from marine and transitional environments. Sediments of the continental shelf are constituted by sandy-silty clay and fossiliferous grey clay; sediments of the coastal environment are constituted by fossiliferous, laminate or massive, bioturbated, fine-to-very-fine grey sand, and by medium-to-thick strata of laminate, medium well-sorted grey sand containing organic matter. The Group C is characterized by a variable thickness increasing southward (ranging from 100 meters in the northern part to 1000-1200 meters in the southern one) and low values of both hydraulic conductivity (ranging from $10^{-6}$ to $10^{-5}$ m/s) and transmissivity (usually lower than $10^{-3}$ $m^2/s$).

- **Group D**

The Group D (Early Pleistocene) is represented by facies coarsening upward and is constituted by silty-clay and silt interbedded by thin layers of fine and very fine sand at the base, medium and fine bioturbated grey sand in the middle part, and polygenic grey gravel alternating with sand at the top. Sediments reveal marine and transitional environments for the deposition of the Group D.

Below the Group D, there are Middle and Late Pliocene sediments, which top is located at about 700 meters below the sea level, essentially constituted by clay.

The shallow aquifer is represented by the Group A all over the plain. In the northern sector of the plain, coincident with the hilly zone, characterized by fluvial terraces, the hydrogeological setting results more complex and the complete succession of the four Groups could not be present everywhere. For example, Group A may be absent in correspondence of ancient terraces, while being present in the valley of the main rivers. Furthermore, in the subsoil, in the northern sector of the plain, the separation between Group A and Group B is not always evident, thus the two groups are connected in this area, until the definition of an aquitard level between the two Groups, which thickness increases toward south (approximately around the latitude of the city of Milan).
The Group A or the corresponding shallow unconfined aquifer in the northern sector of the study area (Groups A and B) is the portion of aquifer that was used in this study to assess the groundwater vulnerability to nitrate contamination.
The groundwater flow is generally oriented north-south toward the base level defined by the Po River, with a deviation to east-south-east in the south-east area of Lombardy. The groundwater depth decreases from north to south, ranging from values higher than 70 m to less than 2 m. There are also some groundwater-fed streams, where the local groundwater depth reduces to zero.

## 2.3 Nitrate contamination in the Lombardy plain area

Nitrate ($NO_3^-$) is the most common non-point-source contaminant found in groundwater in the Po Plain, since the European Union (Nitrate Directive, 91/676/EEC) has classified this area as a Nitrate Vulnerable Zone. Nitrate concentrations have been monitored by a network of about 500 wells covering the entire area with a nearly uniform spatial distribution, where data have been collected every six months from 2001 to 2012 (Regional Environmental Agency – ARPA, unpublished data, 2012). From the network, only the 249 wells monitoring the shallow aquifer, in the period 2010 – 2012, have been used in the non-time-dependent analysis, while the 221 wells monitoring the shallow aquifer and having a minimum of eight measurements, in the period 2001 – 2011, were selected for being used in the time-dependent analyses (Grath et al., 2001).

For the protection of groundwater quality in the European Union (EU), the Water Frame Directive (WFD, 2000/60/EC) and the Groundwater Directive (GWD, 2006/118/EC) require member states to achieve good chemical status of their groundwater bodies within 2015 and to identify significant and sustained trends in the concentration of pollutants.

In order to cope with the EU requirements, this study focuses on the status of nitrate in 2010 – 2012 and its evolution during the decade of 2000s. As demonstrated by various studies, nitrate contamination in the study area is related to agricultural and livestock activities (Masetti et al., 2008), as well as to urban areas (Sorichetta, 2011; Crosta et al., 2015).

This study will deepen the relation between the evolution of nitrate contamination in groundwater and land use changes, starting from the situation in the decade of 2000s and hypothesizing future scenarios for the 2010s.

### 2.3.1 Status at 2011 and evolution in the 2000s

The change in nitrate concentration is quantified by the slope of the regression line from an interpolation of concentration data. The slope defines the rate of nitrate concentration change in mg/L per day. Positive slope values show increasing concentration trends representing water quality deterioration, while non-positive slope values indicate steady or decreasing concentration trend characterizing unaffected or improved groundwater quality.

Until the end of the considered monitoring period in 2011, about 28 % of wells show increasing concentration trends and concentrations exceeding the guideline value of 25 mg/L defined by the EU standard (91/676/EEC), while 35 % of wells show decreasing concentration trends and concentrations lower than the same guideline value. Only 3 % of wells show increasing concentration trends and concentrations exceeding the established threshold of 50 mg/L (91/676/EEC; 2006/118/EC) (Table 2.1, Fig. 2.4).

**Table 2.1 - Nitrate concentration trends related to the last measured concentration in 2011 (percentage of wells).**

| | Concentration ≥ 25 mg/L | Concentration < 25 mg/L | Concentration ≥ 50 mg/L | Concentration < 50 mg/L | ∑ |
|---|---|---|---|---|---|
| Increasing trend | 28 % | 19 % | 3 % | 44 % | 47 % |
| Decreasing trend | 18 % | 35 % | 6 % | 47 % | 53 % |
| ∑ | 46 % | 54 % | 9 % | 91 % | |

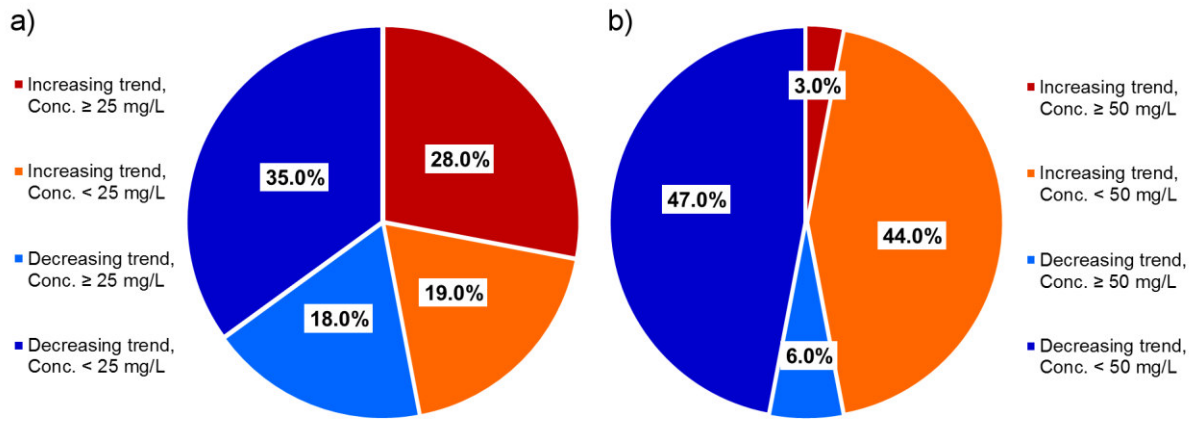


**Fig. 2.4 - Percentage of wells showing increasing or decreasing trends, with concentration lower or higher than 25 mg/L (a) and 50 mg/L (b) in 2011.**

### 2.3.2 Future perspectives

To evaluate predictive scenarios, various hypotheses on the evolution of nitrate concentration can be taken into account. The first one considers that the evolution of nitrate contamination in the decade 2011 – 2020 is equal to its evolution related to the decade of 2000s.

Under this hypothesis, two milestones have been considered: 2015 and 2020. The former is the deadline established by the EU directives (Art. 4, WFD), when groundwater bodies should achieve a good quality of their status of contamination. The latter is the deadline established by the EU strategy, Europe 2020 (http://ec.europa.eu/europe2020/). Its aim is creating the conditions for smart, sustainable and inclusive growth, within 2020, in five main areas: employment; research and development; climate/energy; education; social inclusion and poverty reduction.

It was necessary to calculate the nitrate concentration in 2015, instead of using the real measurements, because data on groundwater quality were not still available at the moment of the study. In fact, the Regional Environment Agency conducts the monitoring in spring and fall, while the analyses can be available after three months, submitting a request to the Agency. This timing was not compatible with the timing of the study.

Results show an improvement of groundwater quality, respect to the end of 2011. A slight decreasing of the number of wells showing a concentration higher than 25 mg/L or 50 mg/L has been observed in 2015 (Table 2.2): –1.6 % and –0.4 %, respectively. Nevertheless, this positive evolution would not remain the same ten years later, in 2020 (Table 2.3). In fact, the number of wells still showing a concentration higher than 25 mg/L is less respect to 2011 and 2015: –2.6 % and –1.0 %, respectively. But, there is an increasing in the number of wells showing a concentration higher than 50 mg/L: +2.3 % and +2.7 %, respect to 2011 and 2015.

This tendency seems caused by the fact that more wells showing an increasing concentration trend will exceed the regulatory thresholds (25 or 50 mg/L), respect to those wells showing a decreasing concentration trend and reaching the good quality status (Fig. 2.5).

**Table 2.2 - Nitrate concentration trends related to the calculated concentration in 2015 (percentage of wells).**

| | Concentration ≥ 25 mg/L | Concentration < 25 mg/L | Concentration ≥ 50 mg/L | Concentration < 50 mg/L |
|---|---|---|---|---|
| Increasing trend | 29.9 % | 17.6 % | 5.9 % | 41.6 % |
| Decreasing trend | 14.5 % | 38.0 % | 2.7 % | 49.8 % |
| ∑ | 44.4 % | 55.6 % | 8.6 % | 91.4 % |

**Table 2.3 - Nitrate concentration trends related to the calculated concentration in 2020 (percentage of wells).**

| | Concentration ≥ 25 mg/L | Concentration < 25 mg/L | Concentration ≥ 50 mg/L | Concentration < 50 mg/L |
|---|---|---|---|---|
| Increasing trend | 33.0 % | 14.5 % | 9.0 % | 38.5 % |
| Decreasing trend | 10.4 % | 42.1 % | 2.3 % | 50.2 % |
| ∑ | 43.4 % | 56.6 % | 11.3 % | 88.7 % |

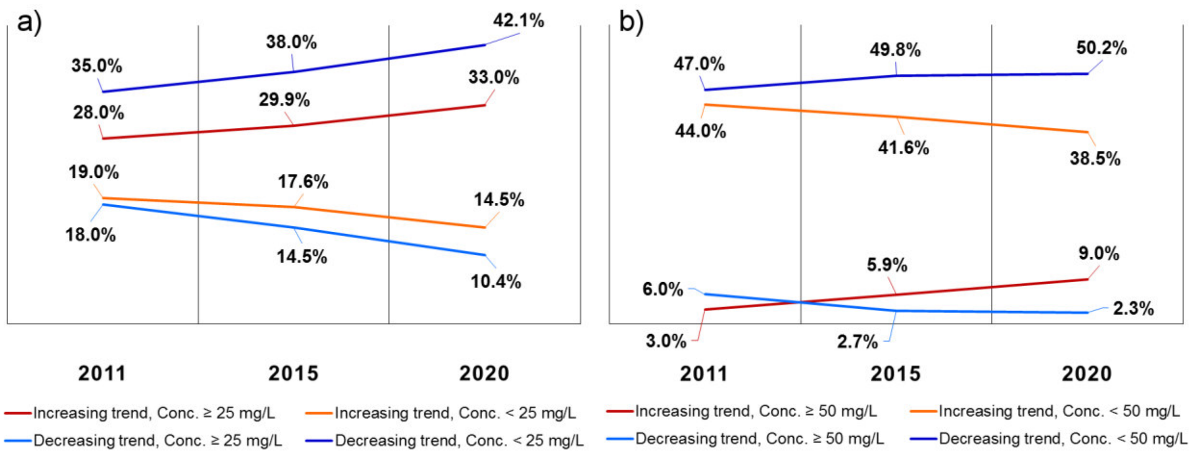


**Fig. 2.5 - Percentage of wells showing increasing or decreasing trends, with concentration lower or higher than 25 mg/L (a) and 50 mg/L (b) in 2011, 2015 and 2020.**

# References

Avanzini M., Beretta G.P., Francani V., Nespoli M., 1995. Indagine preliminare sull'uso sostenibile delle falde profonde nella provincia di Milano. CAP Milano Consorzio per l'acqua potabile

Crosta G.B., Frattini P., Peretti L., 2015. Baseline quality definition for highly productive aquifers in the Milan metropolitan area. Proceedings of the 42° IAH Congress, Rome, Italy

European Community, 1991. Council Directive 91/676/EEC concerning the protection of waters against pollution caused by nitrates from agricultural sources, (Nitrate Directive). OJ L 375, 31 December 1991, pp. 1-8

European Community, 2000. Directive 2000/60/EC of the European Parliament and of the Council of 23 October 2000 establishing a framework for Community action in the field of water policy, (Water Framework Directive). OJ L 327, 22 December 2000, pp. 1-73

European Community, 2006. Directive 2006/118/EC on the protection of groundwater against pollution and deterioration, (Groundwater Directive). OJ L 372, 27 December 2006, pp. 19-31

Francani V., Pozzi R., 1981. Condizioni di alimentazione delle riserve idriche del territorio milanese. La Rivista della Strada, L 303, Milano, Italy

Grath J., Scheidleder A., Uhlig S., Weber K., Kralik M., Keimel T., Gruber D., 2001. The EU Water Framework Directive: Statistical aspects of the identification of groundwater pollution trends, and aggregation of monitoring results. Final Report. Austrian Federal Ministry of Agriculture and Forestry, Environment and Water Management (Ref.: 41.046/01-IV1/00 and GZ 16 2500/2-I/6/00), European Commission (Grant Agreement Ref.: Subv 99/130794), in kind contributions by project partners. Vienna

Martinis B., Mazzarella S., 1971. Prima ricerca idrica profonda nella pianura lombarda. Mem. Ist. Geol. E Min. Univ. Padova, XXVIII

Masetti M., Poli S., Sterlacchini S., Beretta G.P., Facchi A., 2008. Spatial and statistical assessment of factors influencing nitrate contamination in groundwater. Journal of Environmental Management, vol. 86, n. 1, pp. 272-281, doi 10.1016/j.jenvman.2006.12.023

Regione Lombardia, Eni Divisione Agip, 2002. Geologia degli acquiferi Padani della Regione Lombardia (Geology of the Po Valley aquifers in Lombardy Region). S.EL.CA., Firenze, Italy

Sorichetta A., 2011. Groundwater vulnerability assessment using statistical methods. Università degli Studi di Milano, Academic year 2010, 141 pp. http://hdl.handle.net/2434/152913

# Chapter 3

# Groundwater vulnerability

Vulnerability is the degree to which human or environmental systems are likely to experience harm due to perturbation or stress, and can be identified for a specific system, hazard or group of hazards (Popescu et al., 2008). In hydrogeology, vulnerability assessment typically describes the susceptibility of the water table, a particular aquifer, or a water well to contaminants (e.g., nitrates, industrial chemicals, gasoline), which can reduce the groundwater quality (Ligget and Talwar, 2009).
The concept of groundwater vulnerability is derived from the assumption that the physical environment may provide some degree of protection of groundwater against natural and human impacts, especially with regard to pollutants entering to subsurface environment (WHO, 2006). Since the protection provided by the natural environment varies from place to place, some land areas are more vulnerable to pollution than others (Vrba and Zaporozec, 1994).
Although the concept of groundwater vulnerability, which describes the relative ease with which the groundwater resource could be contaminated, is widespread accepted and understood, at present no standardized or rigorous definition for groundwater vulnerability exists (Frind et al., 2006; Liggett and Talwar, 2009). This is because (Foster et al., 2013): (a) all aquifers are to some degree vulnerable to pollution by highly-mobile and persistent contaminants (such as brines and, in many cases, nitrates) and (b) vulnerability is in reality specific to contaminant type and pollution scenario.
Within the scientific community, there is still an on-going debate about whether groundwater vulnerability should consider only the intrinsic characteristics of the aquifer, or whether it should take into account also the properties of the contaminant type, loading, fate and transport (Liggett and Talwar, 2009). While it is clear that general vulnerability to a universal contaminant cannot be really valid, trying to define vulnerability separately for specific pollutant is unlikely to achieve either adequate coverage or universal acceptance (WHO, 2006).
In another way, it is possible to assess groundwater risk, which can consider the vulnerability (intrinsic or specific), the hazard, such as the pollution potential from the surface (i.e., types, loading, distribution, toxicity), and the consequence of losing the resource (i.e., cost of replacement). To generalize, risk (i.e., total risk) is a function of vulnerability, hazard potential, and consequences (i.e., exposure or elements at risk), and expresses the combination of the probability of occurrence of a potentially damaging phenomenon and its negative consequences (UNISDR, 2009). In some cases, no differentiation exists between specific vulnerability and risk assessments, with hazard types, distribution, loading, and transport all included at the risk-assessment stage (e.g., Focazio et al., 2002).

## 3.1 Groundwater vulnerability or groundwater pollution risk?

The term “vulnerability of groundwater to contamination” was probably first introduced by Albinet and Margat in 1970, and describes vulnerability as “the penetrating and spreading abilities of the pollutants in aquifers according to the nature of the surface layers and the hydrogeological conditions”.

After the first attempt, through the years, several definitions of groundwater vulnerability have been proposed (Table 3.1), including different terms like “sensitivity”, “aquifer pollution” or “potential risk”. In absence of a standardized and unanimously accepted definition, distinguishing intrinsic and specific vulnerability, or specific vulnerability and groundwater risk, can become a difficult task when performing a groundwater vulnerability assessment. Thus, it is important to (Sorichetta, 2011): (a) establish the objectives that must be achieved; (b) explicitly refer to the definition of groundwater vulnerability to be used, (c) select the proper assessment method according to (a) and (b).

**Table 3.1 - Definitions of groundwater vulnerability, and related terms, assigned by the different Authors, since the 1970s.**

| Author | Term | Definition |
|---|---|---|
| Civita (1987) | Intrinsic (i.e., natural) aquifer vulnerability | The specific susceptibility of aquifer systems, in their parts, geometric and hydrodynamic settings, to receive and diffuse fluid and/or hydro-vectored contaminants, the impact of which, on the groundwater quality, is a function of space and time. |
| Foster (1987) | Aquifer pollution vulnerability | The intrinsic characteristics that determine the sensitivity of various parts of an aquifer to being adversely affected by an imposed contaminant load. |
| U.S. EPA (1993) | Aquifer sensitivity | The relative ease with which a contaminant (in this case a pesticide) applied on or near the land surface can migrate to the aquifer of interest. It is a function of the intrinsic characteristics of the hydrogeological setting, and is not dependent on the agronomic practices or pesticide characteristics. |
| | Groundwater vulnerability | The relative ease with which a contaminant (in this case a pesticide) applied on or near the land surface can migrate to the aquifer of interest under a given set of agronomic management practices, pesticide characteristics and aquifer sensitivity characteristics. |
| NRC (1993) | Groundwater vulnerability | The tendency or likelihood for contaminants (from non-point sources) to reach a specified position in the ground water system after introduction at some location above the uppermost aquifer. |
| | | The Committee differentiated two general types of vulnerability:<br>- specific vulnerability, referenced to a specific contaminant, contaminant class, or human activity;<br>- intrinsic vulnerability, which does not consider the attributes and behavior of specific contaminants. |

| | | |
|---|---|---|
| Vrba and Zaporozec (1994) | Intrinsic (or natural) vulnerability | An intrinsic property of a groundwater system that depends on the sensitivity of that system to human and/or natural impacts. Thus, it is solely a function of hydrogeological factors, i.e., soil properties, depth to groundwater, lithological properties of the unsaturated (i.e., vadose) and saturated zone, and recharge. |
| | Specific (or integrated) vulnerability | The vulnerability of groundwater to certain pollutants taking into account the potential human impacts, i.e. specific land use practices or contaminants. It considers the travel time of the contaminant through the vadose zone and its residence time in aquifer, and the soil attenuation capacity with respect to the properties of individual contaminants. |
| Focazio et al. (2002) | Intrinsic susceptibility | The intrinsic susceptibility of a ground-water system depends on the aquifer properties (hydraulic conductivity, porosity, hydraulic gradients) and the associated sources of water and stresses for the system (recharge, interactions with surface water, travel through the unsaturated zone, and well discharge). |
| | Groundwater vulnerability | Groundwater vulnerability is a function not only of the properties of the ground-water-flow system (intrinsic susceptibility) but also of the proximity of contaminant sources, characteristics of the contaminant, and other factors that could potentially increase loads of specified contaminants to the aquifer and(or) their eventual delivery to a ground-water resource. |
| Brouyère et al. (2001), COST Action 620 (2003) | Intrinsic vulnerability | The intrinsic vulnerability of groundwater to contaminants takes into account the geological, hydrological and hydrogeological characteristics of an area, but is independent of the nature of the contaminants and the contamination scenario. |
| | Specific vulnerability | The specific vulnerability takes into account the properties of a particular contaminant or group of contaminants and its (their) relationship(s) to the various aspects of the intrinsic vulnerability of the area. |

On the definition and description of groundwater vulnerability, Authors acknowledge and agree that:

- groundwater vulnerability represents, in general, the sensitivity of an aquifer to being adversely affected at any given point by an imposed contaminant pressure (or load) from the land surface (e.g., Foster et al., 2013);

- groundwater vulnerability is a relative, non-measurable and dimensionless property (Vrba and Zaporozec, 1994);
- groundwater vulnerability assesses only contaminants introduced by humans above the water table at or near the land surface (NRC, 1993);
- intrinsic vulnerability takes into account the geological, hydrological and hydrogeological characteristics of an area (i.e., attenuation capacity of soil, characters of the unsaturated and saturated zones, groundwater depth and recharge, which are expressed as advection, hydrodynamic dispersion and dilution processes). But it is independent of the nature of the contaminants (COST Action 620, 2003);
- specific vulnerability takes into account the properties of a particular contaminant (or group of contaminants) and the physical, chemical and biological processes (i.e., adsorption, cation exchange, filtration, sedimentation, biodegradation, oxidation and reduction, complexation, precipitation, volatilization, decay and die off), which determine its (their) fate and transport through the aquifer (COST Action 620, 2003).

The concept of groundwater vulnerability is strictly related to groundwater pollution risk, when it is necessary to develop strategies to protect groundwater quality. In some cases, no differentiation exists between specific vulnerability and risk assessments (e.g., Focazio et al., 2002). Although there is the necessity of a clear distinction of the two concepts and whether they could be assessed, Authors proposed various definitions and different assessment methods or conceptual frameworks.
Besides the properties of both the natural environment and the characteristics of the contaminant(s), which have to be taken into account when performing a specific vulnerability assessment, Vrba and Zaporozec (1994) suggest to include also: land use (e.g., forest or meadow, agricultural lands, urban areas) and population density. According to the Authors, there is a fundamental difference between areas stressed by human activities (e.g., agriculture, settlements) and natural environments (e.g., forests). For example, the more densely an area is populated, the greater the potential and real contaminant load on the groundwater system. Thus, maps showing the distribution of human activities (e.g., contaminant loading) or population densities are integral components of specific vulnerability assessments.
Following the same idea, Focazio et al. (2002) affirm that the vulnerability of a groundwater resource to contamination depends on intrinsic susceptibility as well as the locations and types of sources of naturally occurring and anthropogenic contamination, relative locations of wells, and the fate and transport of the contaminant(s).
On the other hand, Gogu and Dassargues (2000) affirm that overlaying maps of the most vulnerable zones, with maps showing the location of each potential contamination sources or polluting land-use activities (e.g., land-use and census data), generates the map of potential problem areas (or risk maps). Thus, the Authors consider the potential contamination sources or polluting land-use activities as a proper "hazard" in risk assessment terms.
The working group of the European COST Action 620 (2003) in an effort of developing an improved and consistent European approach for the protection of karst groundwater, defined a conceptual framework for vulnerability, hazard and risk mapping. An entire risk assessment procedure can be considered (Brouyère et al., 2001) as a hierarchical process starting with intrinsic vulnerability, then progressing to specific vulnerability, and finally to risk assessment when combining with hazard (i.e.,

potential pollution at the surface). This approach is also based on a source-pathway-receptor model, which can be applied for both groundwater resource and source protection (Fig. 3.1). The source (of contamination) is the assumed place of release of a contaminant (e.g., cattle pasture, spreading of pesticides or fertilizer, leakage in a sewerage system). The pathway is the flow path of a potential contaminant from its point of release (source), through the system, to the point that has to be protected (receptor). The receptor is the groundwater surface in the relevant aquifer under consideration (i.e., resource receptor) or a water well or spring (i.e., source receptor).

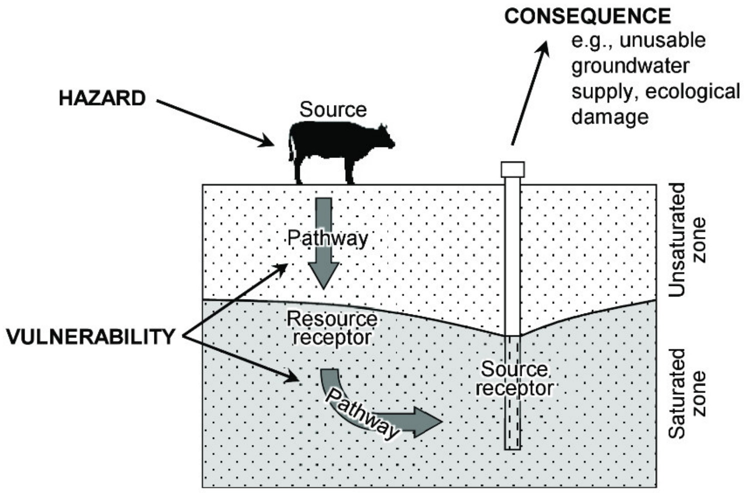


**Fig. 3.1 - Source-pathway-receptor model for contaminants. Risk assessment components: hazard, vulnerability and consequence (modified from Ligget and Talwar, 2009 and COST Action 620, 2003).**

Following the source-pathway-receptor model, the risk of groundwater contamination depends on (COST Action 620, 2003): (a) the hazard posed by a potential polluting activity (equivalent to source); (b) the intrinsic and specific vulnerability of groundwater to contamination (equivalent to pathway); (c) the potential consequences of a contamination event (the receptor is the groundwater). The European approach clearly distinguishes between vulnerability (intrinsic and specific), hazard and risk.
Foster et al. (2003) describe groundwater pollution hazard as the interaction between the aquifer pollution vulnerability (i.e., intrinsic vulnerability) and the contaminant load that is, will be or might be, applied on the subsurface environment because of human activity at the land surface. Adopting such a scheme, there could be high vulnerability but no pollution hazard, because of the absence of a significant subsurface contaminant load. Instead, groundwater pollution risk is defined as the threat posed by this hazard to human health due to pollution of a specific groundwater supply source or to an ecosystem due to pollution of a specific natural aquifer discharge. Furthermore, the Authors highlight the need of a clear distinction between the protection of groundwater resource (aquifers as a whole) and specific sources (such as wells and springs). Although both approaches to groundwater pollution control are complementary, the emphasis placed on one or other depends on the objectives of the research, the resource development situation, and the hydrogeological conditions.

## 3.2 Groundwater vulnerability assessment methods

Groundwater vulnerability assessment methods are a means to synthesize complex hydrogeological information into a form useable by planners, decision and policy makers, geoscientists and the public (Liggett and Talwar, 2009). The outcome is a groundwater vulnerability map. The development of vulnerability maps is useful for many aspects of water management, including for example: prioritizing areas for further investigations, protection and monitoring.

Since vulnerability cannot be directly measured, geological and hydrogeological information are used to assess it. Many methods integrate such information to determine the vulnerability. The methods vary from simple, qualitative, inexpensive, indexing assessments to complex, qualitative, costly, numerical modelling assessments (Focazio et al., 2002). The approach used to determine vulnerability for a particular project will depend on numerous factors, including the purpose and scope of the study, scale, data availability, time, cost, and end-user requirements.

In general, vulnerability assessments are categorized as (Gogu and Dassargues, 2000): index and overlay methods; statistical methods; process-based methods.

Another categorization, proposed by Focazio et al. (2002), divide the methods currently used to assess groundwater vulnerability at a regional scale in (Fig. 3.2): subjective (i.e., knowledge-driven) or objective (i.e., data driven) methods. Subjective methods include overlay and index methods (e.g., DRASTIC, Aller et al., 1987; GOD, Foster, 1987; AVI, Van Stempvoort et al., 1993; and EPIK, Doerfliger and Zwahlen, 1997) and their modifications (e.g., Sener and Davraz, 2013). They are easy to implement and require a limited amount of data to derive a subjective categorization of groundwater vulnerability. However, the various methods produce very different results at any given site (Gogu et al., 2003; Ducci and Sellerino, 2013). On the other hand, objective methods are based on the use of statistical methods or processed-based methods, which allow an objective determination of relations between the predictor factors and the level of contamination in the study area. Statistical methods range from descriptive statistics (e.g., Welch et al., 2000) to regression and conditional probability analyses (e.g., Eckardt and Stackelberg, 1995; Tesoriero and Voss, 1997; Nolan, 2001; Alberti et al., 2001; Worrall and Besien, 2005; Masetti et al., 2009). Processed-based methods refer to approaches that simulate or take into account physical processes of water movement (groundwater flow) and the associated fate and transport of contaminants (e.g., Kralik and Keimel, 2003; Beaujean et al., 2014).

In this regard, only objective methods allow scientifically defensible end products (Focazio et al., 2002) and, most importantly, enable an explicit integration of the time dimension in the groundwater vulnerability assessment (Sorichetta, 2011).

Subjective rating methods produce categories of intrinsic vulnerability (usually high, medium and low), while statistical and process-based methods can assess intrinsic or specific vulnerability (Fig. 3.2). However, Authors often refers to different terms: a generic vulnerability (e.g., Lake et al., 2003; Arthur et al., 2007; Sorichetta et al., 2011; Beaujean et al., 2014), or aquifer susceptibility (e.g., Tesoriero and Voss, 1997), or probability of occurrence of a specific contaminant (e.g., Nolan and Hitt, 2006).

Statistical methods usually evaluate groundwater vulnerability to a single compound, such as nitrates (e.g., Tesoriero and Voss, 1997; Nolan, 2001; Arthur et al., 2007), or the probability of occurrence of natural contaminants, such as arsenic (e.g., Amini et al., 2008; Winkel et al., 2008). Other studies tried to evaluate the vulnerability to a range of pollutant compounds, such as pesticides (e.g., Worral and Kolpin, 2003; Worral and Besien, 2005).

Statistical methods usually take into account pollutant loadings, or land use and population density, besides the natural characteristics of the area, as representing potential sources of contamination (i.e., non-point sources). According to the schools of thought (Paragraph 3.1), considering these information can lead to a vulnerability assessment (e.g., Focazio et al., 2002) or a risk assessment (e.g., Gogu and Dassargues, 2000).

Nevertheless, it is opinion of the Author of this study that risk assessments require the identification of a clear and evident, not only potential, source of contamination and a specific target of the contamination, which, in the case of groundwater, could be a well or a spring. Instead, groundwater vulnerability assessments, which focus on aquifers as a whole resource, endeavor to achieve a degree of protection for the entire groundwater resource and for all groundwater users and aim to produce local, or regional, maps, over extensive areas, of relative degrees of susceptibility to contamination.

Thus, this study would deal with vulnerability assessments to nitrate contamination, using the spatial statistical method “Weights of Evidence” (Bonham-Carter, 1994), taking into account both natural and anthropogenic factors, which can influence the presence of nitrates in groundwater.

Considering the wide spectrum of definitions of groundwater vulnerability and pollution risk, not unanimously accepted, often related to the assessment method, this study follows the same terminology used in the previous studies on groundwater quality performed applying a spatial statistical technique (e.g., Arthur et al., 2007; Sorichetta et al., 2011). Thus, the term “groundwater vulnerability to nitrate contamination” will be used.

Considering the time dimension in groundwater vulnerability assessments, a “zone vulnerable to nitrate contamination” can be defined as an area where the combination of natural (e.g., groundwater depth and velocity) and anthropogenic factors (e.g., growth of urban areas) involves a deterioration of groundwater quality. Whereas, in a static system, a “zone vulnerable to nitrate contamination” can be defined as an area where the combination of the same factors involves a given absolute level of nitrate contamination in the aquifer.

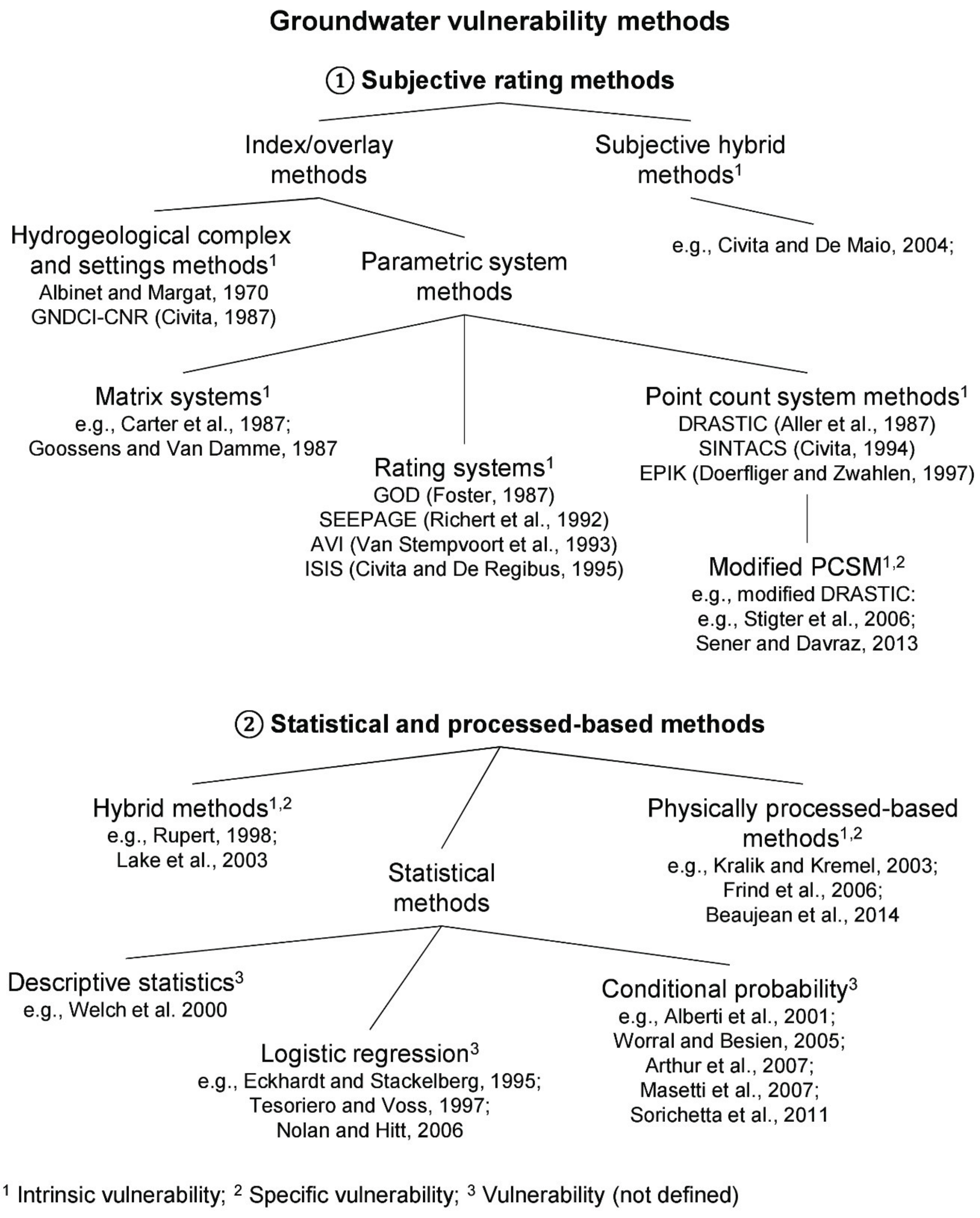


**Fig. 3.2 - Groundwater vulnerability methods, classified according to Focazio et al. (2002) and Gogu and Dassargues (2000).**

## 3.3 Weights of Evidence technique

The Weights of Evidence (WofE) modeling technique combines different spatial datasets in a Geographical Information System (GIS) environment to analyze and describe their interactions and generate predictive patterns (Bonham-Carter, 1994; Raines et al., 2000). WofE can be defined as a data-driven Bayesian method in a log-linear form that uses known occurrences representing the response variable as training sites (training points). These data are used to obtain predictive probability maps (response themes; i.e., groundwater vulnerability maps) from multiple weighted evidences (i.e., evidential themes representing explanatory variables or factors that influence groundwater vulnerability), which determine the spatial distribution of the occurrences in the study area (Raines, 1999).

Training points (TPs) are used in WofE to calculate the prior probability, the weights for each class representing a different range of values of each generalized evidential theme, and the posterior probability values in the response theme.

Prior probability is based on prior knowledge of the TPs' locations in the study area. Prior probability is simply defined by the ratio between the area containing occurrences (i.e., the number of pixels containing a training point D) and the total area (i.e., the total number of pixels). Thus, the prior probability represents the probability that a pixel within the study area contains an occurrence without considering any evidential themes, and it can be expressed as (Bonham-Carter, 1994):

$$P\{D\} = \frac{N_{\mathrm{D}}}{N_{\mathrm{T}}} \tag{3.1}$$

where $N_{\mathrm{D}}$ and $N_{\mathrm{T}}$ are respectively the number of pixels containing a training point and the total number of pixels in the study area.

For each class of each evidential theme, a positive and a negative weight are computed based on the location of the TPs with respect to the study area. For a given class *B*, the positive weight $W^{+}$ and the negative weight $W^{-}$ are, respectively, higher and lower than zero or lower and higher than zero. The resulting combination depends on whether *B* has more or fewer TPs than expected by chance.

The weights can be expressed as (Bonham-Carter, 1994):

$$W^{+} = \log_{\mathrm{e}} \frac{P\{B|D\}}{P\{B|\bar{D}\}} \tag{3.2}$$

$$W^{-} = \log_{\mathrm{e}} \frac{P\{\bar{B}|D\}}{P\{\bar{B}|\bar{D}\}} \tag{3.3}$$

where $P\{B|D\}$ and $P\{B|\bar{D}\}$ are respectively the probability of a pixel of being in the class *B* when the same pixel contains or does not contain a training point, and $P\{\bar{B}|D\}$ and $P\{\bar{B}|\bar{D}\}$ are respectively the probability of a pixel of not being in the class *B* when it contains or does not contain a training point.

The contrast (positive weight minus negative weight) represents the overall degree of spatial association between each class of a given evidential theme and TPs. Thus, it is a measure of the usefulness of the considered class in predicting the location of TPs (Raines, 1999).

A confidence value for the ratio between the contrast and its standard deviation must be selected to provide a useful measure of the significance of the contrast (Raines, 1999). For this study, a confidence value of |1.282|, corresponding approximately to a 90 % level of significance, was chosen as the minimum acceptable value to consider an evidential theme class as statistically significant.
The posterior probability represents the relative probability that a pixel contains an occurrence based on the evidences provided by the evidential themes (i.e., based on the calculated weights). The posterior probability can be expressed as (Bonham-Carter, 1994):

$$\log_e O\{D|B_1^k \cap B_2^k \cap B_3^k \dots \cap B_n^k\} = \sum_{j=1}^{n} W_j^k + \log_e O\{D\} \qquad (3.4)$$

where *n* identifies each single class used to categorize each evidential theme, *k* is either + or - depending on whether the prediction spatial class, $B_n$, is either present or absent, and *O{D}* is the odd form of the probability that a pixel within the study area contains an occurrence.
The relative probability means that a pixel having a higher posterior probability is more likely to contain an occurrence than a pixel having a lower probability, and it represents a measure of the relative likelihood of occurrence of an event (Raines, 1999).
In this study, the WofE response themes were generated using the Spatial Data Modeler (Sawatzky et al., 2009) for ArcGIS 9.3 (ESRI, 2008).

### 3.3.1 Application fields of the WofE modeling technique

The Weights of Evidence technique has been successfully applied both in geosciences and in many other fields such as archaeology (Duke and Steele, 2010), ecology (Romero-Calcerrada and Luque, 2006), wildfire (Romero-Calcerrada et al., 2008) and epidemiology (Lynen et al., 2007).
Applications in geosciences have mainly focused on:

- mineral exploration and resource appraisal (Agterberg et al., 1993; Raines and Mihalasky, 2002; Cheng, 2004; Corsini et al., 2009),
- landslide hazard zonation (Poli and Sterlacchini, 2007; Dahal et al., 2008; Lee, 2013; Goetz et al., 2015),
- groundwater quantity/productivity potential (Lee et al., 2012; Al-Abadi, 2015; Madani and Niyazi, 2015; Sahoo et al., 2015),
- and groundwater quality/vulnerability assessment (Alberti et al., 2001; Arthur et al., 2007; Masetti et al., 2007, 2008; Sorichetta et al., 2011, 2012; Uhan et al., 2011).

Other applications in geosciences include the evaluation of risk of slope failure in open mines (Nelson et al., 2007) and the evaluation of ground subsidence spatial hazard near abandoned underground coal mines (Oh and Lee, 2010).

### 3.3.2 WofE technique in groundwater vulnerability assessments

In groundwater vulnerability assessments of a specific region, the training points are a subset of the monitoring well network of the area, the evidential themes are those natural and anthropogenic factors, which influence groundwater vulnerability, and the posterior probability output (response theme) represents the relative groundwater vulnerability of the area.

The response theme can be categorized so that each vulnerability class contains approximately the same number of different posterior probability values according to the geometric interval method (Sorichetta et al., 2011). The ideal number of classes is five, with the degree of groundwater vulnerability increasing from 1 to 5. This number is selected based on the general criteria used to identify vulnerability classes (Sorichetta et al., 2011) and on visual analytic techniques (Cowan, 2001).

# References


Agterberg F.P., Bonham-Carter G.F., Cheng Q., Wright D.F., 1993. Weights of evidence modeling and weighted logistic regression for mineral potential. In: Davis J.C. and Herzfeld U.C. (ed.), Computers in Geology-25 Years of Progress, pp. 13-32, Oxford University Press, New York, NY

Al-Abadi A.M., 2015. Groundwater potential mapping at northeastern Wasit and Missan governorates, Iraq using a data-driven weights of evidence technique in framework of GIS. Environmental Earth Sciences, vol. 74, n. 2, pp. 1109-1124, doi 10.1007/s12665-015-4097-0

Alberti L., De Amicis M., Masetti M., Sterlacchini S., 2001. Bayes' rule and GIS for evaluating sensitivity of groundwater to contamination. In: Proceedings of the International IAMG Conference - Cancun, Mexico

Albinet M., Margat J., 1970. Cartographie de la vulnérabilité à la pollution des nappes d'eau souterraine [Mapping of groundwater vulnerability to pollution], Bulletin BRGM 2éme Sèrie, vol. 3, n. 4, pp. 13-22

Aller L., Bennet T., Lehr J.H., Petty R.J., 1987. DRASTIC: a standardised system for evaluating groundwater pollution potential using hydrologic settings. US EPA Report, 600/2–87/035, "Robert S. Kerr" Environmental Research Laboratory, Ada, OK

Amini M., Abbaspour K.C., Berg M., Winkel L., Hug S.J., Hoehn E., Yang H., Johnson C.A., 2008. Statistical Modeling of Global Geogenic Arsenic Contamination in Groundwater. Environmental Science and Technology, vol. 42, pp. 3669-3675

Arthur J.D., Wood H.A.R., Baker A.E., Cichon J.R., Raines G.L., 2007. Development and Implementation of a Bayesian-based Aquifer Vulnerability Assessment in Florida. Natural Resources Research, vol. 16, n. 2, pp. 93-107

Beaujean J., Lemieux J.M., Dassargues A., Therrien R., Brouyère S., 2014. Physically Based Groundwater Vulnerability Assessment Using Sensitivity Analysis Methods. Ground Water, vol. 52, n. 6, pp. 864-874, doi 10.1111/gwat.12132

Bonham-Carter G.F., 1994. Geographic Information Systems for Geoscientists-Modelling with GIS. Pergamon Press

Brouyère S., Jeannin P.-Y., Daly D., Dassargues A., Dunne S., Goldscheider N., Malik P., Popescu I.C., Sauter M., Vadillo I., Zwahlen F., 2001. Evaluation and validation of vulnerability concepts using a physically based approach. In: Mudry J., Zwahlen F. (ed.) 7th Conference on limestone hydrology and fissured media. Besancon, France, pp. 67-72

Cheng Q., 2004. Application of Weights of Evidence Method for Assessment of Flowing Wells in the Greater Toronto Area, Canada. Natural Resources Research, vol. 13, n. 2, pp. 77-86, doi 10.1023/B:NARR.0000032645.46747.48

Carter A.D., Palmer R.C., Monkhouse R.A., 1987. Mapping the vulnerability of groundwater to pollution from agricultural practice, particularly with respect to nitrate. In: Duijvenbooden W van, Waegeningh HG van (ed.) Vulnerability of soil and groundwater to pollutants. TNO Committee on Hydrological Research, The Hague, Proceedings and Information, vol. 38, pp. 333-342

Civita M., 1987. La previsione e la prevenzione del rischio d'inquinamento delle acque sotterranee a livello regionale mediante le Carte di Vulnerabilità. In: Atti del Convegno "Inquinamento delle Acque Sotterranee: Previsione e Prevenzione", Mantova, Italy, pp. 9-18

Civita M., 1994. Le carte della vulnerabilità degli acquiferi all'inquinamento. Teoria e pratica. Pitagora, Bologna

Civita M., De Regibus C., 1995. Sperimentazione di alcune metodologie per la valutazione della vulnerabilità degli aquiferi. Quaderni di Geologia Applicata. Pitagora, Bologna, vol. 3, pp. 63-71

Civita M., De Maio M., 2004. Assessing and Mapping groundwater vulnerability to contamination: The Italian "combined" approach. Geofisica Internacional, vol. 43, n. 4, pp. 513- 532

Corsini A., Cervi F., Ronchetti F., 2009. Weight of evidence and artificial neural networks for potential groundwater spring mapping: an application to the Mt. Modino area (Northern Apennines, Italy). Geomorphology, vol. 111, pp. 79-87, doi 10.1016/j.geomorph.2008.03.015

COST Action 620, 2003. Vulnerability and risk mapping for the protection of carbonate (karst) aquifers. In: Zwahlen F. (ed.), Final Report n. EUR 20912. Luxemburg: European Cooperation in the Field of Scientific and Technical Research, DG Research, Brussels, Luxembourg

Cowan N., 2001. The magical number 4 in short-term memory: a reconsideration of mental storage capacity. Behavioral and Brain Sciences, vol. 24, pp. 87-185, doi 10.1017/S0140525X01003922

Dahal R.K., Hasegawa S., Nonomura A., Yamanaka M., Masuda T., Nishino K., 2008. GIS-based weights-of-evidence modelling of rainfall-induced landslides in small catchments for landslide susceptibility mapping. Environmental Geology, vol. 54, n. 2, pp. 311-324, doi 10.1007/s00254-007-0818-3

Doerfliger N., Zwahlen F., 1997. EPIK: a new method for outlining of protection areas in karst environment. In: Günay G., Johnson I. (ed.) Proceedings 5th International symposium and field seminar on karst waters and environmental impacts, Antalya, Turkey. Balkema, Rotterdam

Ducci D., Sellerino M., 2013. Vulnerability mapping of groundwater contamination based on 3D lithostratigraphical models of porous aquifers. Science of the Total Environment, vol. 447, pp. 315-322, doi 10.1016/j.scitotenv.2012.12.090

Duke C., Steele J., 2010. Geology and lithic procurement in Upper Palaeolithic Europe: a weights-of-evidence based GIS model of lithic resource potential. Journal of Archaeological Science, vol. 37, n. 4, pp. 813-824, doi 10.1016/j.jas.2009.11.011

Eckardt D.A., Stackelberg P.E., 1995. Relation of groundwater quality to land use on Long Island, New York. Ground Water, vol. 33, n. 6, pp. 1019-1033

ESRI – Environmental Systems Research Institute, 2008. ArcGIS Desktop 9.3, Redlands, CA. http://www.esri.com/software/arcgis/arcgis-for-desktop

Focazio M.J., Reilly T.E., Rupert M.G., Helsel D.R., 2002. Assessing Ground-Water Vulnerability to Contamination: Providing Scientifically Defensible Information for Decision Makers. U.S. Geological Survey Circular 1224. ISBN: 0-607-89025-8

Foster S., 1987. Fundamental concepts in aquifer vulnerability, pollution risk and protection strategy. In: Duijvenbooden W van, and Waegeningh HG van (ed.), Vulnerability of soil and groundwater to pollutants, vol. 38, pp. 69-86. Proceedings and Information, TNO Committee on Hydrological Research, The Hague

Foster S., Garduno H., Kemper K., Tuinhof A., Nanni M., Dumars C., 2003. Groundwater quality protection: defining strategy and setting priorities. GW-MATE Briefing Note Series, no. 8, World Bank, Washington DC

Foster S., Hirata R., Andreo B., 2013. The aquifer pollution vulnerability concept: aid or impediment in promoting groundwater protection? Hydrogeology Journal, vol. 21, pp. 1389-1392

Frind E.O., Molson J.W., Rudolph D.L., 2006. Well Vulnerability: A Quantitative Approach for Source Water Protection. Ground Water, vol. 44, n. 5, pp. 732-742, doi 10.1111/j.1745-6584.2006.00230.x

Goetz J.N., Brenning A., Petschko H., Leopold P., 2015. Evaluating machine learning and statistical prediction techniques for landslide susceptibility modeling. Computers and Geosciences, vol. 81, pp. 1-11, ISSN: 0098-3004, doi 10.1016/j.cageo.2015.04.007

Gogu R.C., Dassargues A., 2000. Current trends and future challenges in groundwater vulnerability assessment using overlay and index methods. Environmental Geology, vol. 39, n. 6, pp. 549-559

Gogu R.C., Hallet V., Dassargues A., 2003. Comparison of aquifer vulnerability assessment techniques. Application to the Néblon river basin (Belgium). Environmental Geology, vol. 44, n. 8, pp. 881-892, doi 10.1007/s00254-003-0842-x

Goossens M., Van Damme M., 1987. Vulnerability mapping in Flanders, Belgium. In: Duijvenbooden W. van, Waegeningh H.G. van (ed.) Vulnerability of soil and groundwater to pollutants. TNO Committee on Hydrological Research, The Hague, Proceedings and Information, vol. 38, pp. 333-342

Kralik M., Keimel T., 2003. Time-input, an innovative groundwater-vulnerability assessment scheme: application to an alpine test site. Environmental Geology, vol. 44, n. 6, pp. 679-686, doi 10.1007/s00254-003-0809-y

Lake I.R., Lovett A.A., Hiscock K.M., Betson M., Foley A., Sünnenberg G., Evers S., Fletcher S., 2003. Evaluating factors influencing groundwater vulnerability to nitrate pollution: developing the potential of GIS. Journal of Environmental Management, vol. 68, n. 3, pp. 315-328

Lee S., 2013. Landslide detection and susceptibility mapping in the Sagimakri area, Korea using KOMPSAT-1 and weight of evidence technique. Environmental Earth Sciences, vol. 70, n. 7, pp. 3197-3215, doi 10.1007/s12665-013-2385-0

Lee S., Kim Y.S., Oh H.J., 2012. Application of a weights-of-evidence method and GIS to regional groundwater productivity potential mapping. Journal of Environmental Management, vol. 96, n. 1, pp. 91-105, doi 10.1016/j.jenvman.2011.09.016

Liggett J.E., Talwar S., 2009. Groundwater vulnerability assessments and integrated water resource management. Streamline Watershed Management Bulletin, vol. 13, n. 1, pp. 18-29

Lynen G., Zeman P., Bakuname C., Di Giulio G., Mtui P., Sanka P., Jongejan F., 2007. Cattle ticks of the genera Rhipicephalus and Amblyomma of economic importance in Tanzania: distribution assessed with GIS based on an extensive Weld survey. Experimental and Applied Acarology, vol. 43, n. 4, pp. 303-319, doi 10.1007/s10493-007-9123-9

Madani A., Niyazi B., 2015. Groundwater potential mapping using remote sensing techniques and weights of evidence GIS model: a case study from Wadi Yalamlam basin, Makkah Province, Western Saudi Arabia. Environmental Earth Sciences, vol. 74, n. 6, pp. 5129-5142, doi 10.1007/s12665-015-4524-2

Masetti M., Poli S., Sterlacchini S., 2007. The Use of the weights-of-evidence modeling technique to estimate the vulnerability of groundwater to nitrate contamination. Natural Resources Research, vol. 16, n. 2, pp. 109-119, doi 10.1007/s11053-007-9045-6

Masetti M., Poli S., Sterlacchini S., Beretta G.P., Facchi A., 2008. Spatial and statistical assessment of factors influencing nitrate contamination in groundwater. Journal of Environmental Management, vol. 86, n. 1, pp. 272-281, doi 10.1016/j.jenvman.2006.12.023

Masetti M., Sterlacchini S., Ballabio C., Sorichetta A., Poli S., 2009. Influence of threshold value in the use of statistical methods for groundwater vulnerability assessment. Science of the Total Environment, vol. 407, n. 12, pp. 3836-3846, doi 10.1016/j.scitotenv.2009.01.055

Nelson E.P., Connors K.A., Suarez C.S., 2007. GIS-Based Slope Stability Analysis, Chuquicamata Open Pit Copper Mine, Chile. Natural Resources Research, vol. 16, n. 2, pp. 171-190, doi 10.1007/s11053-007-9044-7

Nolan B.T., 2001. Relating nitrogen sources and aquifer susceptibility to nitrate in shallow ground waters of the United States. Ground Water, vol. 39, n. 2, pp. 290-299

Nolan B.T., Hitt K.J., 2006. Vulnerability of shallow groundwater and drinking-water wells to nitrate in the United States. Environmental Science and Technology, vol. 40, n. 24, pp. 7834-7840, doi 10.1021/es060911u

NRC - National Research Council, 1993. Ground water vulnerability assessment: Predictive relative contamination potential under conditions of uncertainty. National Academy Press, Washington DC, ISBN: 978-0-309-04799-9

Oh H.J., Lee S., 2010. Assessment of ground subsidence using GIS and the weights-of-evidence model. Engineering Geology, vol. 115, n. 1-2, pp. 36-48, ISSN: 0013-7952, doi 10.1016/j.enggeo.2010.06.015

Poli S., Sterlacchini S., 2007. Landslide representation strategies in susceptibility studies using weights-of-evidence modeling technique. Natural Resources Research, vol. 16, n. 2, pp. 121-134

Popescu I.C., Gardin N., Brouyére S., Dassargues A., 2008. Groundwater vulnerability assessment using physically-based modelling: From challenges to pragmatic solutions. In: Refsgaard J.C., Kovar K., Haarder E., Nygaard E. (ed.) ModelCARE 2007 Proceedings, Calibration and Reliability in Groundwater Modelling. Denmark. IAHS Publication No. 320

Raines G.L., 1999. Evaluation of weights of evidence to predict epithermal-gold deposits in the Great Basin of the Western United States. Natural Resources Research, vol. 8, n. 4, pp. 257-276

Raines G.L., Bonham-Carter G.F., Kamp L., 2000. Predictive Probabilistic Modeling Using ArcView GIS. ArcUser, vol. 3, n. 2, pp. 45-48

Raines G.L., Mihalasky M.J., 2002. A reconnaissance method for delineation of tracts for regional-scale mineral-resource assessment based on geologic-map data. Natural Resources Research, vol. 11, n. 4, pp. 241-248, doi 10.1023/A:1021138910662

Richert S.E., Young S.E., Johnson C., 1992. SEEPAGE: a GIS model for groundwater pollution potential. Paper no. 922592. ASAE, St. Joseph, MI

Romero-Calcerrada R., Luque S., 2006. Habitat quality assessment using Weights-of-Evidence based GIS modelling: The case of Picoides tridactylus as species indicator of the biodiversity value of the Finnish forest. Ecological Modelling, vol. 196, n. 1-2, pp. 62-76, doi 10.1016/j.ecolmodel.2006.02.017

Romero-Calcerrada R., Novillo C.J., Millington J.D.A., Gomez-Jimenez I., 2008. GIS analysis of spatial patterns of human-caused wildfire ignition risk in the SW of Madrid (Central Spain). Landscape Ecology, vol. 23, n. 3, pp. 341-354, doi 10.1007/s10980-008-9190-2

Rupert M.G., 1998. Probability of detecting atrazine/desethyl-atrazine and elevated concentrations of nitrate (NO2+NO3-N) in ground water in the Idaho part of the upper Snake River basin. U.S.G.S. Water-Resources Investigations Report 98-4203

Sahoo S., Jha M.K., Kumar N., Chowdary V.M., 2015. Evaluation of GIS-based multicriteria decision analysis and probabilistic modeling for exploring groundwater prospects. Environmental Earth Sciences, vol. 74, n. 3, pp. 2223-2246, doi 10.1007/s12665-015-4213-1

Sawatzky D.L., Raines G.L., Bonham-Carter G.F., Looney C.G., 2009. Spatial Data Modeller (SDM): ArcMAP 9.3 geoprocessing tools for spatial data modelling using weights of evidence, logistic regression, fuzzy logic and neural networks, http://arcscripts.esri.com/details.asp?dbid=15341

Sener E., Davraz A., 2013. Assessment of groundwater vulnerability based on a modified DRASTIC model, GIS and an analytic hierarchy process (AHP) method: the case of Egirdir Lake basin (Isparta, Turkey). Hydrogeology Journal, vol. 21, n. 3, pp. 701-714, doi 10.1007/s10040-012-0947-y

Sorichetta A., 2011. Groundwater vulnerability assessment using statistical methods. Università degli Studi di Milano, Academic year 2010, 141 pp. http://hdl.handle.net/2434/152913

Sorichetta A., Masetti M., Ballabio C., Sterlacchini S., Beretta G.P., 2011. Reliability of groundwater vulnerability maps obtained through statistical methods. Journal of Environmental Management, vol. 92, n. 4, pp. 1215-1224, doi 10.1016/j.jenvman.2010.12.009

Sorichetta A., Masetti M., Ballabio C., Sterlacchini S., 2012. Aquifer nitrate vulnerability assessment using positive and negative weights of evidence methods, Milan, Italy. Computers and Geosciences, vol. 48, pp. 199-210, doi 10.1016/j.cageo.2012.05.021

Sorichetta A., Ballabio C., Masetti M., Robinson G.R. Jr, Sterlacchini S., 2013. A Comparison of Data-Driven Groundwater Vulnerability Assessment Methods. Ground Water, vol. 51, n. 6, pp. 866-879, doi: 10.1111/gwat.12012

Stigter T.Y., Ribeiro L., Carvalho Dill A.M.M., 2006. Evaluation of an intrinsic and a specific vulnerability assessment method in comparison with groundwater salinisation and nitrate contamination levels in two agricultural regions in the south of Portugal. Hydrogeology Journal, vol. 14, pp. 79-99, doi 10.1007/s10040-004-0396-3

Tesoriero A., Voss F., 1997. Predicting the probability of elevated nitrate concentrations in the Puget Sound basin: implications for aquifer susceptibility and vulnerability. Ground Water, vol. 35, n. 6, pp. 1029-1039

UNISDR - United Nations International Strategy for Disaster Reduction, 2009. Terminology on Disaster Risk Reduction. UNISDR. 20/2009. Geneva

US EPA - United States Environmental Protection Agency, 1993. A review of methods for assessing aquifer sensitivity and ground water vulnerability to pesticide contamination. USEPA, Office of Water, Washington DC

Uhan J., Vižintin G., Pezdič J., 2011. Groundwater nitrate vulnerability assessment in alluvial aquifer using process-based models and weights-of-evidence method: Lower Savinja Valley case study (Slovenia). Environmental Earth Sciences, vol. 64, n. 1, pp. 97-105, doi 10.1007/s12665-010-0821-y

Van Stempvoort D., Evert L., Wassenaar L., 1993. Aquifer vulnerability index: a GIS compatible method for groundwater vulnerability mapping. Water Quality Research Journal of Canada, vol. 18, pp. 25-37

Vrba J., Zaporozec A., 1994. Guidebook on mapping groundwater vulnerability. International Association of Hydrogeologists, International Contributions to Hydrogeology, Publication No. 16. Verlag Heinz Heise, Hannover

Welch A.H., Westjohn D.B., Helsel D.R., Wanty R.B., 2000. Arsenic in ground water of the United States – Occurrence and geochemistry. Ground Water, vol. 38, n. 4, pp. 589-604

WHO - World Health Organization, 2006. Protecting Groundwater for Health – Managing the quality of Drinking-water sources. Schmoll O., Howard G., Chilton J., Chorus I. (ed.), ISBN: 9241546689, IWA Publishing, London, UK

Winkel L., Berg M., Amini M., Hug S.J., Johnson C.A., 2008. Predicting groundwater arsenic contamination in Southeast Asia from surface parameters. Nature geoscience, vol. 1, pp. 536-542, doi 10.1038/ngeo254

Worrall F., Kolpin D.W., 2003. Direct assessment of groundwater vulnerability from single observations of multiple contaminants. Water Resources Research, vol. 39, n. 12, pp. 1345, doi 10.1029/2002WR001212

Worrall F., Besien T., 2005. The vulnerability of groundwater to pesticide contamination estimated directly from observations of presence or absence in wells. Journal of Hydrology, vol. 303, pp. 92-107, doi 10.1016/j.jhydrol.2004.08.019

## Chapter 4

# Response and explanatory variables

## 4.1 Response variable

Nitrate concentrations have been monitored by a network of about 500 wells covering the entire Lombardy plain area with a nearly uniform spatial distribution, where data have been collected every six months from 2001 to 2012 (Regional Environmental Agency – ARPA, unpublished data, 2012). From the network, only the 249 wells monitoring the shallow aquifer, in the period 2010 – 2012, have been used in the non-time-dependent analysis, while the 221 wells monitoring the shallow aquifer and having a minimum of eight measurements, in the period 2001 – 2011, were selected for being used in the time-dependent analyses (Grath et al., 2001, Fig. 4.1).

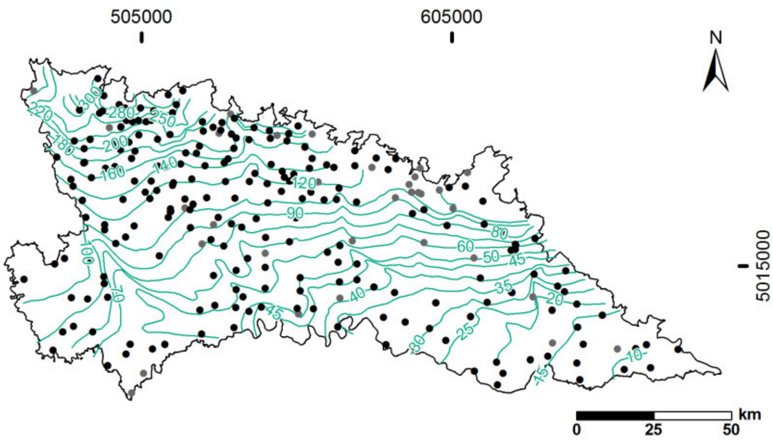


**Fig. 4.1 - Monitoring well network and piezometric levels of the shallow aquifer (*green lines*, expressed as m a.s.l.). *Black dots* represent the 221 wells used in the time-dependent analyses. *Black and grey dots* are the 249 wells selected for the not time-dependent analyses. Coordinates refer to WGS 1984 – UTM Zone 32N projection.**

The most impacted sector, in the period 2010 – 2012, is the northeastern part of the study area, where concentration exceed 50 mg/L, even if most of the whole northern sector shows values greater than the guide value of 25 mg/L (Fig. 4.2a). Nitrate concentration progressively decreases from north to south, where values are consistently lower than 10 mg/L, especially in the southeastern and southwestern areas. It is interesting to note how the southward inflexion of the isoconcentration curves located within the city of Milan represents a local anomaly within the spatial distribution of nitrate concentration in the surroundings. Another anomaly, greater than the previous one, is located in the middle of the plain, again as a southward inflexion of the isoconcentration curves and without any apparent relation with the groundwater flow or with the river network.

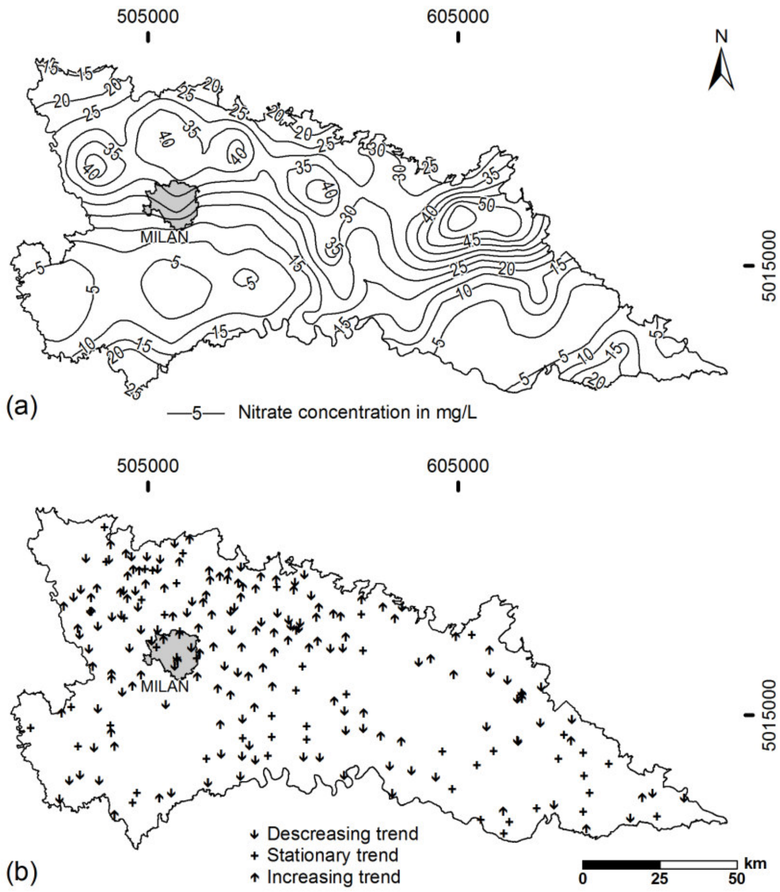


**Fig. 4.2 - (a) Nitrate distribution in the shallow aquifer. (b) Nitrate concentration trend in the monitoring wells. Coordinates refer to WGS 1984 – UTM Zone 32N projection.**

The change in nitrate concentration, in the period 2001 – 2011, is quantified by the slope of the regression line from an interpolation of concentration data. The slope defines the rate of nitrate concentration change in mg/L per day. Positive slope values show increasing concentration trends representing water quality deterioration, while non-positive slope values indicate steady or decreasing concentration trend characterizing unaffected or improved groundwater quality (Fig. 4.3).

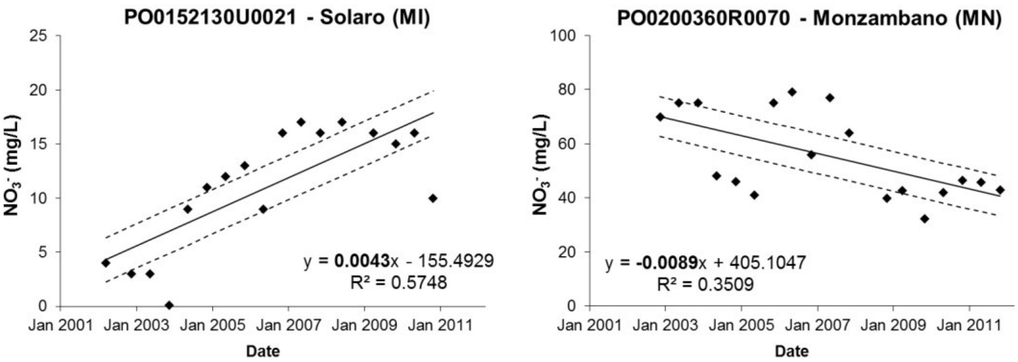


**Fig. 4.3 - Examples of monitoring wells showing an increasing (*left*) and a decreasing (*right*) trend in the period 2001 – 2011.**

Most of the wells showing an increasing concentration trend is located in the northern sector of the area, while wells with a decreasing or stationary trend are mainly located in the southern sector (Fig. 4.2b).

An even distribution of increasing, decreasing and stationary wells localized within the city of Milan shows the local and independent trend in nitrate concentration of each well.

## 4.2 Explanatory variables

Considering the conceptual hydrogeological model, eight explanatory variables have been considered as influencing groundwater vulnerability to nitrate contamination in the study area. These explanatory variables, representing both natural and anthropogenic factors, have been derived from multiple sources of information and are different in type, accuracy, and survey scale.
In order to be used in the WofE technique, as evidential themes, the explanatory variables have been converted in raster maps, with a pixel resolution of 100 m.

### 4.2.1 Natural variables

The natural factors, characterizing geological and hydrogeological conditions of the study area, considered in the study are: soil protective capacity, groundwater depth, groundwater velocity and hydraulic conductivity of the vadose zone.
Natural factors are considered to be steady for the purpose of the study in all the analyses (both not time-dependent and time-dependent analyses), with the exception of groundwater depth.

**Soil protective capacity** is obtained from existing data (Fig. 4.4). It was produced by the Agency of Services of Agriculture and Forest. This soil variable has been mapped at a 1:250,000 scale to assign soil in three protective capacity classes: high, moderate and low. Soil protective capacity is defined according to: hydraulic conductivity of the vadose zone, depth to water-table, grainsize and chemical properties (i.e., pH, CEC). The variable describes soil capacity to reduce water-soluble polluting substances leaching from the surface. It is related to filtering and buffering capacity because of both mechanical and biological/microbiological activities contributing to degradation (Masetti et al., 2007).

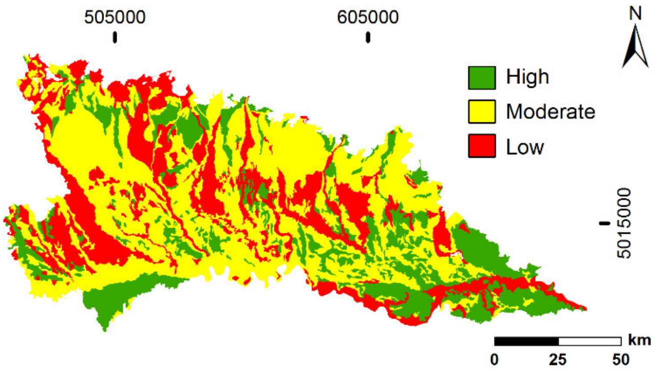


**Fig. 4.4 - Soil protective capacity map. Coordinates refer to WGS 1984 – UTM Zone 32N projection.**

Soils characterized by low protective capacity are located mainly in the northern sector of the plain, in the southwestern area, and in correspondence to local groundwater-fed streams or river valleys, where high permeability, gravel and sand or shallow groundwater are extensively present. Instead, where fine materials, with low permeability, are present, like in correspondence of fluvio-glacial terraces between Ticino and Adda rivers or in the southeastern sector of the plain, soil protective capacity is high.

The other three hydrogeological variables, characterizing the shallow unconfined aquifer, were obtained for this study.

**Groundwater depth** was derived from the difference between the topographic level and groundwater piezometric levels, related to two regional surveys in 2003 and 2014. In both surveys, groundwater depth decreases from north to south, ranging from values higher than 70 m to less than 2 m. At some local areas, there are groundwater-fed streams where groundwater depth is reduced to zero. Groundwater piezometric levels recorded in several wells of the network show that, while groundwater depth has a seasonal variability, it has not significantly changed over the Po Plain in the decade 2000 – 2010. With the beginning of 2010, in some sectors of the study area an increase of the piezometric levels occurred (Fig. 4.5a, c), while in other sectors the piezometric levels last steady (Fig. 4.5b, d). These evidences allow to use the piezometric levels map of the 2003-survey for the analyses related to the period 2000 – 2010, and to consider the piezometric levels map of the 2014-survey to provide estimates of the trend of groundwater depth until 2020, as described in Chapter 9, Paragraph 9.3.2.

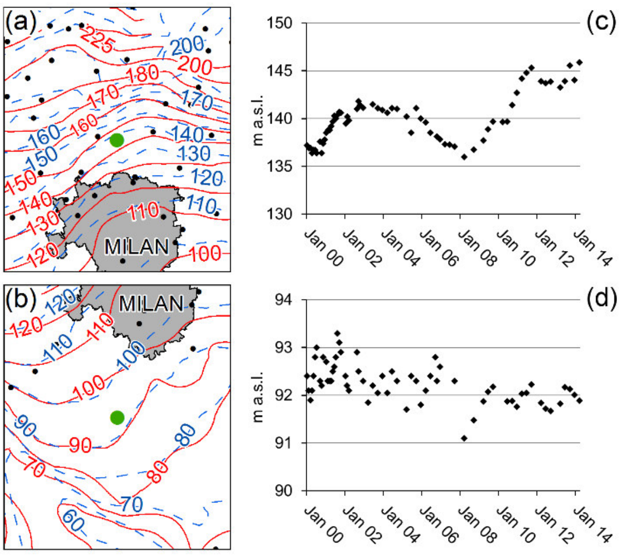


**Fig. 4.5 - (a, b) Piezometric levels (m a.s.l.) in 2003 (*dashed blue lines*) and in 2014 (*solid red lines*) and monitoring well network (*black dots*); extract of an area near the city of Milan. (c, d) Piezometric levels measured in two monitoring wells located in the northern (c) and in the southern (d) sector of the area, located as the *green dots* in maps (a) and (b).**

**Groundwater velocity** was estimated from 1263 wells where pumping tests were available to determine hydraulic conductivity (Fig. 4.6a). These values were used together with the local hydraulic gradient to obtain groundwater velocity. Field data were interpolated through the kriging methodology to obtain a map of the distribution of groundwater velocity. In the study area, groundwater velocity ranges from $4.7\times10^{-8}$ to $7.3\times10^{-5}$ m/s. Higher values are located in the northern sector and in some areas of the southwestern sector (Lomellina), while lower values are mainly found in the southeastern sector.

**Hydraulic conductivity** of the vadose zone was determined from 1597 well stratigraphy records (Fig. 4.6b). For each well, the hydraulic conductivity was calculated with the equivalent vertical permeability method (Anderson and Woessner, 1992), considering the thickness of the layers in the vadose zone in the calculation of the hydraulic conductivity. Data were then interpolated through kriging methodology to obtain the map of the distribution of hydraulic conductivity of the vadose zone in the study area. Hydraulic conductivity of the vadose zone ranges from $4.1 \times 10^{-8}$ to $4.0 \times 10^{-2}$ m/s. Higher values are located in the northern sector, especially along the belt of the heads of groundwater-fed streams and along the main rivers (Ticino and Adda rivers). Whereas, lower values are mainly located in the southern sector, along the Po River banks, which are mainly constituted by fine materials (clay, silt and sand), and in the southeastern sector of the plain.

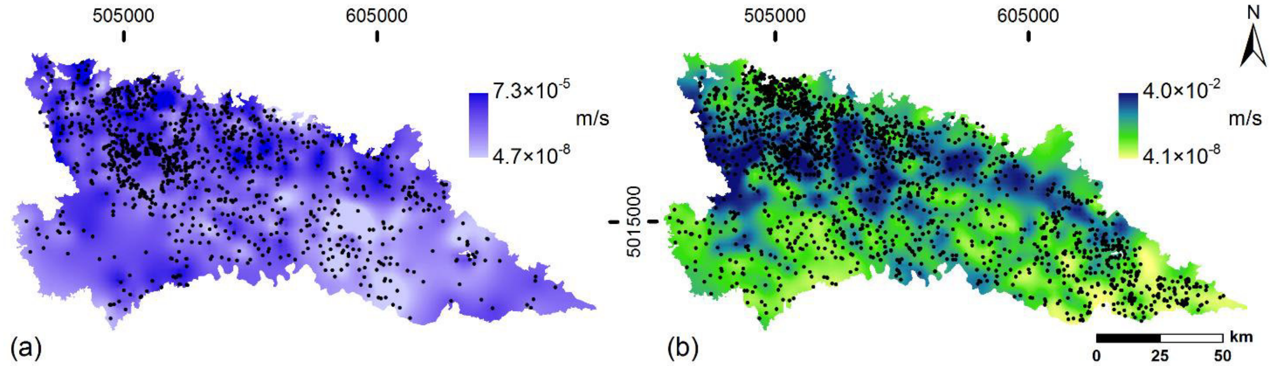


**Fig. 4.6 - a) Groundwater velocity map; (b) hydraulic conductivity of the vadose zone map. *Black dots* represent the locations of pumping test sites and well stratigraphies used to map the spatial distribution of groundwater velocity and hydraulic conductivity of the vadose zone, respectively. Coordinates refer to WGS 1984 – UTM Zone 32N projection.**

## 4.2.2 Anthropogenic variables

Anthropogenic sources of nitrate contamination are categorized in urban sources (presence of sewer leakages or septic tanks) and agricultural sources (fertilizers and manures).

Nitrogen loading derived from urban areas cannot be easily or directly estimated quantitatively. For this reason, it is necessary to explore other variables that can be used as a proxy. Three variables have been explored: population density, urban areas derived from land use / land cover maps or derived from radar satellite data. The last dataset is deeply described in Chapter 5.

**Population density** has been used often as a proxy for urban nitrate sources in groundwater vulnerability assessments (Nolan, 2001; Nolan et al., 2002; Masetti et al., 2009; Sorichetta et al., 2011). Population density is generally referred to administrative units at the specific time of the demographic census or survey. Official national censuses are usually done once every ten years. Consequently, analyses based on population census cover a period of ten years, missing changes in shorter periods.
In this study, population density in each district refers to two consecutive national censuses, in 2001 and 2011 (ISTAT 2001, 2011). Population density referred to 2011 have been used for the not time-

dependent analyses, while a population-density change have been calculated for the time-dependent analyses.

In 2011, population density in the plain area of the Lombardy Region varied in the range from 10 people/km², in rural areas, to 7619 people/km², which is the population density of the city of Milan (Fig. 4.7a). The most populated cities are located in the northwestern sector and close to the city of Milan, which is also the most industrialized sector of Lombardy Region. The southern sector is mainly occupied by agricultural fields, with small cities and scattered farms, characterized by low population densities, whereas only the main cities are enough populated.

The population-density change is calculated as the difference between population densities in each district referred to the two successive national censuses, in 2001 and 2011. Positive values indicate a growth of population, and negative values represent a reduction of population. Between 2001 and 2011, population density changed in the range from –402 to +845 people/km² across Lombardy (Fig. 4.7). Findings from this evaluation support the occurrence of the urban sprawl phenomenon in the Po Plain area, as reported by the European Environment Agency (EEA, 2006). In fact, the most populated cities at the beginning of 2000s have shown a reduction of population density, especially around the city of Milan, or a small increase in 10 years, but not compared with their extension (like Milan or Brescia). While other small cities, located far from the most urbanized area and close to the natural environments, have shown a strong increase in population density. These changes indicate a tendency of people to leave the over-crowded urban areas and reach the more open suburban areas with natural or agricultural surroundings (EEA, 2006).

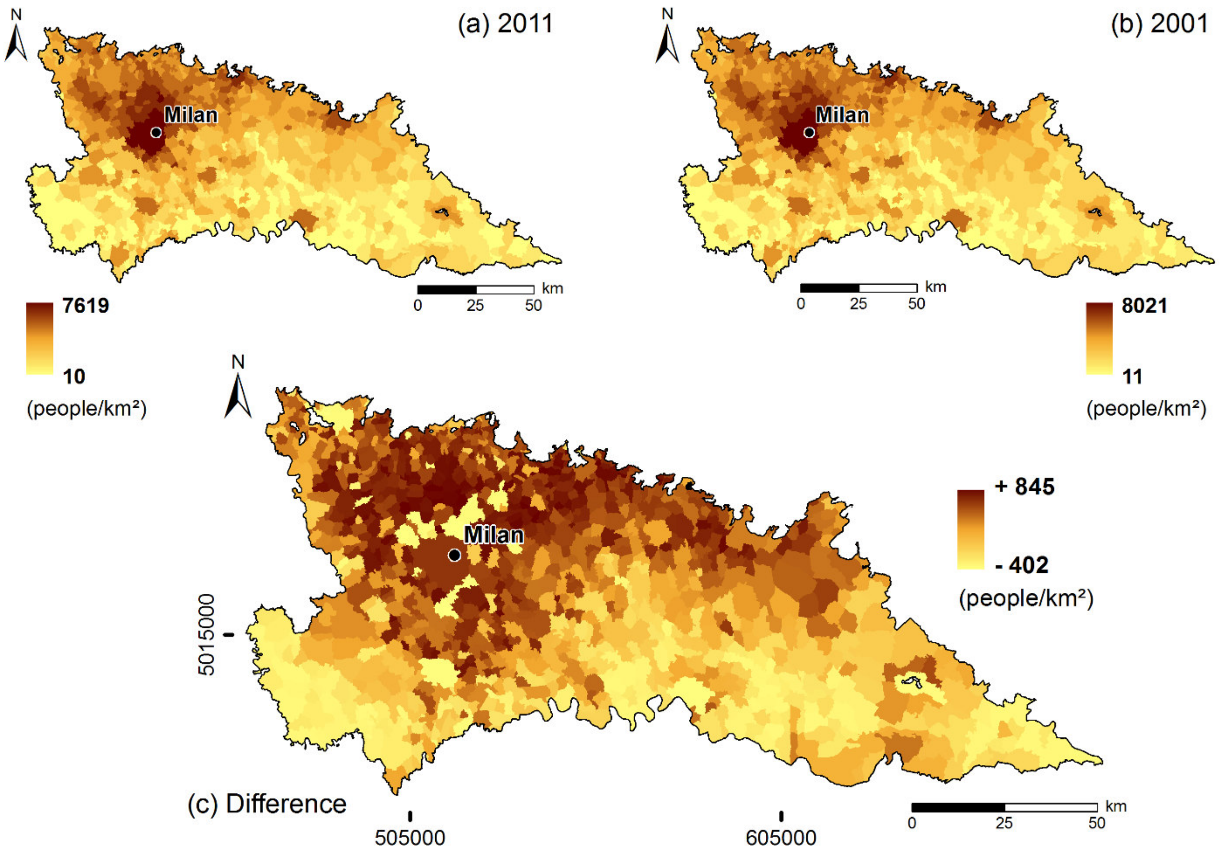


**Fig. 4.7 - Population density maps, at municipality level, in (a) 2011 and (b) 2001, and (c) the final map obtained as the difference between the two maps (a) and (b). Coordinates refer to WGS 1984 – UTM Zone 32N projection.**

High-resolution aerial images in Lombardy have been periodically acquired by the Agency of Services of Agriculture and Forest (ERSAF), creating a database called **DUSAF** (ERSAF, 2014), to identify and categorize the land cover in five main land use classes: urban areas, agricultural areas, woods and semi-natural environments, wetlands and surface water areas. The technical maps are at a 1:10,000 scale. DUSAF is updated at irregular intervals that can be different for different sectors of the region. This limitation does not allow the maps to represent the urban land use at the same time across the whole region.

DUSAF has been used only in the time-dependent analyses, to observe changes in urban extent. For this purpose, the five land use classes have been grouped in two relevant groups: urban areas, and non-urban areas consisting of the remaining four classes in DUSAF. The focal method (described in Chapter 5, Paragraph 5.2) has been applied on the binary variables related to two compilations, in 2000 and 2007/2009. Urban-extent changes are calculated as the percentage change of urban areas in each 1 km² pixel, between two successive compilations, in 2000 (DUSAF version 1.1) and in 2007/2009 (DUSAF versions 2.1 and 3.0), depending on the last available data in different sectors of the study area. Positive values indicate an expansion of urban areas, while negative values indicate a reduction of urban areas. According to DUSAF data, urban-area extent changed in the range from –6.7 % to +30.8 % (Fig. 4.8). Urban areas are mainly located in the northwestern sector and around the city of Milan, while the southern sector consists mainly of agricultural fields. Changes, as increases, in the extension of urban areas mostly occurred along the main roads, along the east-west and north-south transects.

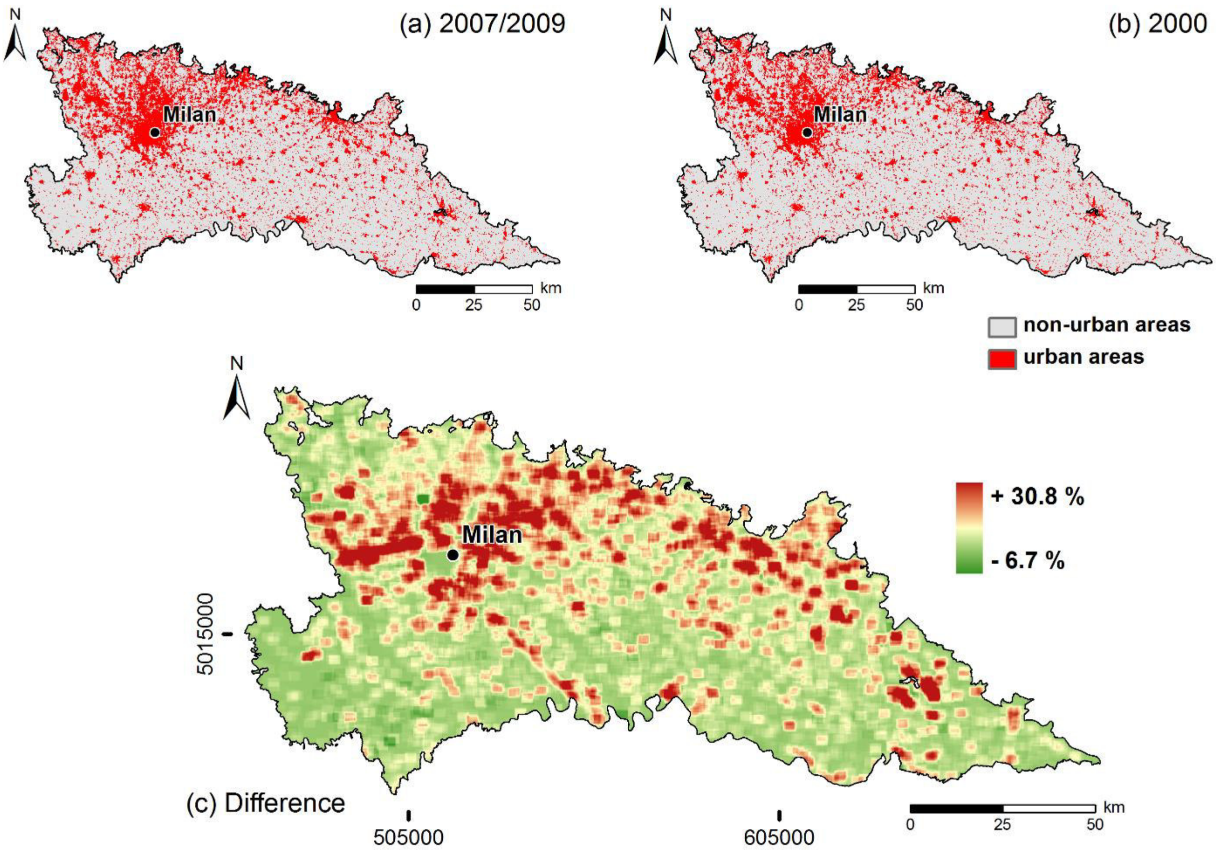


**Fig. 4.8 - DUSAF urban area extent maps in (a) 2007/2009 and (b) 2000, and (c) the final map obtained by calculating the percentage change of urban areas between the two maps (a–b) at a resolution of 1 km². Coordinates refer to WGS 1984 – UTM Zone 32 N projection.**

Nitrogen loadings, related to the use of **fertilizers and manures** in agricultural and breeding activities, are monitored by the Agency of Services of Agriculture and Forest, which controls the amount of fertilizers and manures sold to the farmers every year, in each district of the Region.
Nitrogen fertilizer (and manure) load referred to two surveys, in 2002 and 2010, in each district, has been used both in the not time-dependent and in the time-dependent analyses.
Nitrogen fertilizer load is expressed in kg/ha · year on a district basis, and correlated to the extension of agricultural areas in each district. In 2010, it varied in the range from 0 to 664.2 kg/ha · year (Fig. 4.9a).
The change of nitrogen fertilizer load is calculated as the difference between the amount of fertilizers (and manures) in each district referred to 2002 and 2010. Between 2002 and 2010, nitrogen fertilizer load, used in the plain area of Lombardy Region, changed in the range from –739.8 to +536.5 kg/ha · year (Fig. 4.9).
The distribution of nitrogen fertilizer load reflects the distribution of agricultural fields in Lombardy Region, with some differences among the various provinces, according to the kind of cultivation. The central and eastern sector are characterized by cornfields, while the southwestern sector is mainly constituted by rice fields.
The datasets are not complete and lack of some information. In fact, nitrogen fertilizer load was not available for all the districts in both the surveys. For this reason, those districts with missing data related to one survey, or both surveys, have not been considered in the analyses (white districts in Fig. 4.9).

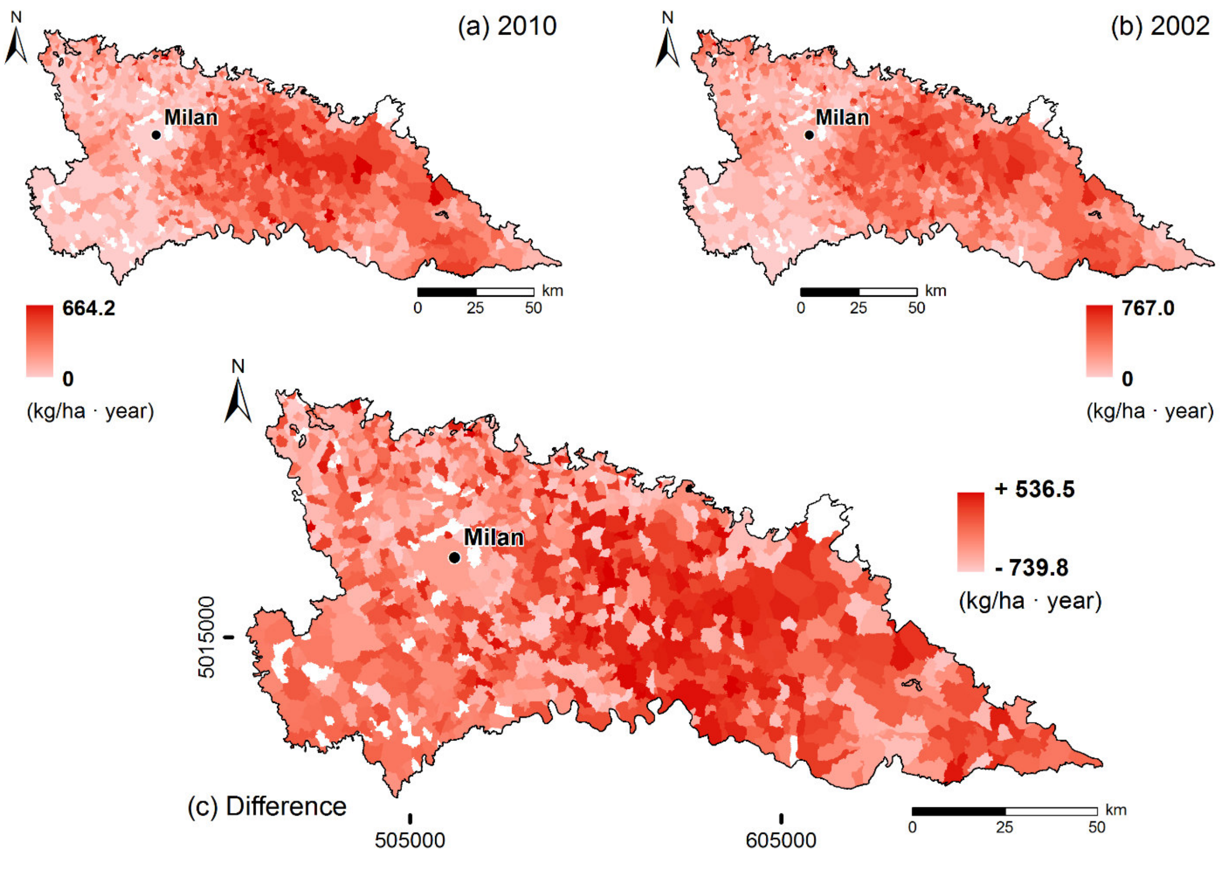


**Fig. 4.9 - Maps of nitrogen fertilizer load, at municipality level, in (a) 2010 and (b) 2002, and (c) the final map obtained as the difference between the two maps (a) and (b). Coordinates refer to WGS 1984 – UTM Zone 32N projection.**

## References

Anderson M., Woessner W., 1992. Applied Groundwater Modeling: Simulation of flow and advection transport. Academic Press, Inc.

EEA – European Environment Agency, 2006. Urban sprawl in Europe: The ignored challenge (EEA Report No. 10/2006). Office for Official Publications of the European Communities, Luxembourg, 56 pp., ISSN: 1725-9177

ERSAF - Ente Regionale per i Servizi all'Agricoltura e alle Foreste, 2014. DUSAF (Destinazione d'Uso dei Suoli Agricoli e forestali). http://www.cartografia.regione.lombardia.it/

Grath J., Scheidleder A., Uhlig S., Weber K., Kralik M., Keimel T., Gruber D., 2001. The EU Water Framework Directive: Statistical aspects of the identification of groundwater pollution trends, and aggregation of monitoring results. Final Report. Austrian Federal Ministry of Agriculture and Forestry, Environment and Water Management (Ref.: 41.046/01-IV1/00 and GZ 16 2500/2-I/6/00), European Commission (Grant Agreement Ref.: Subv 99/130794), in kind contributions by project partners. Vienna

ISTAT - Istituto di Statistica Applicata al Territorio, 2001. 14° General Population and Housing Census. http://dawinci.istat.it/

ISTAT - Istituto di Statistica Applicata al Territorio, 2011. 15° General Population and Housing Census. http://www.istat.it/

Masetti M., Poli S., Sterlacchini S., 2007. The Use of the weights-of-evidence modeling technique to estimate the vulnerability of groundwater to nitrate contamination. Natural Resources Research, vol. 16, n. 2, pp. 109-119, doi 10.1007/s11053-007-9045-6

Masetti M., Sterlacchini S., Ballabio C., Sorichetta A., Poli S., 2009. Influence of threshold value in the use of statistical methods for groundwater vulnerability assessment. Science of the Total Environment, vol. 407, n. 12, pp. 3836-3846, doi 10.1016/j.scitotenv.2009.01.055

Nolan B.T., 2001. Relating nitrogen sources and aquifer susceptibility to nitrate in shallow ground waters of the United States. Ground Water, vol. 39, n. 2, pp. 290-299

Nolan B.T., Hitt K.J., Ruddy B.C., 2002. Probability of nitrate contamination of recently recharged groundwaters in the conterminous United States. Environmental Science and Technology, vol. 36, n. 10, pp. 2138-2145, doi 10.1021/es0113854

Sorichetta A., Masetti M., Ballabio C., Sterlacchini S., Beretta G.P., 2011. Reliability of groundwater vulnerability maps obtained through statistical methods. Journal of Environmental Management, vol. 92, n. 4, pp. 1215-1224, doi 10.1016/j.jenvman.2010.12.009

# Chapter 5

# QuikSCAT-DSM

Radar satellite remote sensing data can be used to identify and delineate urban areas. In fact, satellite radar backscatter is dependent on the number, density, size and material of buildings (e.g., higher backscatter for more buildings, for larger and taller buildings, and for stronger materials like steel rather than wood). Crucially, the satellite global coverage with regular data acquisitions in time spanning over a decadal period allows continuous monitoring of urban changes, and thus enables the trend analysis together with changes in nitrate sources, capturing more detailed variability in annual, interannual, and decadal time scales. Such a satellite dataset has been collected by the SeaWinds scatterometer aboard the QuikSCAT satellite (QSCAT) in the decade of the 2000's. QSCAT backscatter measurement is accurate to 0.2 dB (3-σ) (Nghiem et al., 2004), which is equivalent to approximately 1.57% in root-mean-square error, enabling QSCAT to detect not only large and rapid changes as well as small and slow variations. Applied on the original QSCAT backscatter data, the Dense Sampling Method (DSM), based on a newly invented mathematical transform called Rosette Transform (Nghiem et al., 2009), is a breakthrough enabling quantitative measurements of urban parameters (i.e., location, shape, extent, and typology) to map land cover features at a posting pixel scale of 1 km², and to calculate the rate of urban change in the decadal period of 2000 – 2009 in every pixel across the world.

In DSM, backscatter signature of an area is characterized by the composition of a spatially-dependent mean part and a fluctuation part that is a function of location, azimuth angle (buildings are different on different sides; roads have preferential directions; hilly surfaces in a city, etc.), and any changes in time (vehicles and people move in a city; there can be rain, snow, hail, etc. at different times in different sections of a city). Thereby, DSM allows azimuthal and temporal changes to occur, and high-resolution results from DSM include information from both the mean value and the variability of backscatter at each location where the Rosette Transform is applied on an ensemble of backscatter data whose centroids are collocated in each unit area. At the expense of the daily temporal resolution, DSM is a breakthrough method to increase the spatial resolution in urban areas, where the inherent azimuth and motion changes invalidate the use of the traditional deconvolution method to enhance the resolution of satellite remote sensing data.

Moreover, advantages of QSCAT-DSM (Nghiem et al., 2009) include the delineation of urban and suburban contours both in metropolitan and rural areas, and the identification of urban development both fast and expansive or slow and restrained. Some limitations are due to complex mountainous topography, persistent snow cover on cold land at high latitudes (e.g., tundra and taiga), or extensive water surfaces, which affect backscatter signatures, but such factors are ineffective in the study area. The pointing accuracy of DSM was verified precisely with an accurate overlay of the Príncipe Island (Gulf of Guinea) on its true geographic location (Nghiem et al., 2009). DSM was validated and used to accurately delineate urban extent for a number of cities in different countries such as Dallas-Fort Worth and Phoenix in the United States, Bogotá in Colombia, Dhaka in Bangladesh, Guangzhou and Beijing in China, and Quito in Ecuador (Nghiem et al., 2009; Nghiem et al., 2014).

QSCAT-DSM is able to recognize and delineate urban areas and natural features even in a complex area such as the Italian peninsula (Fig. 5.1a).
The peculiar shape of the country is well defined by QSCAT-DSM. Coastal areas, with inlets, lagoons, promontories, and islands are recognizable (e.g., Aeolian Islands in south Tyrrhenian Sea, Fig. 5.1d). Water bodies are characterized by low backscatter values. However, only extended basins, like oceans, seas and lakes can be recognized, whereas rivers are not easily identifiable. In the mainland of Italy, only the major basins can be identified, like the Garda Lake in the Lombardy-Veneto Prealps (Fig. 5.1b) or the two volcanic lakes in Central Italy (Trasimeno and Bolsena Lakes). Moreover, the delineation of lakes in the Italian peninsula is difficult because they are surrounded by mountainous chains (Alps and Prealps in the northern sector, or Appennines along the peninsula).
The main cities can be recognized because of the high backscatter values respect to rural areas and natural environments. Some areas characterized by high values coincide not only with a main city but also with the surrounding suburbs, like the Milan area, the Florence Plain or the Naples area, which consist of different cities, with various extensions, located one next to each other, without any gap between the residential or industrial areas of these cities. Thus, these urban areas can be bigger than the city of Rome, which is the largest and most populated city in Italy (Fig. 5.1c).
As most of the main cities are located along the main roads and highways, this characteristic is well shown by QSCAT-DSM, like the main east-west highway in the north of Italy, which connects Venice, Milan and Turin in the Po Plain.

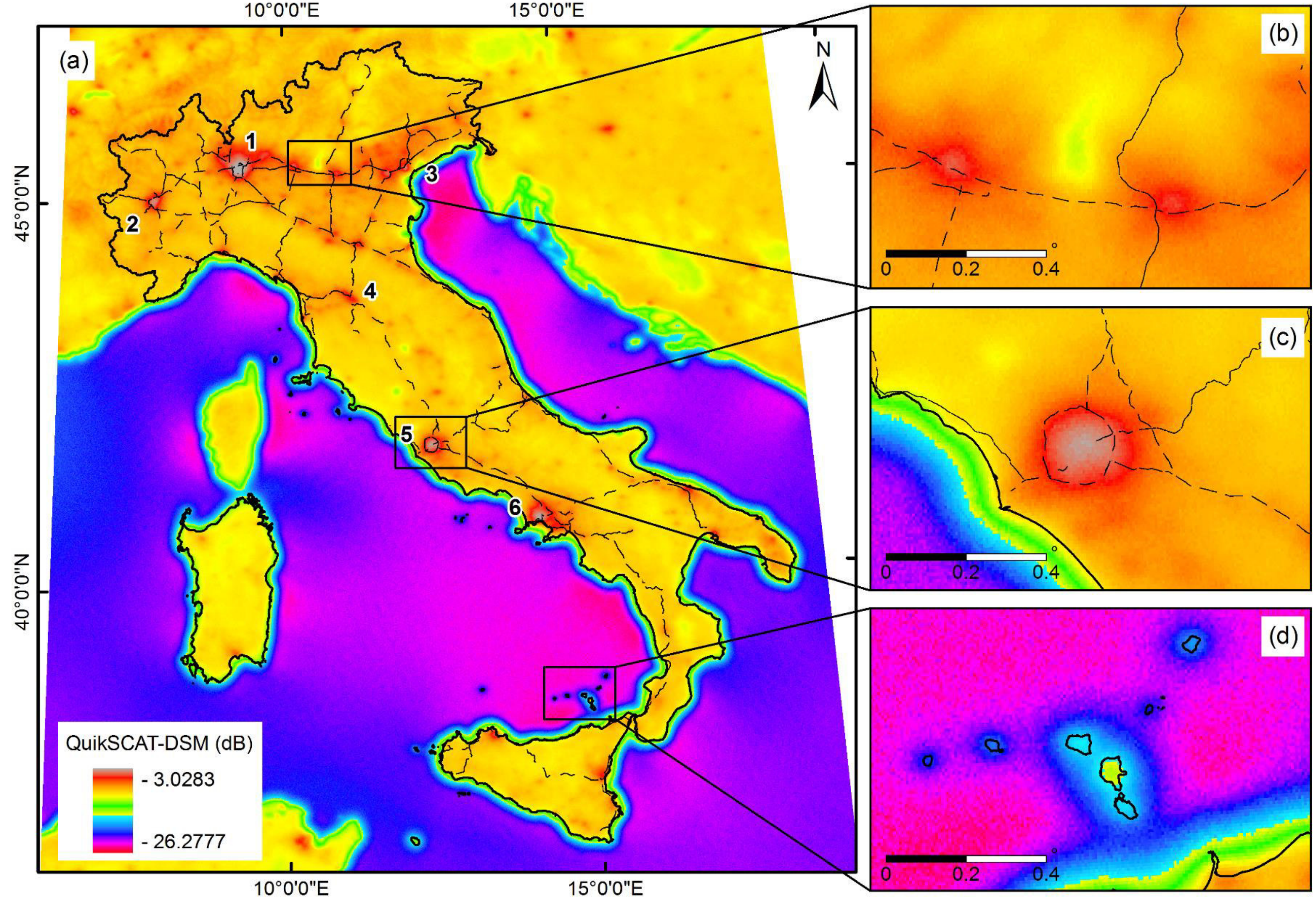


**Fig. 5.1 - (a) QSCAT-DSM backscatter map, at a posting of 1 km², averaged on ten years data, from 2000 to 2009. Numbers indicate the main cities (*red to grey areas*): 1 = Milan, 2 = Turin, 3 = Venice and Lagoon, 4 = Florence, 5 = Rome, 6 = Naples. (b) Lake of Garda (*green to yellow area* in the center) and Cities of Brescia (left) and Verona (right). (c) City of Rome and Tyrrhenian Sea. (d) Aeolian Islands (*yellow to blue areas*) in the Tyrrhenian Sea. *Black dashed lines* represent the main highways. Coordinates refer to GCS WGS 1984.**

## 5.1 Urbanization in Lombardy

The zoom on the Lombardy Region reveals details not recognizable at the country scale (Fig. 5.2). Natural environments and rural areas are represented by low to medium backscatter values. Among the natural environments, valleys and lakes can be distinguished from the mountains. The main and wide valleys in the northern sector can be easily identified because of the presence of various cities in the valley bottom, which involves higher backscatter values respect to the mountainous area. An example is Valtellina Valley (central Alps), which crosses the region along an east-west direction. The main lakes can be identified because of the low backscatter values due to the presence of water, like the Garda Lake in the east side of the Region. Some low values in mountainous areas are not explained by the presence of water bodies, but can be related to the kind of vegetation (e.g., broad-lived woods) or the altitude and slope of the mountains, like the south-west sector which corresponds to the Appennines chain or the mountainous area between Valcamonica Valley and Garda Lake in the east side. Glaciers and exposed rocks can influence the backscatter acquisition, which varies every year, as the shape of glaciers changes every season, whereas rocks have not a regular shape, thus the reflection of the signal is not consistent at each passage of the satellite. However, at a regional scale it is not possible to exactly distinguish different kinds of vegetation (e.g., broad-lived or conifer woods), different altitudes or slopes of the mountains, or glaciers and exposed rocks, but it is possible to identify a coarse relation between QSCAT-DSM values and these natural features.

The plain area of Lombardy region can be divided in two sectors: the northern and the southern sector. The northern sector is characterized by medium to high backscatter values, because of the presence of an extended urban area, where residential buildings and industries are located, around the city of Milan or along the main roads and highways.

The city of Milan, like any European city, is very different respect to U.S. cities or other mega-cities, like Beijing. In fact, the structure of the latter cities shows: (a) a central core with skyscrapers and commercial buildings, mainly made of steel, (b) a ring of small residential and commercial buildings, mainly made of concrete or wood, around the central core, and (c) rural or natural environments which surround the city. This structure is translated in QSCAT-DSM acquisition as very high, medium and low backscatter values, with clear transitions between the sectors (Nghiem et al., 2009). Instead, the center of the city of Milan is mainly constituted of buildings made of concrete and natural stones, while new skyscrapers made of steel, located in the central-north area of the city, have been built after 2009. Buildings, both residential and commercial, within the city have approximately the same height, with few differences in their heights and not related with the distance to the city core. Thus, it is not possible to recognize the city center within the city. Anyway, it is possible to distinguish the entire city of Milan among the other urban areas and main cities of the region, because of the conspicuous difference between backscattered values acquired over Milan and over the other cities. These cities, like Monza or Brescia, are less extended respect to Milan and characterized by smaller buildings, mainly made of concrete or covered by natural stones.

The southern sector is characterized by low to medium backscatter values, because of extended agricultural fields and scattered towns, which are not distinguishable. Thus, only the main cities, like Cremona and Mantua can be easily identified, as the backscatter values are higher respect to the surrounding rural area.

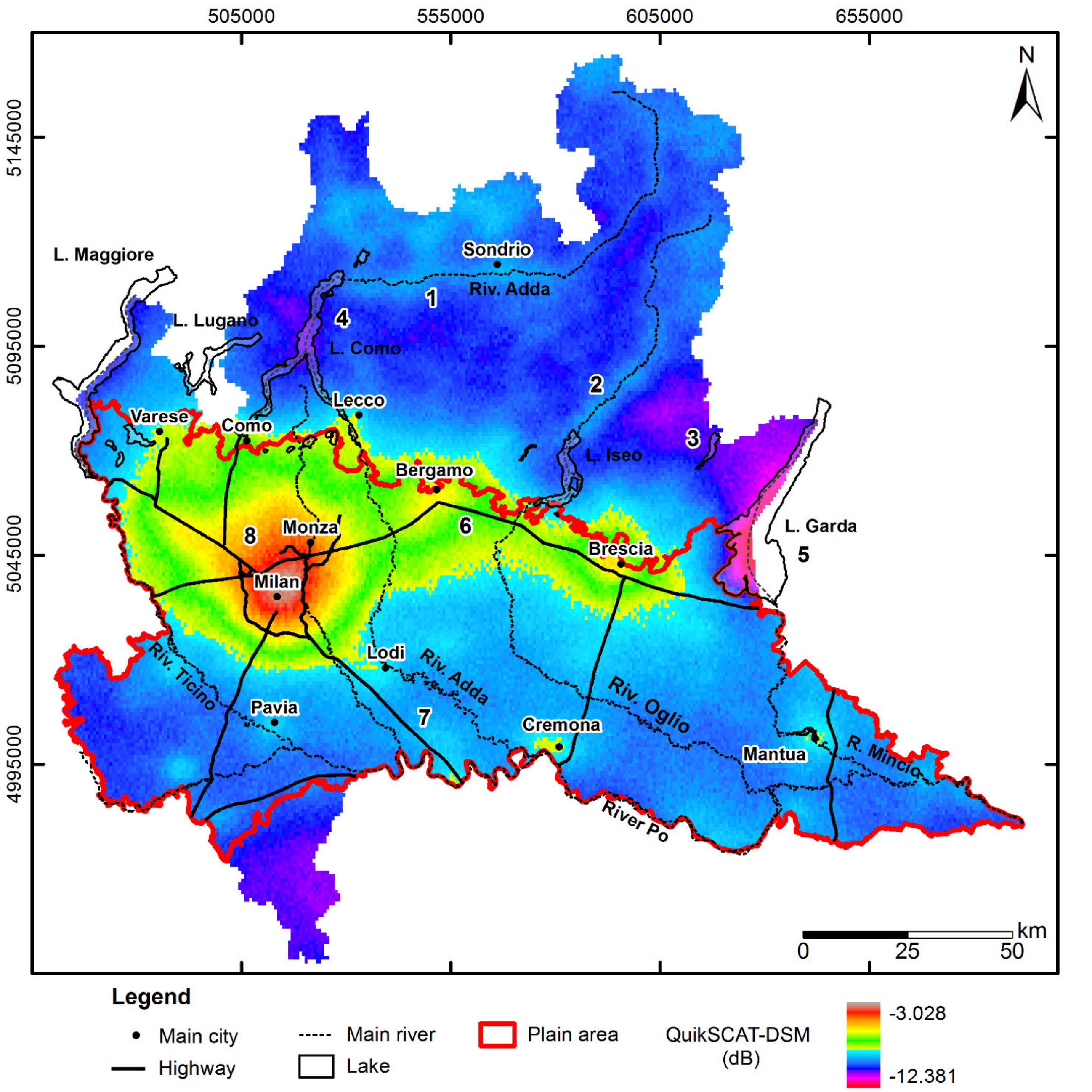


**Fig. 5.2 - QSCAT-DSM backscatter map, at a posting of 1 km², averaged on ten years data, from 2000 to 2009. 1, 2 and 3 = Valleys (Valtellina, Valcamonica, Val Sabbia), 4 and 5 = Main lakes (L. Como and L. Garda), 6 and 7 = Main highways, 8 = Milan area (*from yellow to grey*). Coordinates refer to WGS 1984 – UTM Zone 32N projection.**

QSCAT-DSM data obtained for each year in 2000 – 2009 show the expansion of urban areas in the northern sector of the plain area of Lombardy Region (Fig. 5.3). The highest backscatter values correspond to the city of Milan, which shows an increase of backscatter values from –3.43 dB in 2000 to –2.53 dB in 2009, being the main city of the region (red and grey areas). Urban areas have expanded northward and eastward, creating a unique urban area, without any spatial gap represented by rural areas (green to yellow areas). These connections have been developed along the main roads and highways.

Low to medium backscatter values represent rural areas with agricultural fields (mainly cornfields, as blue areas) and urban areas (light blue areas). While very low values represent humid areas close to lakes and rice fields, which are periodically flooded during the growth season (violet areas).

The rate of land cover change, including both urban and rural areas, is determined by the slope of the linear regression with QSCAT-DSM data obtained for each year in 2000 – 2009, expressed in decibel per year (dB/year). Positive slope values represent increasing or growth of urban areas (yellow to red areas), while non-positive and shallow slope values indicate steady rural areas or natural environments (blue to yellow areas). In the plain area of Lombardy Region, QSCAT-DSM slope varies within the range of −0.0699 to +0.1268 dB/year, or equivalently −16.0 to +29.6 %/decade (Fig. 5.3), as the slope in dB/year can be converted to the 10-year percentage change given by 10 times of $100\times(10^{\mathrm{dB/year}/10} - 1)$.

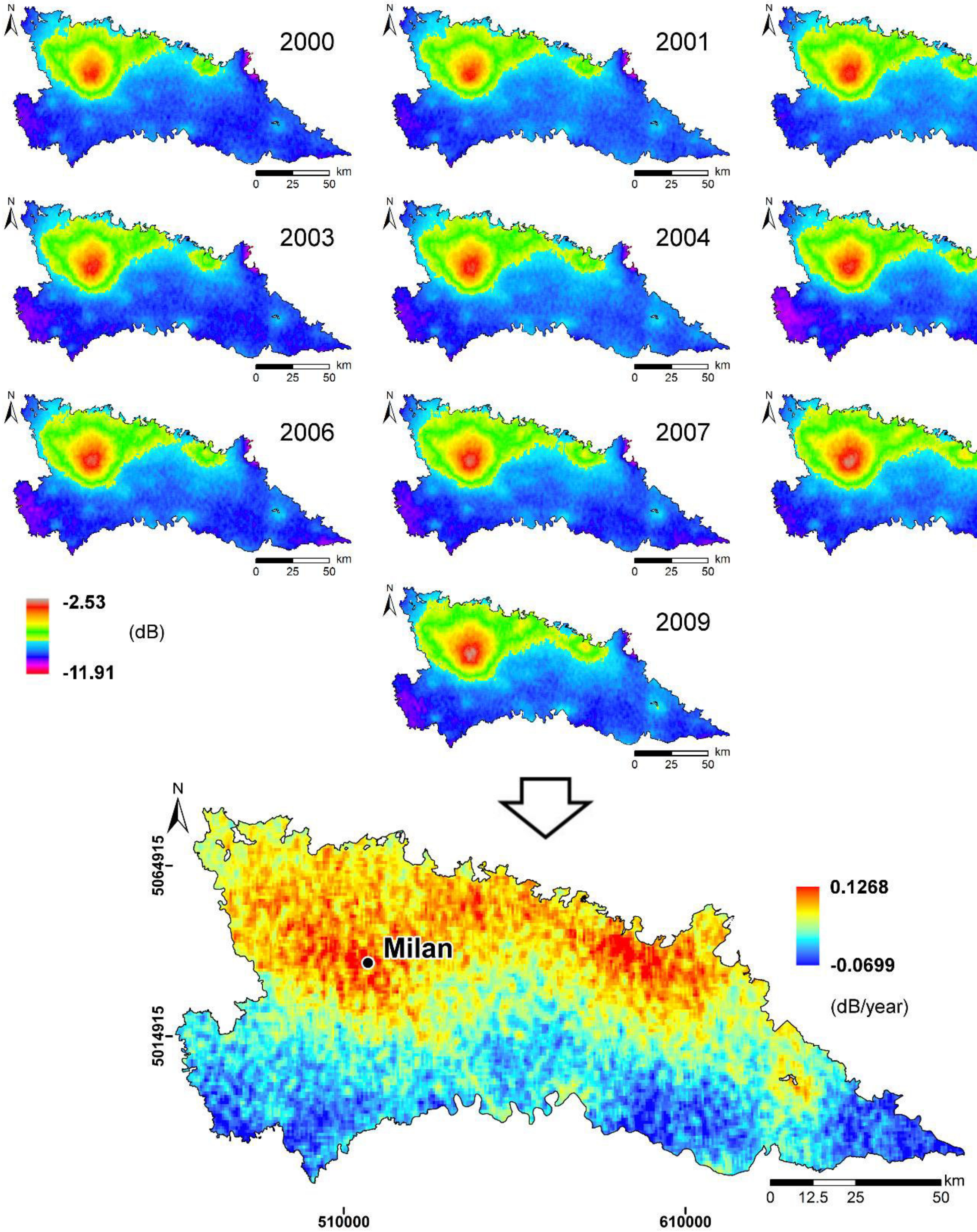


**Fig. 5.3 - QSCAT-DSM backscatter maps, at a posting of 1 km², from 2000 to 2009, and the final map of the linear regression slope. Coordinates refer to WGS 1984 – UTM Zone 32N projection.**

## 5.2 Application of QuikSCAT-DSM on groundwater issue

In this study's approach to assess impacts on groundwater contamination, the focal method is adapted particularly for applications to QSCAT-DSM and hydrogeological data. The algorithm in the focal method considers both the value of each cell and the values of the surrounding cells with a deterministic mathematic function (e.g., arithmetic mean). It can account for groundwater flow direction: among the surrounding cells of each cell, only the cells located upstream are considered in the calculation. The extent of the area of calculation is 9 km² for a 3×3 window above each pixel of 1 km² (Fig. 5.4).

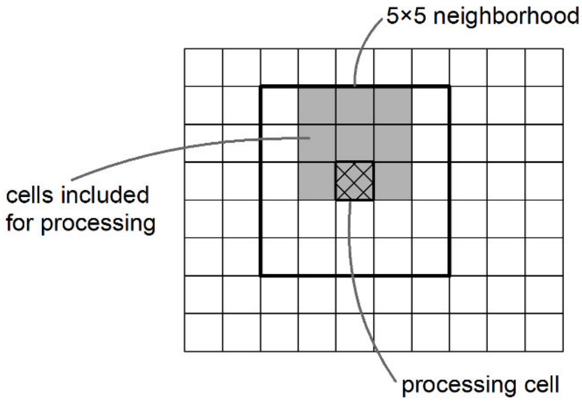


**Fig. 5.4 - Focal method.**

QSCAT-DSM data have been used both in the time-dependent and in the non-time dependent analyses. The comparison of QSCAT-DSM data with the other two proxies representing urban nitrate sources of contamination (population density and land use derived from aerial images) allows to evaluate its reliability in groundwater vulnerability assessments.

## References

Nghiem S.V., Leshkevich G.A., Stiles B.W., 2004. Wind fields over the Great Lakes measured by the SeaWinds Scatterometer on the QuikSCAT Satellite. Journal of Great Lakes Research, vol. 30, n. 1, pp. 148-165

Nghiem S.V., Balk D., Rodriguez E., Neumann G., Sorichetta A., Small C., Elvidge C.D., 2009. Observations of urban and suburban environments with global satellite scatterometer data. ISPRS – Journal of Photogrammetry and Remote Sensing, vol. 64, n. 4, pp. 367-380, doi 10.1016/j.isprsjprs.2009.01.004

Nghiem S.V., Sorichetta A., Elvidge C.D., Small C., Balk D., Deichmann U., Neumann G., 2014. Remote Sensing of Urban Environments – The Beijing Case Study. In: Njoku E (ed.), Encyclopedia of Remote Sensing, pp. 869-878, ISBN 978-0-387-36698-2, Springer, Heidelberg, Germany

# Chapter 6

# Groundwater vulnerability assessments

Groundwater vulnerability studies are crucial to understand the cause-effect relationship between groundwater quality and both natural and anthropogenic factors to develop effective groundwater protection plans. Mapping areas where groundwater is most vulnerable to contamination and identifying primary factors influencing the contamination level are imperative to manage and protect groundwater and thus human health.

Groundwater vulnerability is commonly treated as a static property (NRC, 1993). Groundwater vulnerability maps refer to a specific time in a given area (Vrba and Zaporozec, 1994). However, groundwater vulnerability maps are time dependent, requiring updating to portray changes in a groundwater system and in the location and nature of human impacts (Vrba and Zaporozec, 1994).

This study aims to develop a time-dependent method to assess groundwater vulnerability, which could take into account both the current groundwater quality status and its changes, and to predict the impacts of human activities on groundwater resources in the future.

The proposed time-dependent approach is shown, in a simplified version, in Fig. 6.1. Each model has been developed using the Weights of Evidence technique. The spatial model considers the status of nitrate contamination and nitrate anthropogenic sources at a generic time $t_1$. The spatial model is described in Chapter 7, considering the status in 2011. The temporal model takes into account the evolution of nitrate contamination and nitrate anthropogenic sources in the period between $t_0$ and $t_1$. The temporal model is described in Chapter 8, considering the period 2000 – 2011. The spatio-temporal model considers both the status and the evolution of nitrate contamination and nitrate anthropogenic sources, at a generic time $t_1$ and between $t_0$ and $t_1$, respectively. The predictive spatio-temporal model considers both the status and the evolution of nitrate contamination and nitrate anthropogenic sources, referred to a hypothetical condition at time $t_2$, under the hypothesis of a given evolution between $t_1$ and $t_2$. The spatio-temporal and predictive spatio-temporal models are described in Chapter 9. The former considers the status at 2011, together with the evolution in the period 2000 – 2011. The latter considers a hypothetical evolution from 2011 to 2020 and the calculated status at 2020.

The complete procedure of the proposed time-dependent approach, described in Chapter 9, includes the comparison between the outputs at time $t_1$ and $t_2$, which is necessary to understand the differences in the impacts of nitrate anthropogenic sources on groundwater quality, between the current and the future (hypothetical) condition.

The proposed time-dependent approach would answer to the requirements of the European Union on the identification of areas where groundwater is or will be potentially affected by nitrate contamination and suffers significant and sustained upward trends in the concentration of contaminants.

The outcomes of the time-dependent approach are groundwater vulnerability maps to nitrate contamination, which consider both the natural and anthropogenic factors that can influence nitrate distribution in groundwater.

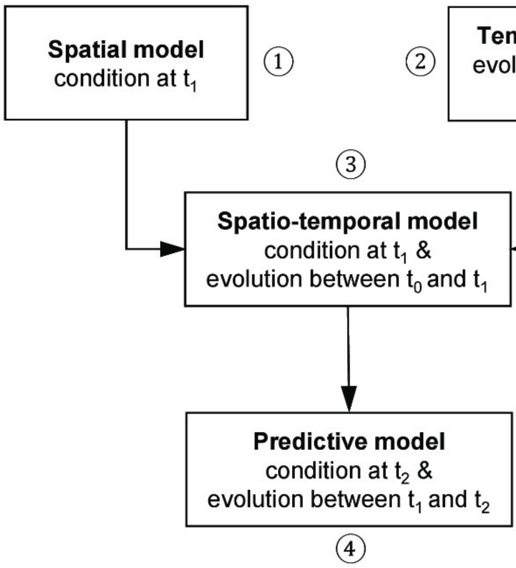


**Fig. 6.1 - Simplified proposed time-dependent approach.**

# References

NRC - National Research Council, 1993. Ground water vulnerability assessment: Predictive relative contamination potential under conditions of uncertainty. National Academy Press, Washington DC, ISBN: 978-0-309-04799-9

Vrba J., Zaporozec A., 1994. Guidebook on mapping groundwater vulnerability. International Association of Hydrogeologists, International Contributions to Hydrogeology, Publication No. 16. Verlag Heinz Heise, Hannover

# Chapter 7

# Definition of the vulnerable zones to nitrate contamination

## 7.1 Introduction

The European Community has identified the Po Plain area as a nitrate vulnerable zone, as a result of the implementation of EU Nitrate Directive (91/676/EEC), which aimed to prevent and reduce nitrate water pollution from agricultural sources. Nitrate occurs naturally from mineral sources and animal wastes, and anthropogenically as a by-product of agriculture activities and urban wastes (Madison and Burnett, 1985).

Determining areas where groundwater is at risk of nitrate contamination and which factors mainly influence nitrate presence in groundwater represents an important step in managing and protecting groundwater and, thus, human health (Masetti et al., 2008).

In this Chapter, both natural and anthropogenic factors influencing the occurrence of high nitrate concentration in groundwater have been considered and analyzed. Among natural factors, soil protective capacity, groundwater depth, groundwater velocity and hydraulic conductivity of the vadose zone have been selected. Nitrogen fertilizer loading was selected to represent agriculture nitrate sources. Since nitrogen loading derived from urban areas cannot be easily or directly estimated quantitatively, other variables have to be chosen as a proxy. In this Chapter, two variables have been selected and compared: population density and urban areas derived from radar satellite data.

Nitrogen fertilizer loading and population density are both mapped using municipality boundaries as territorial unit. Radar backscatter can identify and map urban extent and surface features at a posting scale of about 1 km². Data have been acquired by the SeaWinds scatterometer aboard the QuikSCAT satellite, with a footprint of about 25 km in azimuth by 37 km in range, on which the Dense Sampling Method has been applied to improve the resolution at 1 km² (QSCAT-DSM; Nghiem et al., 2009).

Recent studies (Masetti et al., 2008, 2009; Sorichetta et al., 2011, 2013) have shown that, in some areas of the Po Plain, nitrate occurrence in groundwater is strongly related to urban sources (using population density as a proxy) more than to agricultural activities. Moreover, the Weights of Evidence (WofE) technique have allowed to combine the different factors, both natural and anthropogenic factors, and to observe their combined influence in predicting nitrate occurrence in groundwater (and characterizing groundwater vulnerability).

In this Chapter, a groundwater vulnerability assessment, using the WofE technique, over the Po Plain area of Lombardy Region (Chapter 2, Paragraph 2.1) is performed. The reliability and usefulness of QSCAT-DSM in groundwater vulnerability assessments is tested through the comparison with population density, usually used as a proxy to represent urban nitrate sources.

## 7.2 Response variable and evidential themes

The response variable is represented by nitrate concentration in groundwater, measured from the 249 wells monitoring the shallow aquifer, in the period 2010 – 2012, with a minimum of two samples over the three years (Chapter 4, Paragraph 4.1). The average nitrate concentration in each well, over the period 2010 – 2012, has been calculated and used in the analysis.

The frequency histogram of nitrate concentrations shows a bimodal (left-skewed) distribution with a main relative peak at about 40 mg/L and a minor peak at about 1.25 mg/L (Fig. 7.1a). A statistical technique, already applied by Masetti et al. (2009) on groundwater issue, has been used to determine the threshold value, which separates the population in two subsets, as the WofE modelling technique requires a binary formulation of the response variable. The use of cumulative probability plots allows to distinguish two or more populations within the dataset of nitrate concentration in groundwater, and the inflection points are defined as threshold values (Panno et al., 2006). The value of 16 mg/L, which identifies the change of slope of the cumulative curve and divides the two populations, has been selected as an appropriate threshold to be used in the analyses (Fig. 7.1b).

Wells showing a nitrate concentration higher than 16 mg/L are considered "impacted" wells (152), and those below the threshold value as "non-impacted" wells (97). The "impacted" wells represent the training set, and they have been selected to be used in the analysis. While "non-impacted" wells represent the control set.

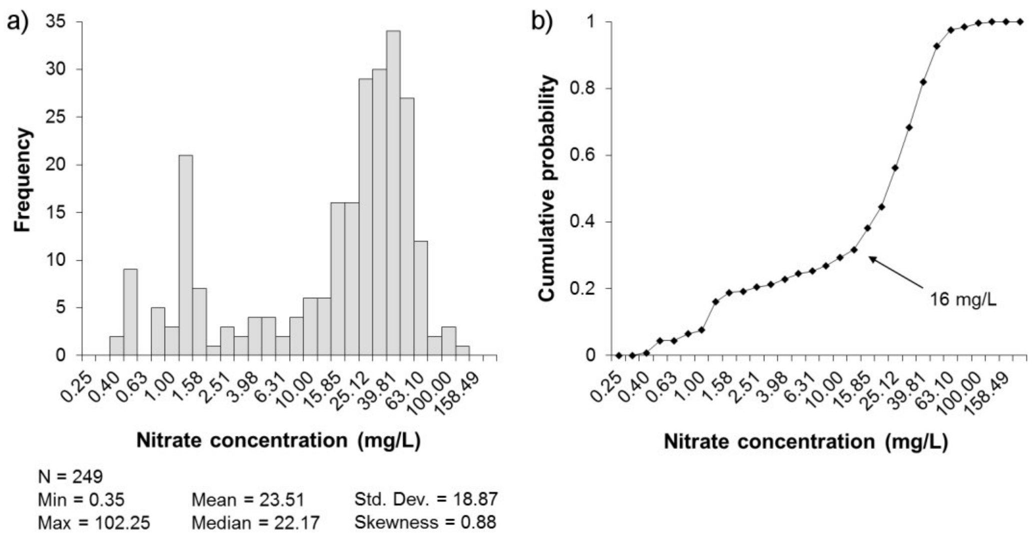


**Fig. 7.1 - Frequency histogram (a) and cumulative probability graph (b) of nitrate concentration.**

From the hydrogeological conceptual model, seven explanatory variables (described in Chapter 4, Paragraph 4.2, and Chapter 5), were considered for being used as evidential themes in the analysis (Table 7.1). The variables representing urban sources of nitrate contamination have been evaluated separately and the obtained groundwater vulnerability maps have been compared.

**Table 7.1 - Explanatory variables used as evidential themes.**

| Explanatory variable | Type | Range |
|---|---|---|
| Population density [2011] (people/km²) | Continuous | 11 ÷ 8021 |
| QuikSCAT-DSM [2009] (dB) | Continuous | –11.47 ÷ –2.53 |
| Nitrogen fertilizer load [2010] (kg/ha/year) | Continuous | 0 ÷ 664 |
| Soil protective capacity | Categorical | Low, Moderate, High |
| Groundwater depth [2003] (m) | Continuous | 0 ÷ 70 |
| Groundwater velocity (m/s) | Continuous | $4.7\times10^{-8} \div 7.3\times10^{-5}$ |
| Hydraulic conductivity of the vadose zone (m/s) | Continuous | $4.1\times10^{-8} \div 4.0\times10^{-2}$ |

## 7.3 Results and discussion

### 7.3.1 Contrasts of the generalized evidential themes

The contrasts of statistically significant evidential themes enable an assessment of the influence of the variables under consideration on groundwater contamination. Contrast values, both for anthropogenic and natural factors, are presented in Fig. 7.2 and Fig. 7.3. Positive contrast values mean a direct relationship (or, a positive correlation) between the presence of the class and the training points, whereas negative contrast values mean an inverse relationship (or, a negative correlation) and values close to zero a general low correlation.

The process of generalization of evidential themes has been performed following the objective (semi-guided) procedure developed by Sorichetta et al. (2012), which guarantees the achievement of the maximum number of statistical significant classes for each evidential theme.

Soil protective capacity shows an inverse relationship between high-protected areas and high nitrate concentrations. The low protective class shows an anomalous negative contrast, but with an absolute value close to zero, which indicates a poor influence in the process of propagation of nitrates. Groundwater depth reveals that large values of water-table depth are positively related to high concentrations, while low values (close to surface or less than 10 m) are negatively associated. Groundwater velocity and hydraulic conductivity of the vadose zone show positive correlations with high nitrate concentrations and the threshold values are about $1.8\times10^{-6}$ m/s and $3.9\times10^{-6}$ m/s, respectively.

The two variables, representing urban nitrate sources, show a direct relation between the extension of urban areas, or population density, and the occurrence of high nitrate concentration values in groundwater. Threshold values, corresponding to the transition from negative to positive contrasts, are 346 people/km² and –8.0051 dB, respectively for population density and QSCAT-DSM. Observed from these variables, classes with positive contrast values are clustered in the northwestern sector, especially around the cities of Milan, Bergamo and Brescia, while classes with negative contrast values are mainly in the southern sector.

The evidential theme, representing agricultural nitrate sources, shows an inverse relation between nitrogen fertilizer load and high nitrate concentrations, which disagrees with the expectations. But, contrast values are close to zero, meaning a general low correlation with the presence of high nitrate concentrations in groundwater.

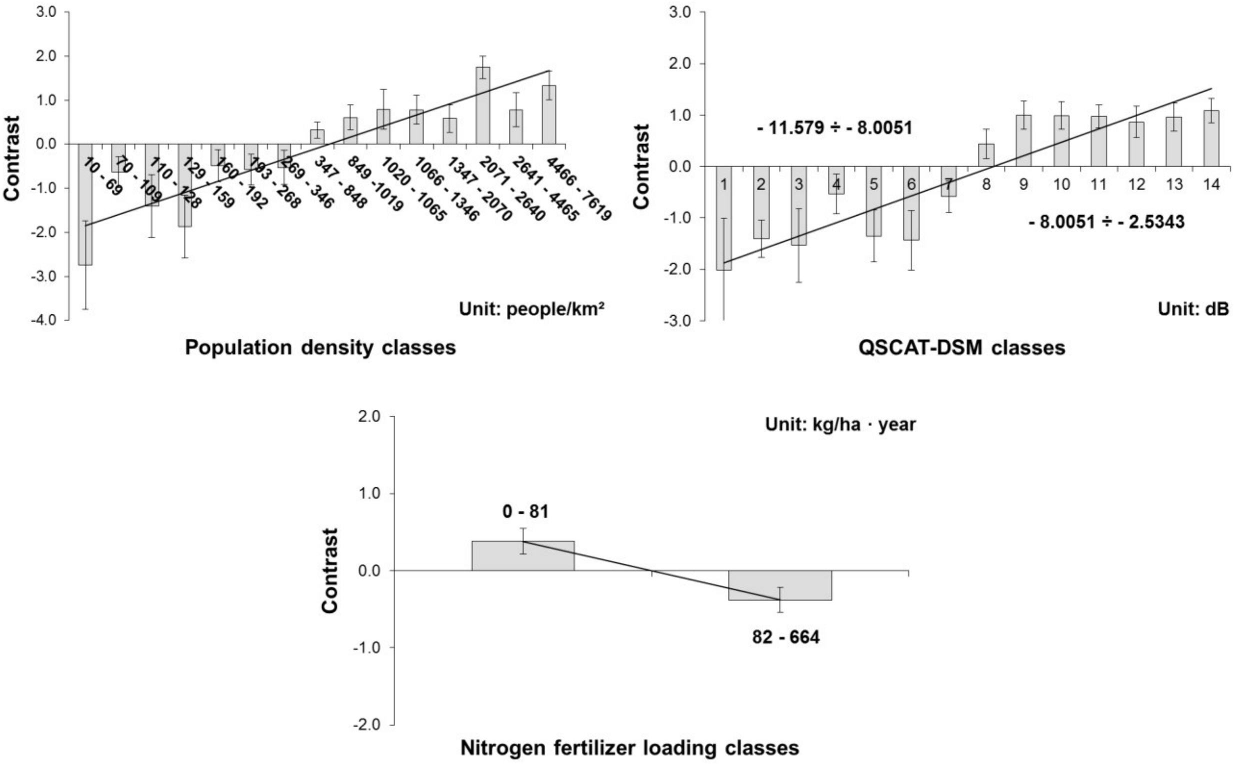


**Fig. 7.2 - Contrasts and error bars of the statistically significant classes of anthropogenic evidential themes used to generate the maps in Fig. 7.4.**

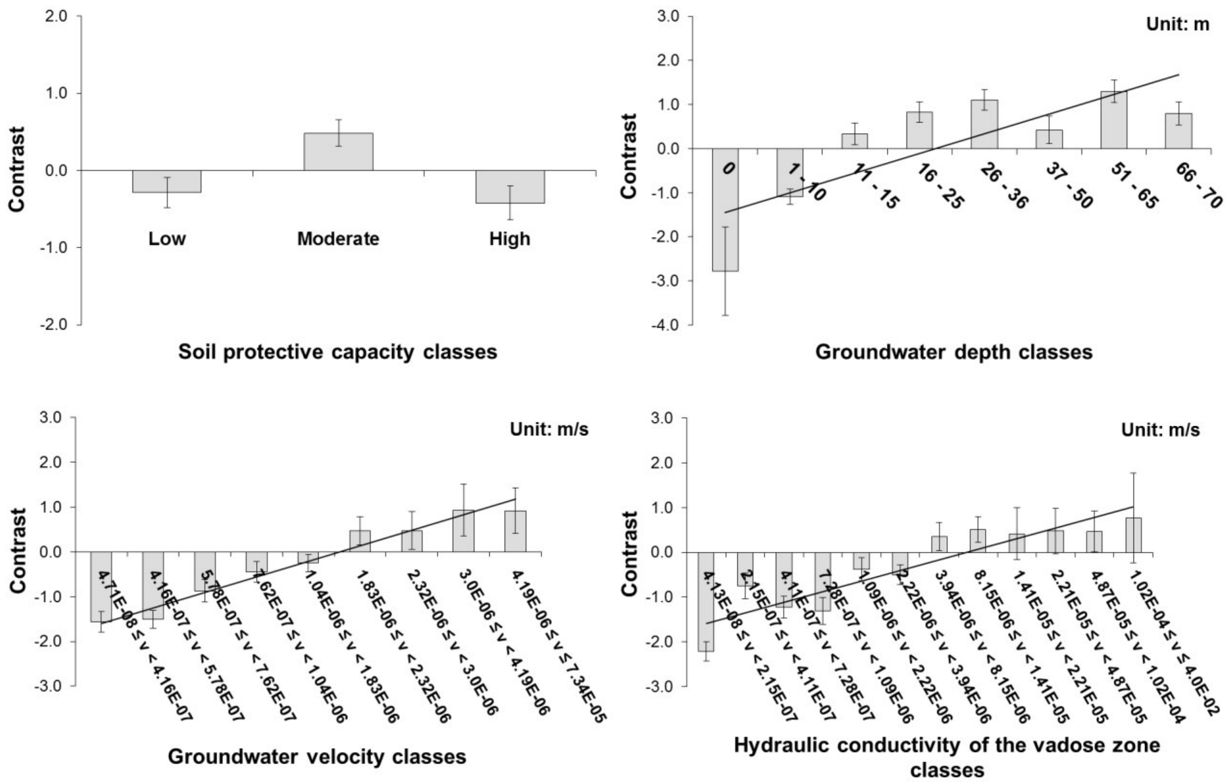


**Fig. 7.3 - Contrasts and error bars of the statistically significant classes of natural evidential themes used to generate the maps in Fig. 7.4.**

### 7.3.2 Response theme

Based on the results obtained through the generalization of evidential themes, three different kind of variables can be distinguished:
1) variables that are not statistically significant. These variables have not to be used for generating the response themes;
2) variables that are significant both from a statistical and a physical point of view, meaning that the relation between the variable and the training points is coherent with the physical processes that influence groundwater contamination. These variables can be used for generating the groundwater vulnerability maps;
3) variables that are significant from a statistical point of view but not from a physical point of view, meaning that the relation between the variable and the training points is not coherent with the physical processes. It is preferable not to use these variables for producing the vulnerability maps.

In this Chapter, two response themes were obtained and compared (Fig. 7.4). Each response theme considers one of the two urban variables, and the evidential themes representing the associated natural factors (Table 7.2). Despite the anomaly in the low class of soil protective capacity, this variable has been used for generating the response themes. On the other hand, the evidential theme representing agricultural sources has not been used, because the relation between the variable and the training points is not coherent with the distribution of nitrate contamination in groundwater.
Each response theme was categorized so that each vulnerability class in the corresponding map contains approximately the same number of different posterior probability values according to the geometric interval method (Sorichetta et al., 2011). Five classes were identified with the degree of groundwater vulnerability increasing from 1 to 5.

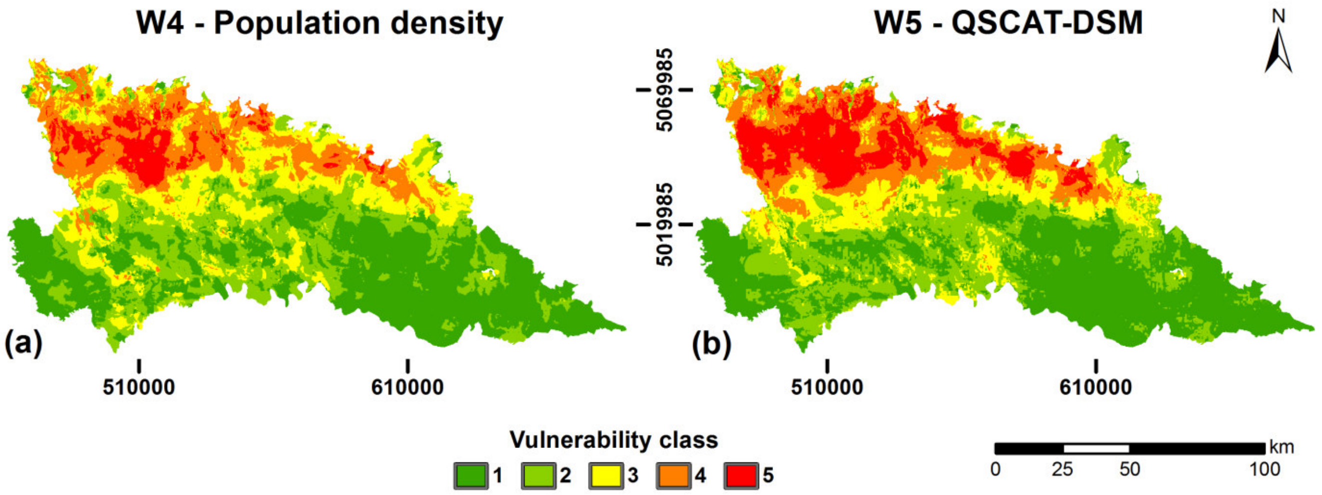


**Fig. 7.4 - Vulnerability maps obtained using natural factors, with (a) population density, and (b) QSCAT-DSM, as representing urban nitrate sources. Coordinates refer to WGS 1984 – UTM Zone 32N projection.**

### 7.3.3 Validations

The general quality of each response theme (i.e., post probability map) can be evaluated with the area-under-the-curve (AUC) value or by the success rate curve (SRC) method (Chung and Fabbri, 1999). SRC is performed by plotting on the X-axis the cumulative percentage of vulnerable areas (from the highest probability values to the lowest) and, on the Y-axis, the cumulative percentage of occurrences being in the training set. According, the steeper is the curve, the better is the capability of the model to adequately describe the groundwater vulnerability of the study area (Sorichetta et al., 2011). SRCs are represented in
Fig. 7.5, which shows that the two curves have a similar performance, but the response theme W4 performs relatively worse in the middle-high post probability values.
AUC is a direct measure of the performance of the statistical approach, and is given by the area under the curve (integral) in the SRC plot. The calculated AUC values are presented in Table 7.2 showing the consistent quality of the two maps.

**Table 7.2 - Combination of evidential themes used to obtain response themes and AUC values (pop = population density, spc = soil protective capacity, gwd = groundwater depth, gwv = groundwater velocity, hcv = hydraulic conductivity of the vadose zone, QSCAT-DSM = land use derived from satellite data).**

| Response theme | Combination of evidential themes | AUC value |
|---|---|---|
| W4 | pop, spc, gwd, gwv, hcv | 78.3% |
| W5 | QSCAT-DSM, spc, gwd, gwv, hcv | 78.4% |

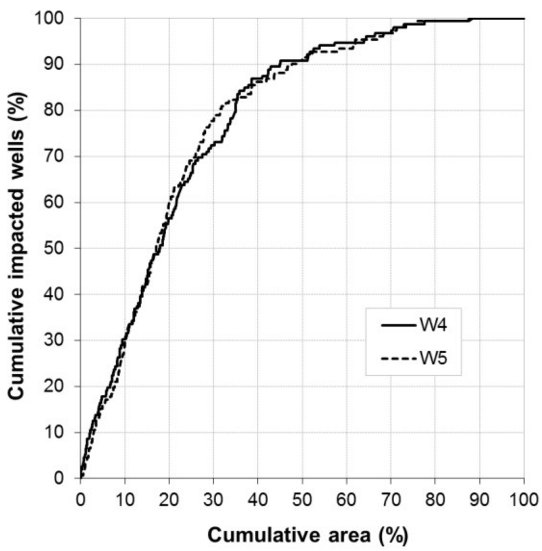


**Fig. 7.5 - Success rate curves of the response themes.**

Then, the reliability of each reclassified map was evaluated by considering its overall performance in classifying the occurrences. Three statistical validation procedures were used: (1) frequency of training set, (2) average nitrate concentration of all wells, and (3) density of control set in each vulnerability class.

The evaluation of the frequency, $F$, is expressed by the ratio:

$$F = \left(N_{\mathrm{W}j}/T_{\mathrm{W}j}\right) \tag{7.1}$$

where $N_{\mathrm{W}j}$ is the number of "impacted" wells in a vulnerability class $j$ and $T_{\mathrm{W}j}$ is the total number of wells in the same class $j$. This technique adds new information to the validation process because it also includes the wells not used in the modeling. Frequency is expected to increase monotonically as the degree of vulnerability increases. The expected trend is verified. In fact, in both the two vulnerability maps, the highest frequency of "impacted" wells is in the highest vulnerability class and the lowest frequency of "impacted" wells is in the lowest vulnerability class (Fig. 7.6).

The evaluation of the average nitrate concentration of all wells, $C_{\mathrm{AVG}}$, is expressed as:

$$C_{\mathrm{AVG}} = \sum_{i=1}^{T_{\mathrm{W}j}} C_{ij} \Big/ T_{\mathrm{W}j} \tag{7.2}$$

where $C_{ij}$ is the nitrate concentration of well $i$ in the vulnerability class $j$, and $T_{\mathrm{W}j}$ is the total number of wells in the same class $j$. This analysis was carried out using all wells stored in the database. The concentration should monotonically increase as the degree of vulnerability increases and the central vulnerability class should give a value close to the overall mean value. The histograms show a direct correlation between average nitrate concentration and the degree of vulnerability, even if, in both cases, the average nitrate concentration in vulnerability class 3 is higher than the overall mean value of nitrate considering all wells (Fig. 7.6).

Considering that the study area was divided in pixels having the same dimension (100 m × 100 m), the density, $D$, can be expressed as:

$$D = \left(NP_{\mathrm{W}j}/TP_j\right) \tag{7.3}$$

where $NP_{\mathrm{W}j}$ is the number of pixels of vulnerability class $j$ containing non-impacted wells, and $TP_j$ is the total number of pixels in the same vulnerability class. Histograms were derived using wells being part of the control set. The density of the non-impacted wells is expected to monotonically decrease as the degree of vulnerability increases. Comparing the density of the central vulnerability class with the prior probability calculated considering the wells being part of the control set is expected that the two values should be as close as possible. In fact, the prior probability expresses the probability that a pixel contains an occurrence without considering any influencing factor, and it is, ideally, similar to the presence of an average combination of factors, which can be represented by the central vulnerability class. The histograms show a monotonic decrease of density values as the vulnerability class increases and the density values for vulnerability class 3 are close to the prior probability value, as expected (Fig. 7.6).

With these three techniques, the quality of each vulnerability map was evaluated based on the slope coefficient of the regression line and the regression coefficient, so that a map should be deemed reliable if it passes these tests.

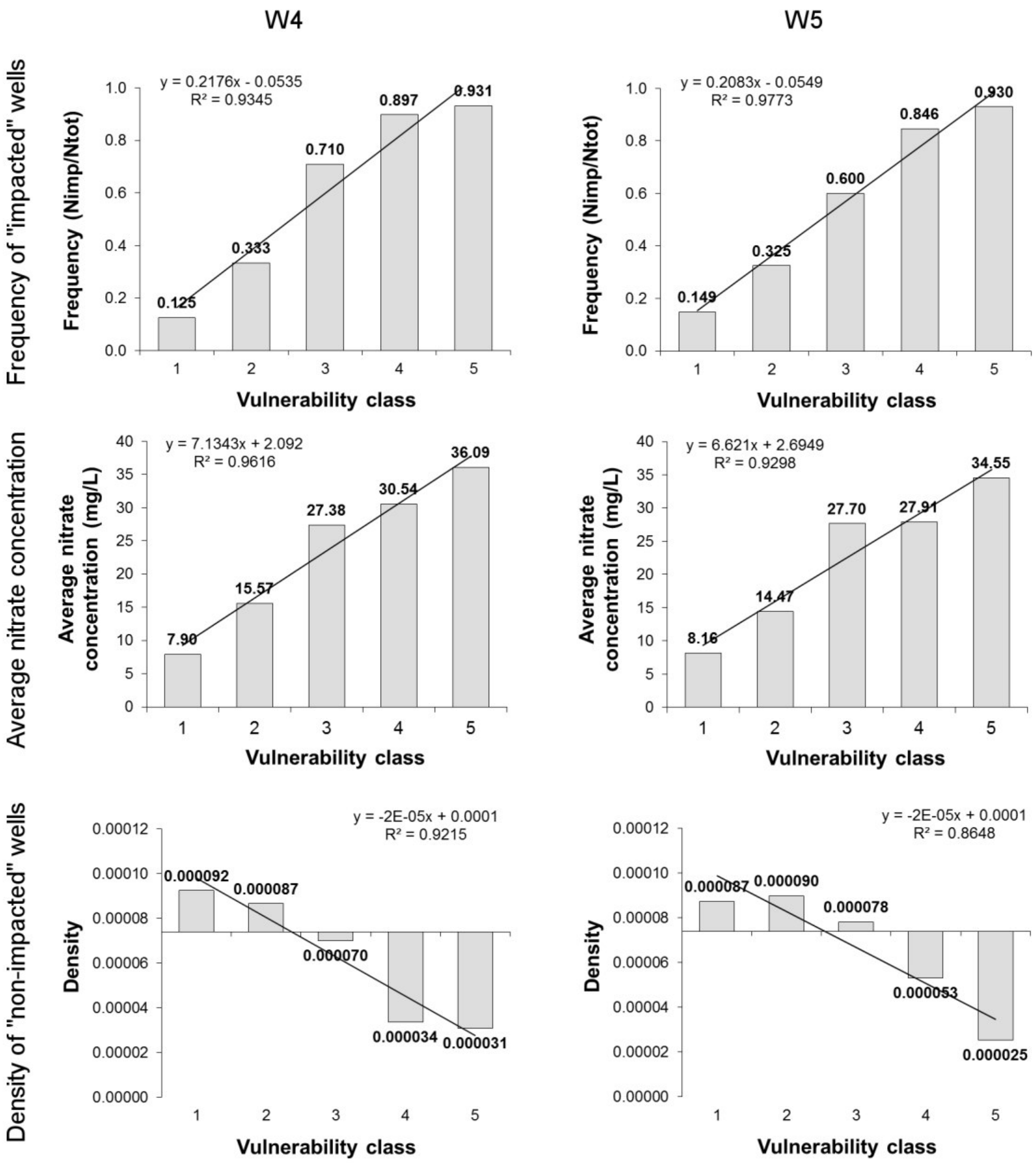


**Fig. 7.6 - Histograms of the frequency of the "impacted" wells (*top*), of the average nitrate concentration (*middle*), and of the density of the "non-impacted" wells (*bottom*) in each vulnerability classes of the maps in Fig. 7.4. The degree of vulnerability increases from class 1 to class 5.**

## 7.3.4 Discussion

The influence of each factor on the presence of high nitrate values in groundwater can be analyzed considering the positive and negative weights, and the derived contrast. Results obtained for the entire plain area within Lombardy Region are compared to previous studies executed on two sectors of the study area: Province of Milan (Sorichetta et al., 2013) and Province of Lodi (Masetti et al., 2008). The former is located in the northern sector of the plain, the latter in the southern sector.

Comparing the small areas, analyzed in the previous studies, similarities and discordances appear.

Soil protective capacity is not statistically significant in the Province of Milan, whereas it shows the expected negative correlation in the Province of Lodi. These results may be explained by the fact that soil protects groundwater only against pollutants introduced at the land surface. In the case of nitrate sources, fertilizers or manures are spread at the land surface, whereas leakages from the sewer systems occur near the surface, but under the soil layer. Thus, soil can act as a filter only in the first case. Results reflect the distribution of nitrate sources of contamination in the two areas: urban areas (i.e., leakages from the sewer system) prevail in the Province of Milan, whereas agricultural activities (i.e., fertilizers and manures) prevail in the Province of Lodi. Soil protective capacity is inhibited in the Province of Milan, whereas it is active in the Province of Lodi.

Groundwater depth and hydraulic conductivity of the vadose zone are positively correlated with the presence of nitrate contamination in both areas. The direct relationship between groundwater depth and probability of high nitrate concentration is in agreement with previous observations for shallow aquifer in USA (Kolpin et al., 1999; Nolan, 2001; Nolan et al., 2002) and Canada (Best et al., 2015). The explanation can be found in bio-geochemical conditions of the vadose zone. In fact, very shallow water table leads to waterlogged conditions conducive to denitrification processes, in which denitrification rates tend to decrease as water-table depth increases. Within the vadose zone, high concentrations could not be attenuated at depth in high hydraulic conductivity, mainly related to coarse-grained sediments (Best et al., 2015), and oxidizing conditions, where the transport process prevails on dilution and denitrification is not facilitated. Moreover, there could be preferential flow paths, created by interconnected higher permeable units, which accelerate the percolation of contaminants in the subsurface (Masetti et al., 2016).

As hydraulic conductivity of the vadose zone influences the movements of contaminants from surface to aquifers, groundwater velocity controls the movements within aquifers, in terms of transport and dilution processes. Groundwater velocity in the saturated zone shows a positive correlation with the occurrence of high nitrate concentrations, but with low contrast values, in the Province of Milan, while a negative correlation in the Province of Lodi. In the first case, the transport process prevails on dilution, even if low contrast values indicate a small influence on the post probability results. In the second case, the dilution process prevails on transport, increasing the contaminant dispersion.

Nitrate sources of contamination result urban areas, expressed in terms of population density, in the Province of Milan and nitrogen fertilizer loads in the Province of Lodi. In the first case, population density is positively correlated with high nitrate concentrations, while nitrogen fertilizer loads are negatively correlated. This fact means that high nitrate concentrations in groundwater are sourced mainly from subsurface leakages of municipal sewage systems, and not from nitrogen fertilizer loadings (agricultural and breeding activities). This unexpected result may be explained by the fact that nitrogen fertilizer loading and population density are both mapped using municipality boundaries as territorial unit, with the result that the latter may overwhelm and mask the influence of agricultural and breeding nitrate sources on nitrate concentration in groundwater (Sorichetta et al., 2013). In the second case, results show the opposite situation: population density is not correlated with high nitrate concentration, while nitrogen fertilizer loadings are positive correlated, meaning a small influence of urban nitrate

sources against a great influence of agricultural ones. These results reflect the different patterns of the study areas: the Milan area is very urbanized in its northern and central sectors, while rural areas are mainly located in the southern sector, whereas the Lodi area is mainly occupied by an extensive agricultural activity, with only the 10 % of the Province covered by urban areas.
Both study cases emphasize the importance of geological and hydrogeological characteristics of the areas, which can mitigate nitrate contamination (such as high soil protection neutralizing nitrates or shallow water table depth favoring denitrification).

Changing the scale of the study area, similarities and discrepancies with the two small areas can be highlighted.
Soil protective capacity shows a negative correlation, with an anomaly in the low protective class. This result agrees with results obtained in the two small areas, emphasizing the importance of soil protective capacity in protecting groundwater against contaminants, even at the regional scale. Although, it seems difficult to identify a physical process responsible for the anomaly in the low protective class.
The positive correlation of groundwater depth with high nitrate concentrations has been observed at different scales, from the field dimension (Best et al., 2015), to sub-basins (e.g., Masetti et al., 2008), to regional scales (this study), and to country scales (e.g., Nolan et al., 2002). This outcome, at different scales, disagrees with the assumption on which the subjective rating systems are based; they usually associate a decrease of vulnerability with the increase of groundwater depth.
At the regional scale, groundwater velocity and hydraulic conductivity of the vadose zone are positively correlated with high nitrate concentration, meaning that the transport process is generally prevalent over the dilution one, both in groundwater and in the vadose zone. Although, at the sub-basin scale, the behavior could be different, as in the Province of Lodi (Masetti et al., 2008).
Regarding anthropogenic sources of nitrate contamination, the outcome at the regional scale shows that urban nitrate sources, as urban extent or population density, are prevalent on agricultural sources. This result may be related to the mask effect that urban sources have on agricultural ones, and to the simultaneous presence of these factors together with geological and hydrogeological conditions, which prevent the propagation of nitrates through the vadose zone.

The two vulnerability maps at the regional scale show a similar distribution of vulnerable areas. Classes 4 and 5 are mainly located in the northern sector, with a prevalence in the northwestern sector, where there is a frequent combination of the presence of urban nitrate sources with high groundwater depth and high hydraulic conductivity in the vadose zone, which prevent denitrification processes. Class 3 is prevalent in the northern and central sector, with some spot in the southwestern sector. Classes 1 and 2 occupy more than half of the study area, in both maps, and are mainly located in the southern sector, where low groundwater depth and low hydraulic conductivity of the vadose zone are present, favoring denitrification processes.
Vulnerability maps are calibrated and validated. The similarity in calculated high AUC values for maps W4 and W5 asserts the consistent quality of the two maps. Although, success rates curves prove a better result for map W5. Validations on the reclassified maps are excellent for both map W4, which shows higher regression coefficients in average nitrate concentration and density of “non-impacted wells” histograms, and W5. Moreover, both maps show density values of the central vulnerability class close

to the prior probability value. Instead, no map presents the mean of nitrate concentration on the total number of wells as average concentration in the central vulnerability class.
In summary, QSCAT-DSM can be successfully used as an alternative to population density as a proxy for nitrate contamination from urban sources.

## 7.4 Conclusions

The application of the WofE technique at a regional scale, in the plain area of Lombardy Region, has shown that:

- Natural factors, such as soil protective capacity, groundwater depth, groundwater velocity and hydraulic conductivity of the vadose zone, influence groundwater vulnerability, confirming results from previous studies (e.g., Nolan et al., 2002; Masetti et al., 2008; Sorichetta et al., 2013);
- Urban nitrate sources are prevalent on agricultural ones in the study area. This outcome is strictly related to the distribution of both anthropogenic activities and natural factors, whose combination can mitigate or facilitate nitrate contamination;
- Approaching the problem at different scales (i.e., local and regional scales) can lead to both concordant and contrasting results. At a local scale there could be some variables (e.g., nitrogen fertilizer loading) that significantly influence the presence of nitrates in groundwater, not perceivable at a regional scale, because of the presence of other variables, more affecting nitrate occurrences over the entire territory;
- QSCAT-DSM satellite dataset (Nghiem et al., 2009) has proven to be a reliable variable to be used in groundwater vulnerability assessments as a proxy for urban nitrate sources, in alternative to population density.

QSCAT-DSM data have the advantages of a worldwide coverage, a continuous data collection and an adequate resolution without spatial gaps. These characteristics, which are not completely covered by population density dataset, allow QSCAT-DSM to detect changes in urban areas over a decadal period and different scales. These advantages allow to introduce the time dimension in groundwater vulnerability assessments (Chapter 8).

# References

Best A., Arnaud E., Parker B., Aravena R., Dunfield K., 2015. Effects of glacial sediment type and land use on nitrate patterns in groundwater. Groundwater Monitoring & Remediation, vol. 35, n. 1, pp. 68-81, doi 10.1111/gwmr.12100

Chung C.F., Fabbri A.G., 1999. Probabilistic prediction models for landslide hazard mapping. Photogrammetric Engineering and Remote Sensing, vol. 65, n. 12, pp. 1389-1399

European Community, 1991. Council Directive 91/676/EEC concerning the protection of waters against pollution caused by nitrates from agricultural sources, (Nitrate Directive). OJ L 375, 31 December 1991, pp. 1-8

Kolpin D., Burkart M., Goolsby D., 1999. Nitrate in groundwater of the Midwestern United States: a regional investigations on relations to land use and soil properties. In: Impact of Land-Use Change on Nutrient Loads from Diffuse Sources (Proceedings of IUGG 99 Symposium HS3, Birmingham, July 1999). Heathwaite L (ed.), Denmark. IAHS Publication No. 257

Madison R.J., Burnett J.O., 1985. Overview of the occurrence of nitrate in groundwater of the United States. U.S. Geological Survey Water Supply Paper, vol. 2275, pp. 93-105

Masetti M., Poli S., Sterlacchini S., Beretta G.P., Facchi A., 2008. Spatial and statistical assessment of factors influencing nitrate contamination in groundwater. Journal of Environmental Management, vol. 86, n. 1, pp. 272-281, doi 10.1016/j.jenvman.2006.12.023

Masetti M., Sterlacchini S., Ballabio C., Sorichetta A., Poli S., 2009. Influence of threshold value in the use of statistical methods for groundwater vulnerability assessment. Science of the Total Environment, vol. 407, n. 12, pp. 3836-3846, doi 10.1016/j.scitotenv.2009.01.055

Masetti M., Pedretti D., Sorichetta A., Stevenazzi S., Bacci F., 2016. Impact of a storm-water infiltration basin on the recharge dynamics in a highly permeable aquifer. Water Resource Management, vol. 30, n. 1, pp. 149-165, doi: 10.1007/s11269-015-1151-3

Nghiem S.V., Balk D., Rodriguez E., Neumann G., Sorichetta A., Small C., Elvidge C.D., 2009. Observations of urban and suburban environments with global satellite scatterometer data. ISPRS – Journal of Photogrammetry and Remote Sensing, vol. 64, n. 4, pp. 367-380, doi 10.1016/j.isprsjprs.2009.01.004

Nolan B.T., 2001. Relating nitrogen sources and aquifer susceptibility to nitrate in shallow ground waters of the United States. Ground Water, vol. 39, n. 2, pp. 290-299

Nolan B.T., Hitt K.J., Ruddy B.C., 2002. Probability of nitrate contamination of recently recharged groundwaters in the conterminous United States. Environmental Science and Technology, vol. 36, n. 10, pp. 2138-2145, doi 10.1021/es0113854

Panno S.V., Kelly W.R., Martinsek A.T., Hackley K.C., 2006. Estimating background and threshold nitrate concentrations using probability graph. Groundwater, vol. 44, n. 5, pp. 697-709, doi 10.1111/j.1745-6584.2006.00240.x

Sorichetta A., Masetti M., Ballabio C., Sterlacchini S., Beretta G.P., 2011. Reliability of groundwater vulnerability maps obtained through statistical methods. Journal of Environmental Management, vol. 92, n. 4, pp. 1215-1224, doi 10.1016/j.jenvman.2010.12.009

Sorichetta A., Masetti M., Ballabio C., Sterlacchini S., 2012. Aquifer nitrate vulnerability assessment using positive and negative weights of evidence methods, Milan, Italy. Computers and Geosciences, vol. 48, pp. 199-210, doi 10.1016/j.cageo.2012.05.021

Sorichetta A., Ballabio C., Masetti M., Robinson G.R. Jr, Sterlacchini S., 2013. A Comparison of Data-Driven Groundwater Vulnerability Assessment Methods. Ground Water, vol. 51, n. 6, pp. 866-879, doi: 10.1111/gwat.12012

# Chapter 8

# Groundwater vulnerability maps derived from a time dependent method using satellite scatterometer data

## 8.1 Introduction

As groundwater resources have become more vulnerable in recent years, it is necessary to urgently close the gap between the information required for land use planning to efficiently safeguard groundwater quality and techniques required to accurately assess groundwater vulnerability. In fact, the EU Groundwater Directive (2006/118/EC) requires the identification of areas where groundwater suffers increasing trends in contaminant concentration, highlighting the need to carefully manage such areas even if the concentration is below the regulatory limit.

A current limitation in groundwater vulnerability studies is related to the lack of consideration of temporal trends (Stuart et al., 2007), and this emphasizes the need to consider the time dimension in assessing groundwater vulnerability. Methods currently used to assess groundwater vulnerability at a regional scale (Focazio et al., 2002) can be subjective (i.e., knowledge-driven) or objective (i.e., data driven). In this regard, only objective methods allow scientifically defensible end products (Focazio et al., 2002) and, most importantly, enable an explicit integration of the time dimension in the groundwater vulnerability assessment (Sorichetta, 2011).

Objective methods, however, face a major challenge that requires an extensive dataset, including a series of contaminant concentration measurements and natural and anthropogenic variables, to be consistent both in space and in time (Brunner et al., 2007). Addressing such a challenge demands a determination of the relationship between temporal changes in groundwater contamination and in land use across a vast spatial extent encompassing natural environments, agricultural regions, and urban areas. This effort will enable breakthrough advances to improve the mapping of hazardous areas with different levels of vulnerability, and to assess the efficacy of land use planning toward groundwater protection.

In this context, this Chapter focuses on advancing the use of statistical methods, adopting the Weights of Evidence technique (WofE), to assess groundwater vulnerability by explicitly introducing the time dimension in the analysis. The objectives are to address recent requirements from transnational policies and to close the critical information gap described earlier.

In view of current and projected acceleration in global urbanization, urban areas are widely considered as one of the most important non-point sources of contamination impacting groundwater quality (Kuroda and Fukushi, 2008). Urban sprawl is one of the most important types of land-use changes impacting the regional environment, the social structure, and the economy in Europe (EEA, 2006). Nitrate is an abundant contaminant of groundwater. With a high mobility and multiple sources, nitrate is an effective indicator of groundwater contamination. A sufficient frequency for monitoring nitrate concentration in

groundwater over the long term allows the use of nitrate in temporal analyses to determine the contamination trend.
The previous Chapter has shown that, in the Lombardy plain area, nitrate occurrence in groundwater is strongly related to urban sources more than to agricultural activities; however, the problem has never been analyzed in the time dimension. It is unclear whether a relationship exists between recent changes in groundwater nitrate contamination and in land use. To analyze how urban development could affect groundwater quality in the 2000s, recent trends in groundwater nitrate concentration need to be correlated with the evolution of potential urban nitrate sources across this region.
The use of an innovative dataset to delineate urban areas with satellite scatterometer data has been explored to identify zones where different rates of urban growth occurred across the entire study area, and in which an increase of potential urban sources may exist and consequently impact groundwater. Radar backscatter data acquired by the SeaWinds scatterometer aboard the QuikSCAT satellite together with the Dense Sampling Method (QSCAT-DSM; Nghiem et al., 2009) have been used to identify and map urban extent and surface features at a posting scale of about 1 km². QSCAT-DSM results are to be compared with those obtained from two different sources of urban information: 1) changes of population density and 2) changes in land use derived from high-resolution aerial images acquired in different years.
This Chapter aims to describe the reliability of a new approach that introduces the time dimension in groundwater vulnerability assessment, by using an innovative remote sensing dataset to obtain a quantitative assessment of groundwater quality changes through time.

## 8.2 Response variable and evidential themes

The response variable is represented by nitrate concentration trend in groundwater. Nitrate concentrations have been collected through the monitoring network described in Chapter 4, Paragraph 4.1. Only the 221 wells monitoring the shallow aquifer and having a minimum of eight measurements in the period 2001 – 2011, have been selected to be used in the analysis. The change in nitrate concentration is quantified by the slope of the regression line from an interpolation of concentration data, which defines the rate of nitrate concentration change in mg/L per day.
A frequency histogram of nitrate concentration trend shows a nearly bimodal distribution with two main relative peaks at about –0.0008 and +0.00016 mg/L per day (Fig. 8.1). Another minor peak can also be identified at value 0. The intermediate values of –0.0004 and +0.0004 mg/L per day, which separate three populations, were considered to be appropriate values to be used as thresholds.
Wells showing concentration trends higher than +0.0004 mg/L per day are considered as “increasing” wells (87), and those below –0.0004 mg/L per day as “decreasing” wells (86). Wells showing concentration trends included in the range –0.0004 and +0.0004 mg/L per day are considered as “neutral” wells (48). In these wells, the uncertainty in the slope coefficient value, which is close to zero, does not allow one to precisely categorize them as “increasing” or “decreasing” wells.
The “increasing” wells, showing a clear increase in concentration trends, represent the training set, and they have been selected to be used in the analysis. While “decreasing” and “neutral” wells are grouped in a unique set, representing the control set. The binary formulation of the response variable is a requirement of the WofE modelling technique.

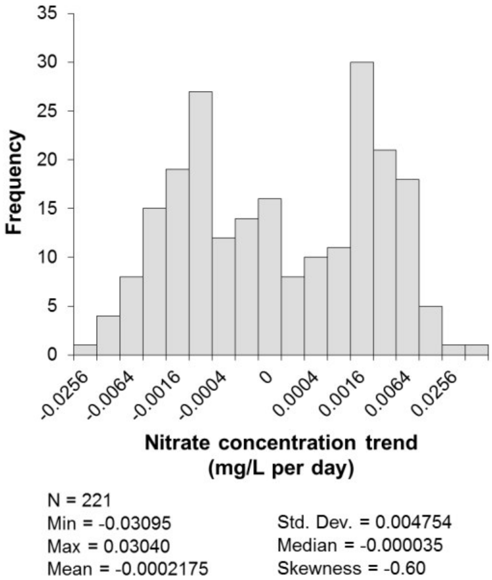


**Fig. 8.1 - Frequency histogram of nitrate concentration trend.**

From the hydrogeological conceptual model, seven explanatory variables (described in Chapter 4, Paragraph 4.2, and Chapter 5), were considered for being used as evidential themes in the analysis (Table 8.1). The three variables representing urban sources of nitrate contamination have been evaluated separately and the obtained groundwater vulnerability maps have been compared. The aim is identifying the most appropriate variable representing urban nitrate sources.

**Table 8.1 - Explanatory variables used as evidential themes.**

| Explanatory variable | Type | Range |
|---|---|---|
| Population density change [2001 – 2011] (people/km$^2$) | Continuous | –402 ÷ 845 |
| Slope QuikSCAT-DSM [2000 ÷ 2009] (dB/year) | Continuous | –0.0699 ÷ 0.1268 |
| DUSAF urban change [2000 – 2007/2009] (%) | Continuous | –6.7 ÷ 30.8 |
| Soil protective capacity | Categorical | Low, Moderate, High |
| Groundwater depth [2003] (m) | Continuous | 0 ÷ 70 |
| Groundwater velocity (m/s) | Continuous | $4.7\times10^{-8} \div 7.3\times10^{-5}$ |
| Hydraulic conductivity of the vadose zone (m/s) | Continuous | $4.1\times10^{-8} \div 4.0\times10^{-2}$ |

# 8.3 Results and discussion

## 8.3.1 Contrasts of the generalized evidential themes

The contrasts of statistically significant evidential themes enable an assessment of the influence of the variables under consideration on groundwater contamination. Contrast values, both for anthropogenic and natural factors, are presented in Fig. 8.2. All three variables, representing urban nitrate sources and their evolution, show a positive correlation between the increase of urban areas or population growth and the occurrence of increasing nitrate concentration trends in groundwater.

Threshold values, corresponding to the transition from negative to positive contrasts, are +44 people/km², +0.0260 dB/year and +1.81 % over the study period, respectively for population density change, QSCAT-DSM slope and DUSAF urban extent change. Observed from these variables, classes with positive contrasts are clustered in the northern sector, while classes with negative contrasts are mainly in the southern sector.
Soil protective capacity is not statistically significant. Also, it does not show a discernible correlation, with negative contrasts for low and high classes and a positive contrast for the moderate class. Groundwater depth reveals that large values of water-table depth are positively related to increasing concentration trends, while low values (close to surface or less than 13 m) are negatively associated. Groundwater velocity and hydraulic conductivity of the vadose zone show positive correlations and the threshold values are about $1.5\times10^{-6}$ m/s and $4.7\times10^{-6}$ m/s, respectively.

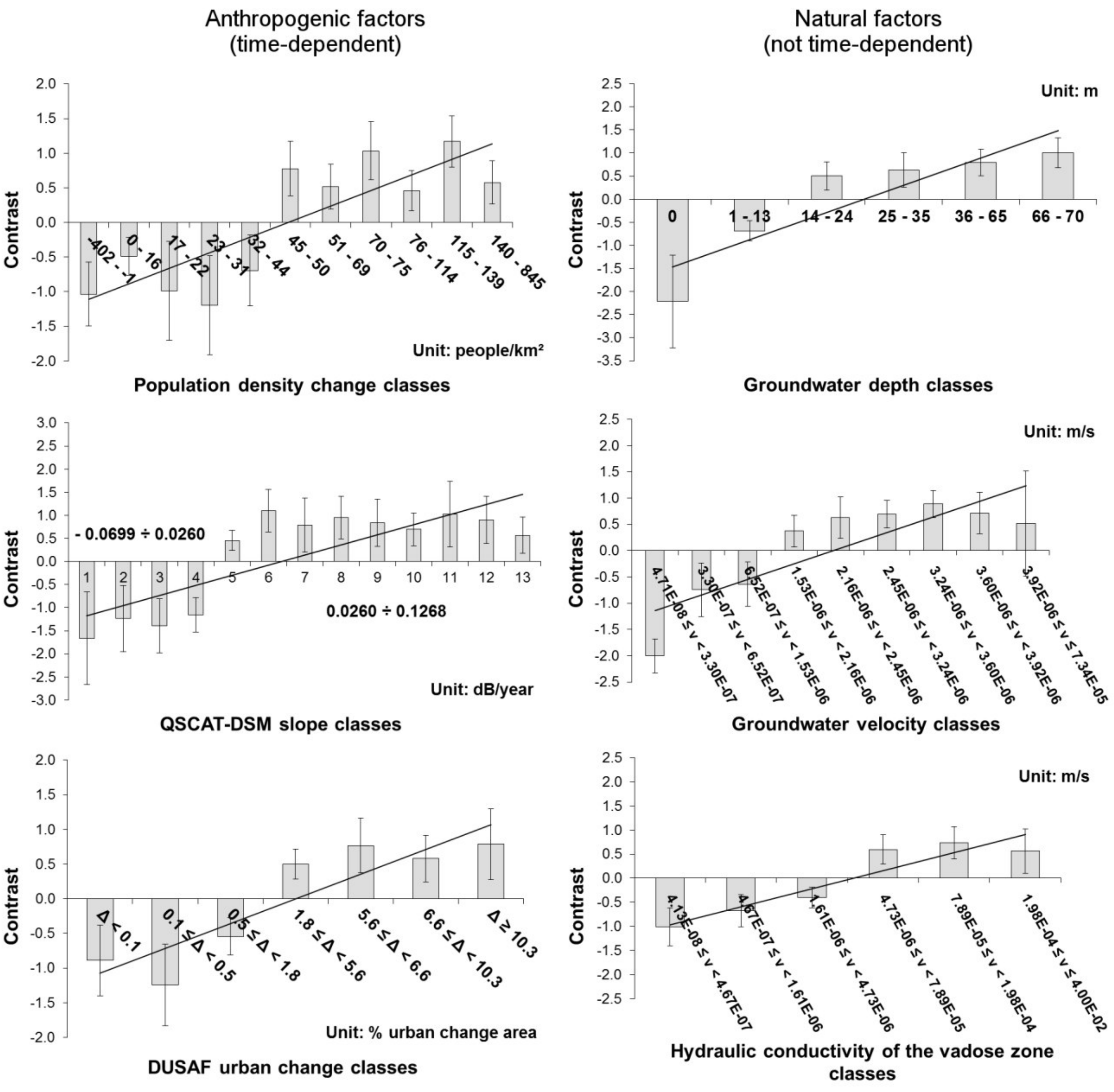


**Fig. 8.2 - Contrasts and error bars of the statistically significant classes of each evidential theme used to generate the maps in Fig. 8.3.**

## 8.3.2 Response theme

In order to evaluate the reliability of each variable as a proxy of urban nitrate sources, three response themes were obtained and compared (Fig. 8.3). Each response theme considers one of the three urban variables, and the three statistically significant evidential themes representing the associated natural factors (Table 8.2).

Each response theme was categorized so that each vulnerability class in the corresponding map contains approximately the same number of different posterior probability values according to the geometric interval method (Sorichetta et al., 2011). Five classes were identified with the degree of groundwater vulnerability increasing from 1 to 5.

It is important to note that these response themes are time dependent. This means that groundwater vulnerability classes reflect the tendency toward a deterioration of the quality of the aquifer rather than the absolute severity of the aquifer contamination in a static condition.

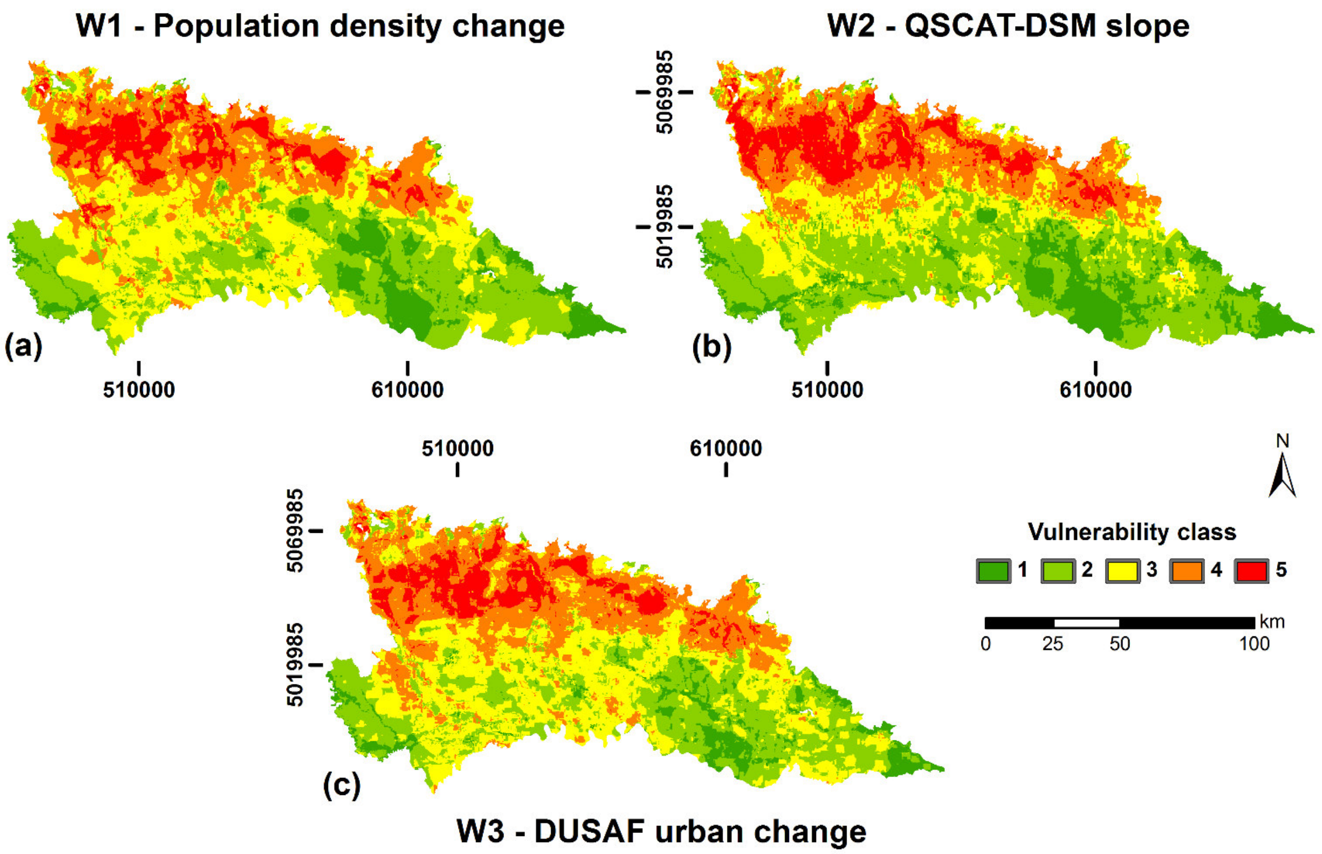


**Fig. 8.3 - Vulnerability maps obtained using static variables, representing natural factors, with (a) population density change, (b) QSCAT-DSM slope, and (c) DUSAF-based urban extent change as time-dependent variables. Coordinates refer to WGS 1984 – UTM Zone 32N projection.**

## 8.3.3 Validations

The general quality of each response theme (i.e., post probability map) can be evaluated with the area-under-the-curve (AUC) value. AUC is a direct measure of the performance of the statistical approach, and is given by the area under the curve (integral) in a binary plot considering cumulated area/cumulated training points expressed in percentage. The calculated AUC values are presented in Table 8.2 showing the consistent quality of the different maps.

**Table 8.2 - Combination of evidential themes used to obtain response themes and AUC values (pop = population density change, gwd = groundwater depth, gwv = groundwater velocity, hcv = hydraulic conductivity of the vadose zone, QSCAT-DSM = land use changes derived from satellite data, DUSAF = land use changes derived from aerial photographs).**

| Response theme | Combination of evidential themes | AUC value |
|---|---|---|
| W1 | pop, gwd, gwv, hcv | 74.4% |
| W2 | QSCAT-DSM, gwd, gwv, hcv | 74.3% |
| W3 | DUSAF, gwd, gwv, hcv | 73.7% |

Then, the reliability of each classified map was evaluated again by considering its overall performance in classifying the occurrences. Two statistical validation procedures were used: (1) frequency of training set, and (2) average nitrate concentration trend of all wells in each vulnerability class.

The evaluation of the frequency, $F$, is expressed by the ratio:

$$F = \left(N_{\mathrm{W}j}/T_{\mathrm{W}j}\right) \tag{8.1}$$

where $N_{\mathrm{W}j}$ is the number of "increasing" wells in a vulnerability class $j$ and $T_{\mathrm{W}j}$ is the total number of wells in the same class $j$. This technique adds new information to the validation process because it also includes the wells not used in the modeling. Frequency is expected to increase monotonically as the degree of vulnerability increases. The expected trend is verified. In fact, for all the three vulnerability maps, there are no "increasing" wells in the lowest vulnerability class and the highest frequency of "increasing" wells is in the highest vulnerability class (Fig. 8.4).

The evaluation of the average nitrate concentration trend of all wells, $C_{\mathrm{AVG}}$, is expressed as:

$$C_{\mathrm{AVG}} = {\sum_{i=1}^{T_{\mathrm{W}j}} C_{ij}} \Big/ {T_{\mathrm{W}j}} \tag{8.2}$$

where $C_{ij}$ is the nitrate concentration trend of well $i$ in the vulnerability class $j$, and $T_{\mathrm{W}j}$ is the total number of wells in the same class $j$. This analysis was carried out using all wells stored in the database. The concentration should monotonically increase as the degree of vulnerability increases and the central vulnerability class should give a value close to the overall mean value. Despite some anomalies, all three histograms show a direct correlation between average nitrate concentration trend and the degree of vulnerability (Fig. 8.4).

With these two techniques, the quality of each vulnerability map was evaluated based on the slope coefficient of the regression line and the regression coefficient, so that a map should be deemed reliable if it passes these tests.

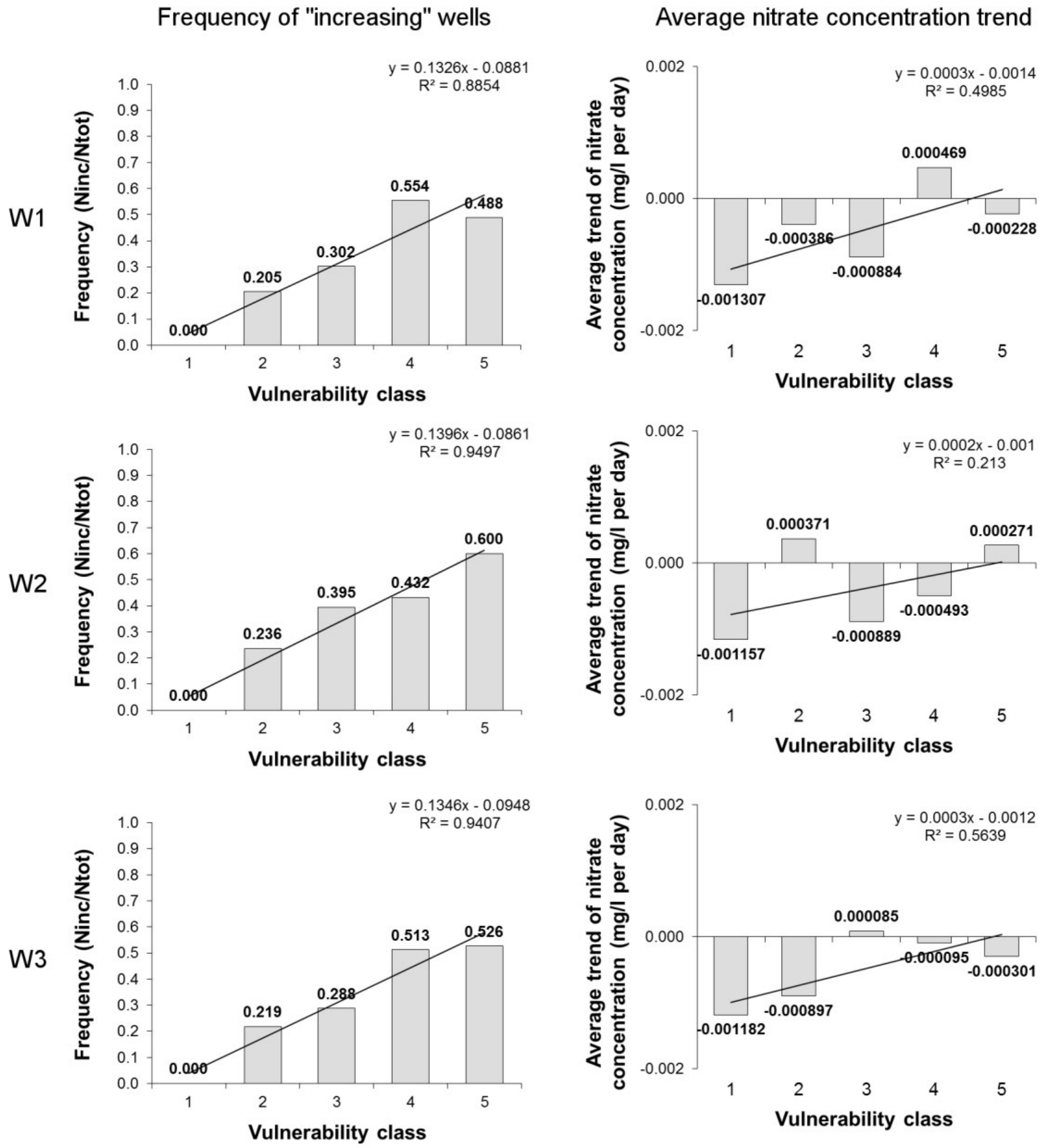


**Fig. 8.4 - Histograms of the frequency of the "increasing" wells (*left*) and of the average nitrate concentration trend (*right*) in each vulnerability classes of the maps in Fig. 8.3. The degree of vulnerability increases from class 1 to class 5.**

## 8.3.4 Spatial agreement

A spatial agreement is quantitatively evaluated through a pixel-by-pixel analysis representing the difference, expressed as percentage, in the unit-cell classification for the three vulnerability maps (Fig. 8.5). Results from this analysis show a high level of agreement between the maps in the paired map-to-map comparison: almost 61–67 % of the study area is classified with the same degree of vulnerability, 33–38 % is classified within a difference of one degree of vulnerability, while only 0.3–0.8 % within a difference of two degrees of vulnerability.

Another method to evaluate the reliability of each vulnerability map is overlaying each map with the classes of its urban change variable with positive contrast values to examine their consistency (Fig. 8.6). Map W2, obtained using QSCAT-DSM slope, is the only one where the highest vulnerability classes are consistently overlain by the classes of urban extent change variable with positive contrast values. Instead, in the other two cases there are anomalous mismatches. In map W1, obtained using population density changes, some cities (like Monza or Brescia) show negative contrast values, meaning that their population density change is lower than +44 people/km². In map W3, obtained using DUSAF maps, some areas in the northern sector show negative contrast values (like Milan), while agricultural areas of the southern sector are characterized by positive contrast values (e.g., Provinces of Cremona and Mantua). The first anomaly could be explained by the urban sprawl phenomenon, with residential citizens moving from the largest cities to the smallest cities, while the rate of urbanization is increasing almost everywhere. The second anomaly could be caused by the focal application applied to the binary land-use categorization in the DUSAF maps: small changes in urban extent cannot be accurately detected in large urban areas.

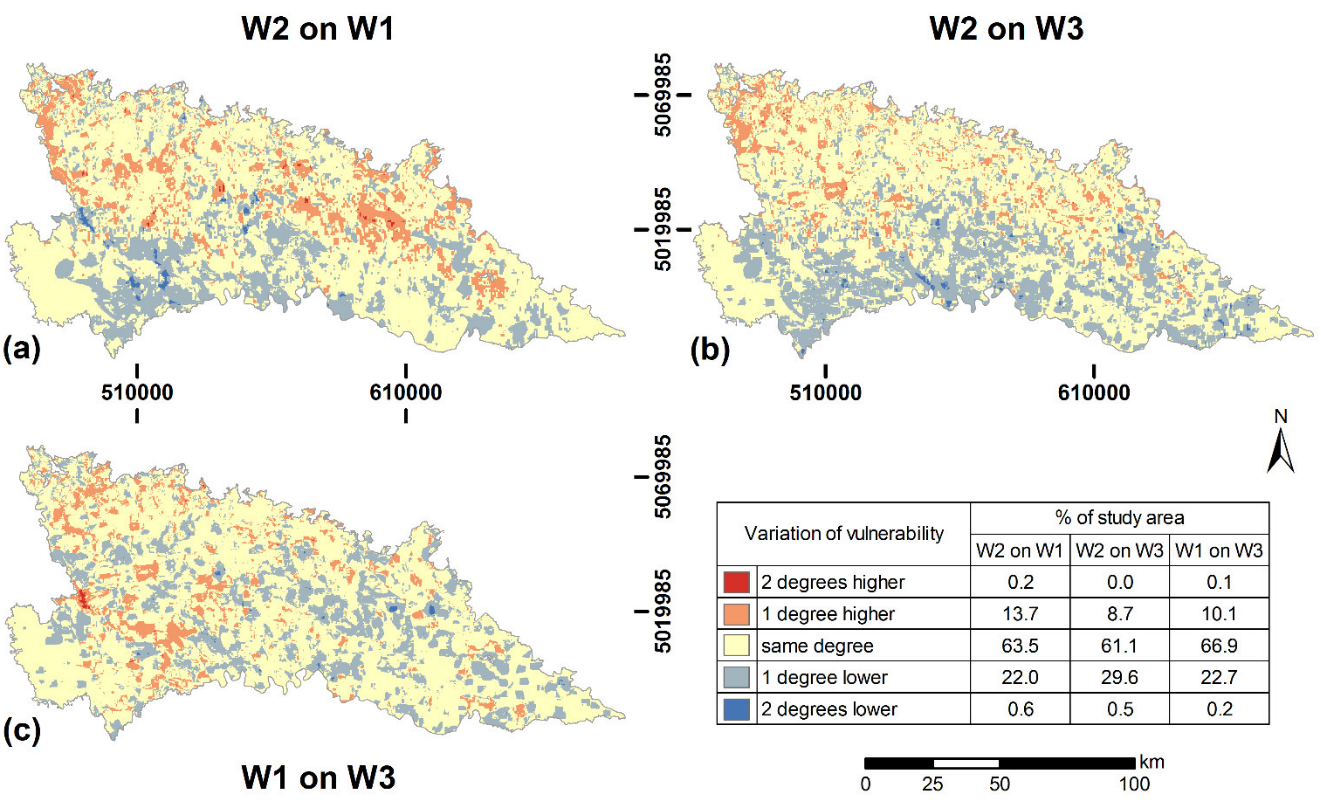


| Variation of vulnerability | % of study area | | |
|---|---|---|---|
| | W2 on W1 | W2 on W3 | W1 on W3 |
| 2 degrees higher | 0.2 | 0.0 | 0.1 |
| 1 degree higher | 13.7 | 8.7 | 10.1 |
| same degree | 63.5 | 61.1 | 66.9 |
| 1 degree lower | 22.0 | 29.6 | 22.7 |
| 2 degrees lower | 0.6 | 0.5 | 0.2 |

**Fig. 8.5 - Variation of vulnerability from map-to-map: (a) map W2 on map W1; (b) map W2 on map W3; (c) map W1 on map W3. The variation is expressed as the agreement in percentage between the vulnerability depicted in the first map with respect to the one depicted in the second map. Coordinates refer to WGS 1984 – UTM Zone 32N projection.**

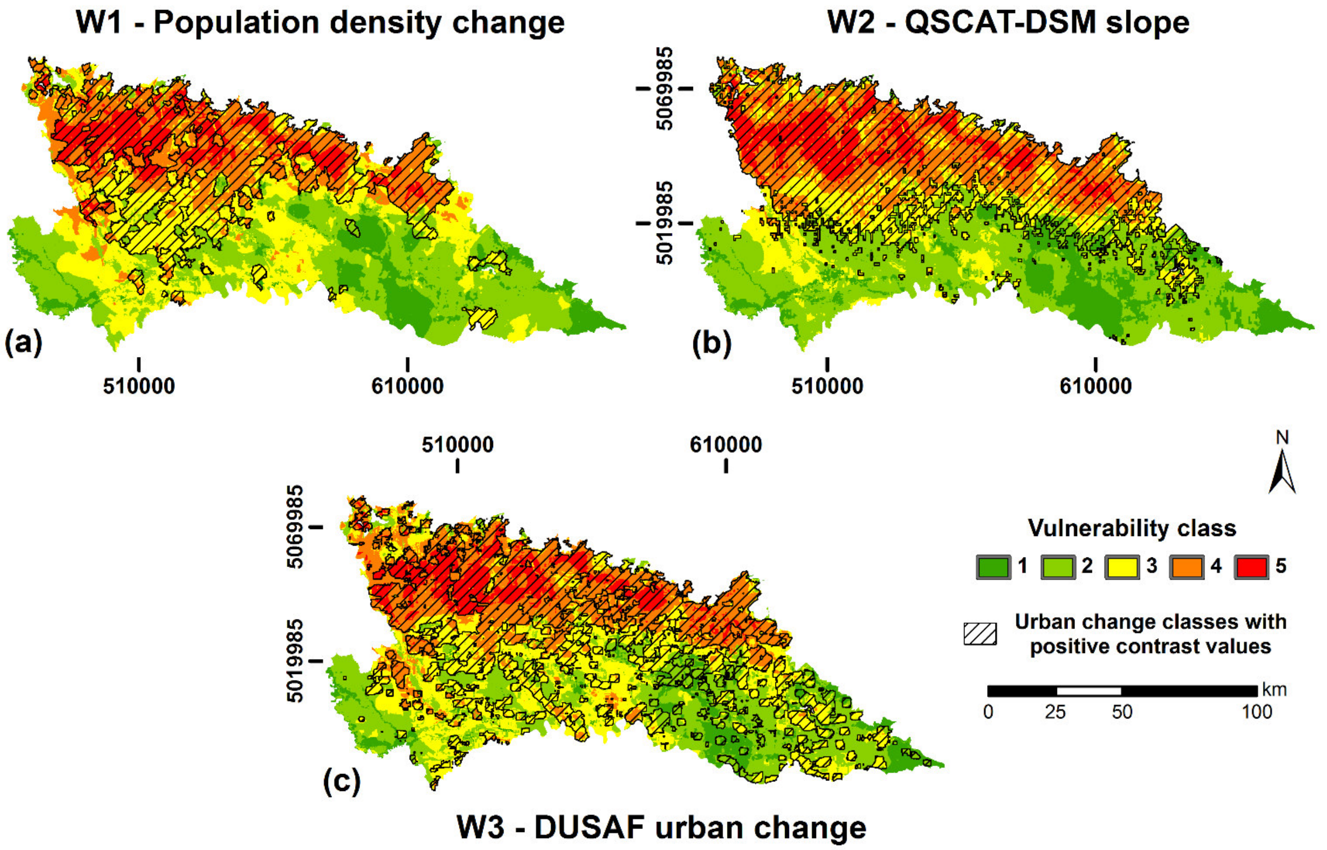


**Fig. 8.6 - Vulnerability maps obtained using (a) population density change, (b) QSCAT-DSM slope and (c) DUSAF urban extent change as time-dependent variables, overlain by the corresponding evidential theme classes with positive contrast values. Coordinates refer to WGS 1984 – UTM Zone 32N projection.**

## 8.3.5 Discussion

The direct correlation for all of the three anthropogenic evidential themes means that increasing nitrate concentration is related to areas of urban development or population increase.

The three urban variables consistently identify that the most important changes are clustered around the biggest cities or in the northern sector where cities and industries in the Lombardy Region are mostly located, while the southern sector primarily consists of agricultural fields. There are anomalies in population density changes because some sectors in large cities have decreasing trends while small towns show significantly increasing trends. These changes indicate a tendency that people like to move away from over-crowded urban areas and sprawl to more open suburban areas with natural or agricultural surroundings (EEA, 2006).

The direct relationship between groundwater depth and increasing concentration trends is consistent with earlier static observations for shallow aquifer in USA (Nolan, 2001; Nolan et al., 2002) and in the Lombardy plain area (Chapter 7). The explanation can be found in bio-geochemical conditions of the vadose zone. In fact, very shallow water table leads to waterlogged conditions conducive to denitrification processes, in which denitrification rates tend to decrease as water-table depth increases.

The result in this Chapter supports this hypothesis and indicates that nitrate concentration changes are related to bio-geochemical activities in the vadose zone.

Groundwater velocity and hydraulic conductivity of the vadose zone are two hydrogeological variables that influence the movements of contaminants from surface to aquifers and within aquifers. The first controls transport and dilution of contaminants within aquifers, and the latter controls the rate at which a contaminant can reach groundwater. In terms of increasing concentration trends in the study area, positive correlations mean that the transport process is generally prevalent over the dilution one, both in groundwater and in the vadose zone. Static analyses (Chapter 7) have found that these variables have positive correlations with the occurrence of high nitrate concentrations. From this Chapter, increasing concentration trends are shown to relate to increasing groundwater velocity or increasing hydraulic conductivity in the vadose zone. Thus, both static and time-dependent analyses confirm the impacts of these hydrogeological factors on the distribution of contaminants, which are necessary to include in groundwater vulnerability assessment.

Vulnerability maps are calibrated and validated. The similarity in calculated high AUC values for maps W1, W2 and W3 asserts the consistent quality of the maps. Histograms of frequency are excellent for all the maps, with a monotonic increase corresponding to higher vulnerability. Nevertheless, according to the criteria used in evaluating the frequency histograms, map W2 can be considered the one that performs best. In fact, it has the highest regression coefficients and it is the one with the highest frequency of impacted wells in the highest vulnerability class.

Histograms of average nitrate concentration trends show a general positive trend, although with low values. Maps W1 and W3 have the highest angular and regression coefficients, but only map W2 shows the mean positive value in the higher vulnerability class. No map presents the mean or median value of the whole distribution as average concentration trend in the central vulnerability class.

In summary, QSCAT-DSM can be successfully used as a proxy for nitrate contamination from urban sources and, among the three obtained vulnerability maps, the map that uses QSCAT-DSM slope to characterize the evolution of urban nitrate sources (map W2) appears to be the best.

## 8.4 Conclusions

Introducing the time variable to monitor trends in groundwater vulnerability assessment is an innovative approach to study the evolution of non-point-source pollution in an area and to forecast future changes. With the application of a Bayesian spatial statistical approach, it is found that:

- Natural factors, such as groundwater depth, groundwater velocity and hydraulic conductivity of the vadose zone, influence groundwater vulnerability, confirming results from previous studies on nitrate contamination (Nolan, 2001; Sorichetta et al., 2013);
- The innovative use of QSCAT-DSM satellite data (Nghiem et al., 2009) in the analysis enables the production of a time-dependent vulnerability map, which is compared with two other vulnerability maps obtained using different time-dependent factors related to urban changes (i.e., population density from census and changes in land use derived from the DUSAF database);
- All of the time-dependent factors indicate that increasing nitrate concentration occurs in areas related to urban development or population increase;

- The calibration and validation procedures affirm all of the three vulnerability maps have a high reliability, while the one obtained with QSCAT-DSM is the better one.

The latter result is remarkable for those areas where there are insufficient or inaccurate data for population or land use and their changes, and thus satellite observations of urban change become particularly useful. Moreover, QSCAT-DSM data have the advantages of a worldwide coverage, a continuous data collection and an adequate resolution without spatial gaps.

In conclusion, the approach developed in this Chapter allows the inclusion of the time variable in groundwater vulnerability assessment with the use of innovative remote sensing data to carry out a quantitative statistical analysis of groundwater quality changes.

New approaches to combine groundwater vulnerability maps obtained by explicitly accounting for the time variable with traditional vulnerability maps should be advanced for better intervention strategies and for more efficient policy measures. Indeed, their combined use would allow to not only identify already highly contaminated areas where expensive remediation measures need to be implemented, but also to detect areas where pro-active interventions need to be planned.

With the method demonstrated in this Chapter, existing and future satellite scatterometer data can be used to make and update maps of groundwater vulnerability as urbanization accelerates across the world.

## References

Brunner P., Hendricks Franssen H.-J., Kgotlhang L., Bauer-Gottwein P., Kinzelbach W., 2007. How can remote sensing contribute in groundwater modeling? Hydrogeology Journal, vol. 15, n. 1, pp. 5-18, doi:10.1007/s10040-006-0127-z

EEA – European Environment Agency, 2006. Urban sprawl in Europe: The ignored challenge (EEA Report No. 10/2006). Office for Official Publications of the European Communities, Luxembourg, 56 pp., ISSN: 1725-9177

European Community, 2006. Directive 2006/118/EC on the protection of groundwater against pollution and deterioration, (Groundwater Directive). OJ L 372, 27 December 2006, pp. 19-31

Focazio M.J., Reilly T.E., Rupert M.G., Helsel D.R., 2002. Assessing Ground-Water Vulnerability to Contamination: Providing Scientifically Defensible Information for Decision Makers. U.S. Geological Survey Circular 1224. ISBN: 0-607-89025-8

Kuroda K., Fukushi T., 2008. Groundwater contamination in urban areas. In: Takizawa S. (ed.) Groundwater management in Asian cities. Springer, Heidelberg, Germany, pp. 125–149

Nghiem S.V., Balk D., Rodriguez E., Neumann G., Sorichetta A., Small C., Elvidge C.D., 2009. Observations of urban and suburban environments with global satellite scatterometer data. ISPRS – Journal of Photogrammetry and Remote Sensing, vol. 64, n. 4, pp. 367-380, doi 10.1016/j.isprsjprs.2009.01.004

Nolan B.T., 2001. Relating nitrogen sources and aquifer susceptibility to nitrate in shallow ground waters of the United States. Ground Water, vol. 39, n. 2, pp. 290-299

Nolan B.T., Hitt K.J., Ruddy B.C., 2002. Probability of nitrate contamination of recently recharged groundwaters in the conterminous United States. Environmental Science and Technology, vol. 36, n. 10, pp. 2138-2145, doi 10.1021/es0113854

Sorichetta A., 2011. Groundwater vulnerability assessment using statistical methods. Università degli Studi di Milano, Academic year 2010, 141 pp. http://hdl.handle.net/2434/152913

Sorichetta A., Masetti M., Ballabio C., Sterlacchini S., Beretta G.P., 2011. Reliability of groundwater vulnerability maps obtained through statistical methods. Journal of Environmental Management, vol. 92, n. 4, pp. 1215-1224, doi 10.1016/j.jenvman.2010.12.009

Sorichetta A., Ballabio C., Masetti M., Robinson G.R. Jr, Sterlacchini S., 2013. A Comparison of Data-Driven Groundwater Vulnerability Assessment Methods. Ground Water, vol. 51, n. 6, pp. 866-879, doi: 10.1111/gwat.12012

Stuart M.E., Chilton P.J., Kinniburgh D.G., Cooper D.M., 2007. Screening for long-term trends in groundwater nitrate monitoring data. Quarterly Journal of Engineering Geology and Hydrogeology, vol. 40, n. 4, pp. 361-376, doi 10.1144/1470-9236/07-040

# Chapter 9

# A new approach to introduce the time variable in groundwater vulnerability assessments

## 9.1 Introduction

Water scarcity and associated risks are a centerpiece of our present societal challenges. The challenge for the future will be to ensure the short-term and long-term provision of accessible and safe freshwater supply to meet the needs of the growing human population and ecosystems, with protection playing a key role in this situation (Kumar, 2015). Rapid changes in land use modify the amount and distribution of point and non-point sources of contamination and climate changes are going to modify the amount and distribution of water availability. Within this framework, groundwater is going to represent the most strategically important water resource, considering its attitude to be less impacted by both climate changes and contamination respect to surficial water. Anyway, also groundwater is vulnerable to contamination and is going to be under increasing risks in these changing scenarios. Thus, there is the urgent need to better quantify time-dependent processes that can affect groundwater quality and to develop methods that allow to evaluate the effect of future scenarios of land use and climate changes on groundwater vulnerability.

Chapter 7 has proven the importance of the combination of natural and anthropogenic factors in influencing groundwater contamination and demonstrated the reliability of satellite data (QuikSCAT-DSM, Nghiem et al., 2009) to be used in groundwater vulnerability assessments as a proxy for urban nitrate sources. Chapter 8 has proven the usefulness of groundwater vulnerability maps also in identifying areas characterized by an upward contamination trend, together with the advantages of satellite data in recognizing urban changes in the decade of the 2000's.

This Chapter presents a time-dependent approach, which allows to evaluate groundwater vulnerability to nitrate contamination, considering both the last status of groundwater contamination and its evolution. The approach would answer to the European Union requirements on the identification of areas where groundwater suffers because of the contamination by various pollutants and is characterized by increasing contamination trends (Groundwater Directive, 2006/118/EC). The approach allows also evaluating a hypothetical scenario in the future and its impacts on groundwater contamination.

In particular, it focuses on the status of nitrate contamination in 2011 and its evolution in the decade 2000 – 2011, and evaluates groundwater vulnerability influenced by the presence of natural and anthropogenic factors and their evolution in the decade of 2000s. Moreover, a prediction scenario, referred to 2020, considers the evolution of nitrate anthropogenic sources and changes in natural factors in the period 2011 – 2020. The referred year 2020 has been chosen as it represents the deadline established by the EU strategy, Europe 2020 (http://ec.europa.eu/europe2020/).

As the proposed approach introduces the time dimension in groundwater vulnerability assessment, and develops a hypothetical scenario in the future, the Author proposes not to use the term "vulnerability" in this case. In fact, the term "vulnerability" refers to the present natural and anthropogenic conditions, as well as to the present status of contamination. Indeed, the Author proposes to use the term “severity” or “criticality”, which describes the areas where the probability that a deterioration of groundwater quality would happen in the future is higher, or lower, respect to the previous conditions.

## 9.2 Spatio-temporal approach

### 9.2.1 General aspects

The Weights of Evidence (WofE) technique has been used to develop the models within the spatio-temporal approach: each time that a model had to be create, the WofE technique has been applied. In order to obtain a model that can take into account both the last status of nitrate contamination and its evolution, the next steps have been followed (Fig. 9.1):

1) a “spatial model” (Chapter 7), which considers the status of nitrate contamination and nitrate anthropogenic sources at time $t_1$, has been created. It identifies the areas where the combination of natural and anthropogenic factors involves nitrate concentrations higher than a specific value;

2) a “temporal model” (Chapter 8), which takes into account the evolution of both nitrate contamination and nitrate anthropogenic sources between $t_0$ and $t_1$, has been created. It identifies the areas where the combination of natural and anthropogenic factors involves an increase of nitrate concentrations;

3) a “spatio-temporal model”, which considers both the status at $t_1$ and the evolution between $t_0$ and $t_1$ of nitrate contamination and nitrate anthropogenic sources, has been generated. It helps to identify areas where the combination of natural and anthropogenic factors causes the presence of nitrates and their increasing concentration trends in groundwater;

4) a “predictive spatio-temporal model” considers a hypothetical status of nitrate contamination and nitrate anthropogenic sources at time $t_2$ and their evolution between $t_1$ and $t_2$. Various scenarios can be considered, which hypothesize: (a) a different evolution of nitrate sources of contamination (e.g., different growth rates of urban areas), or (b) a variation of hydrogeological conditions (e.g., groundwater depth variations);

5) the “spatio-temporal” (3) and the “predictive spatio-temporal” (4) models are compared in order to find the differences between the status at $t_1$ and at $t_2$;

6) a “model of criticality” has been created combining the “comparison model” (5) and the “spatial model” (1). It represents the critical areas where the combination of natural and anthropogenic factors involves both the presence of nitrates and their increasing contamination in groundwater, at $t_2$, considering the vulnerable areas at $t_1$.

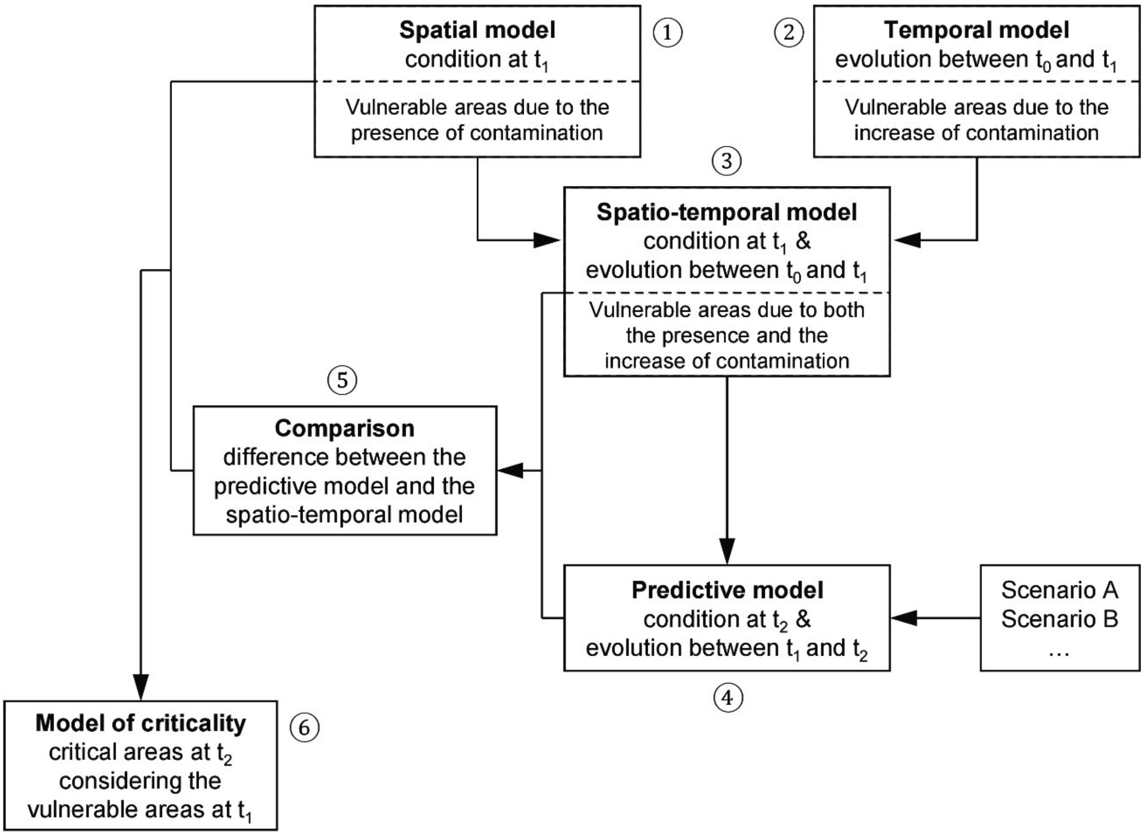


**Fig. 9.1 - Study flow for groundwater vulnerability mapping.**

## 9.2.2 Response variable

The response variable is represented either by nitrate concentration in groundwater at time $t_n$ or by nitrate concentration trend from $t_{n-1}$ to $t_n$ or by the combination of these two variables. Nitrate concentrations have been collected through the monitoring network described in Chapter 4, Paragraph 4.1. The 249 wells monitoring the shallow aquifer, in the period 2010 – 2012, with a minimum of two samples over the three years, have been used to develop the spatial model (Chapter 7). Whereas, only the 221 wells monitoring the shallow aquifer and having a minimum of eight measurements in the period 2001 – 2011, have been selected to be used in the analyses of the temporal (Chapter 8), spatio-temporal and predictive models.

The WofE modelling technique requires a binary formulation of the response variable. Thus, it is necessary to establish a threshold value allowing to distinguish between occurrences and non-occurrences (a training and a control set, respectively).

In the spatial model, which refers to a specific time $t_1$, the value representing the inflection point of the cumulative probability plot has been selected as an appropriate threshold to be used in the analysis (Chapter 7, Paragraph 7.2). Wells with a nitrate concentration higher than the threshold value represent the training set, and they have been selected to be used in the analysis. Whereas wells with a nitrate concentration lower than the threshold value form the control set.

The temporal model considers the evolution through time of nitrate concentrations, focalizing on the cases showing an increase in nitrate concentration. The change in nitrate concentration is quantified by the slope of the regression line from an interpolation of concentration data. Thus, wells showing a clear increase in concentration trends (positive slope values) represent the training set, and wells showing a decrease trend or a trend close to zero (non-positive slope values) represent the control set (Chapter 8, Paragraph 8.2).

In the spatio-temporal model, the training set is identified considering both the nitrate concentration measured in the wells and their contamination trend, expressed as the slope of the regression line from an interpolation of concentration data. Each well of the network is classified considering its nitrate concentration at time $t_1$ and its contamination trend from $t_0$ to $t_1$. Eleven classes of nitrate concentration and five classes of contamination trend have been defined to be used in the analysis (Table 9.1 and 9.2).

**Table 9.1 - Classification of the wells based on the last measured nitrate concentration, in 2011, or the closest year to 2011 (Sorichetta, 2011).**

| Concentration class | Concentration in mg/L |
|---|---|
| 1 | C > 50 |
| 2 | 45 < C ≤ 50 |
| 3 | 40 < C ≤ 45 |
| 4 | 35 < C ≤ 40 |
| 5 | 30 < C ≤ 35 |
| 6 | 25 < C ≤ 30 |
| 7 | 20 < C ≤ 25 |
| 8 | 15 < C ≤ 20 |
| 9 | 10 < C ≤ 15 |
| 10 | 5 < C ≤ 10 |
| 11 | C ≤ 5 |

**Table 9.2 - Classification of the wells based on the nitrate concentration trend of the period 2001 – 2011.**

| Trend class | Trend in mg/L per day |
|---|---|
| 1 | T > + 0.0015 |
| 2 | + 0.0003 < T ≤ + 0.0015 |
| 3 | – 0.0003 < T ≤ + 0.0003 |
| 4 | – 0.0015 < T ≤ – 0.0003 |
| 5 | T ≤ – 0.0015 |

Then, in order to rank each well with respect to both its concentration and trend class, the formula written below could be used (Stillwell et al., 1981):

$$R = \frac{(n - r_j + 1)}{\sum_{j=1}^{n}(n - r_j + 1)} \qquad (9.1)$$

where $n$ is the number of classes and $r_j$ is the rank of class $j$.

Once each well is ranked with respect to both its concentration and trend, the average rank (5th column, Table 9.3) on which identifying the training set to be used in the analysis can be computed as the simple average of the concentration rank value (2nd column, Table 9.3) plus the trend rank value (4th column, Table 9.3).

**Table 9.3 - Classification of the wells in the monitoring network based on both their nitrate contamination trend from 2001 to 2011 and last measured nitrate concentration (in 2011, or the closest year to 2011).**

| Concentration class | Concentration rank | Trend class | Trend rank | Average rank |
|---|---|---|---|---|
| 6 | 0.0909 | 1 | 0.3333 | 0.2121 |
| 7 | 0.0758 | 5 | 0.0667 | 0.0712 |
| 11 | 0.0152 | 4 | 0.1333 | 0.0742 |
| 1 | 0.1667 | 2 | 0.2667 | 0.2167 |
| … | … | … | … | … |

The frequency histogram of the average rank shows a light right-skewed (non-normal) distribution (Fig. 9.2), and the median value has been identified as the best measure of its central tendency and it was selected to be used as the threshold. Wells showing average rank higher than the median value of 0.1167 constitute the training set, while wells showing an average rank lower than the threshold represent the control set, with 0.1167 representing a sort of "reference critical value" for groundwater quality.
The same procedure, used for the spatio-temporal model, can be followed to identify the training set for the predictive spatio-temporal model, with the exception that the nitrate concentration at time $t_2$ is calculated hypothesizing a given trend between $t_1$ and $t_2$. Then, in order to easily compare the spatio-temporal and the predictive spatio-temporal models, the same threshold value is selected and the same number of training points is used. These "a priori" rules involve that the prior probability of the two models is the same and the "reference critical value" of groundwater quality, too.

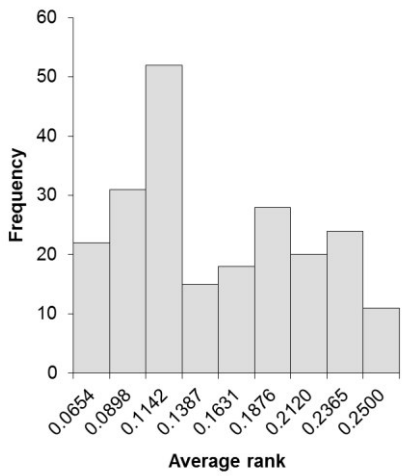


N = 221
Min = 0.0409
Max = 0.2500
Mean = 0.1377
Std. Dev. = 0.0596
Median = 0.1167
Skewness = 0.22

**Fig. 9.2 - Frequency histogram of the average rank.**

### 9.2.3 Evidential themes

Considering the conceptual hydrogeological model, six explanatory variables (described in Chapter 4, Paragraph 4.2, and Chapter 5) have been considered as influencing groundwater vulnerability to nitrate contamination in the study area (Table 9.4).

**Table 9.4 - Explanatory variables used as evidential themes.**

| Explanatory variable | Type | Range |
|---|---|---|
| QuikSCAT-DSM [2000, 2001, …, 2009] (dB) | Continuous | –11.91 ÷ –2.53 |
| Slope QuikSCAT-DSM [2000 ÷ 2009] (dB/year) | Continuous | –0.0699 ÷ 0.1268 |
| Nitrogen fertilizer load [2002] (kg/ha/year) | Continuous | 0 ÷ 767 |
| Nitrogen fertilizer load [2010] (kg/ha/year) | Continuous | 0 ÷ 664 |
| Soil protective capacity | Categorical | Low, Moderate, High |
| Groundwater depth [2003] (m) | Continuous | 0 ÷ 70 |
| Groundwater depth [2014] (m) | Continuous | 0 ÷ 75 |
| Groundwater velocity (m/s) | Continuous | $4.7\times10^{-8} \div 7.3\times10^{-5}$ |
| Hydraulic conductivity of the vadose zone (m/s) | Continuous | $4.1\times10^{-8} \div 4.0\times10^{-2}$ |

The six explanatory variables selected to be used in the analyses are handled in order to respect the assumptions of the spatio-temporal and predictive spatio-temporal models.
Natural factors are considered not time-dependent. Anthropogenic factors, which represent urban and agricultural nitrate sources, are handled applying a formula that considers both the status of the variable at $t_1$ (or $t_2$) and its evolution from $t_0$ to $t_1$ (or $t_1$ to $t_2$), as written below:

$$\frac{|\text{Value at } t_1|}{\text{Mean of the value}} + \frac{\text{Variation from } t_0 \text{ to } t_1}{\text{Mean of the variation}} \qquad (9.2)$$

where the mean is calculated over the entire study area. The division by the mean has been done in order to normalize the values of the two variables, and to allow the sum of the two variables.

### 9.2.4 Response themes, post-probability maps and map of criticality

Once all the models have been evaluated through the WofE, the post-probability maps have been obtained. The spatial, temporal and spatio-temporal response themes are categorized, applying the geometrical interval method (Sorichetta et al., 2011), in 5 classes, which represent 5 degrees of groundwater vulnerability, increasing from 1 to 5.
Instead, the post-probability maps obtained from the spatio-temporal and the predictive spatio-temporal models are compared calculating the difference, in percentage, of the post probabilities in each pixel, and the obtained map is categorized in 5 classes of percentage (columns, Table 9.5). The map shows the areas where the post-probability has increased, or decreased, between the conditions at time $t_1$ and $t_2$.

Then, the comparison map is combined with the spatial response theme as in matrix in Table 9.5. The 5 new classes represent five degrees of "criticality", where the degree increases from 1 to 5. The aim of the map of criticality is to recognize the critical areas at $t_2$, given the vulnerable areas at $t_1$. For example, two areas with the same increment of post probability shown by the comparison map (e.g., higher than 50 %) have two different meaning (that is, criticality) if the vulnerability class, according to the spatial response theme at $t_1$, is the less vulnerable (1) or the most vulnerable (5). The former area is less critical (3rd class) than the second one (5th class).

**Table 9.5 - Matrix of criticality. Criticality increases from 1 to 5.**

| | | Difference of Post Probabilities (%) | | | | |
|---|---|---|---|---|---|---|
| | | <-25% | -25÷0% | 0÷25% | 25÷50% | >50% |
| | | 1 | 2 | 3 | 4 | 5 |
| Vulnerability class | 1 | 1 | 1 | 1 | 2 | 3 |
| | 2 | 1 | 1 | 2 | 3 | 4 |
| | 3 | 1 | 2 | 3 | 4 | 5 |
| | 4 | 2 | 3 | 4 | 5 | 5 |
| | 5 | 3 | 4 | 5 | 5 | 5 |

# 9.3 Demonstration of the method

## 9.3.1 Spatial, Temporal and Spatio-Temporal models

The spatio-temporal approach is illustrated for the Po Plain area in Lombardy Region (Chapter 2, Paragraph 2.1):

- the spatial model refers to the status of nitrate contamination and nitrate sources at 2011 (described in Chapter 7);
- the temporal model refers to the evolution of nitrate contamination and nitrate sources from 2000 to 2011 (described in Chapter 8);
- the spatio-temporal model refers to the status of nitrate contamination and nitrate sources at 2011 and their evolution from 2000 to 2011 (this Chapter).

Table 9.6 shows the combinations of the significant evidential themes used to generate the response themes.

Evidential themes not statistically or physically significant have not been considered in the analyses. In the spatio-temporal model, soil protective capacity and nitrogen fertilizer load have been excluded because the first is not statistically significant, whereas the second is not physically significant. Regarding nitrogen fertilizer load, it seems that urban nitrate sources mask the contribution of agricultural sources in the area (Chapter 7, Paragraph 7.3.4).

**Table 9.6 - Combination of evidential themes used to obtain response themes and AUC values (QSCAT-DSM [2009] = land use from satellite data in 2009, Slope QSCAT-DSM [2000 ÷ 2009] = land use changes from satellite data between 2000 and 2009, spc = soil protective capacity, gwd [2003] = groundwater depth measured in 2003, gwv = groundwater velocity, hcv = hydraulic conductivity of the vadose zone).**

| Model | Combination of evidential themes | AUC value Success Rate | AUC value Prediction Rate |
|---|---|---|---|
| Spatial (Map W5) | QSCAT-DSM [2009], spc, gwd [2003], gwv, hcv | 78.4% | 43.2% |
| Temporal (Map W2) | Slope QSCAT-DSM [2000 ÷ 2009], gwd [2003], gwv, hcv | 74.3% | 62.1% |
| Spatio-temporal | QSCAT-DSM [2009] & Slope QSCAT-DSM [2000 ÷ 2009], gwd [2003], gwv, hcv | 75.5% | 51.9% |

Spatial, temporal and spatio-temporal response themes are shown in Fig. 9.3. Each response theme was categorized so that each vulnerability class in the corresponding map contains approximately the same number of different posterior probability values according to the geometric interval method (Sorichetta et al., 2011).

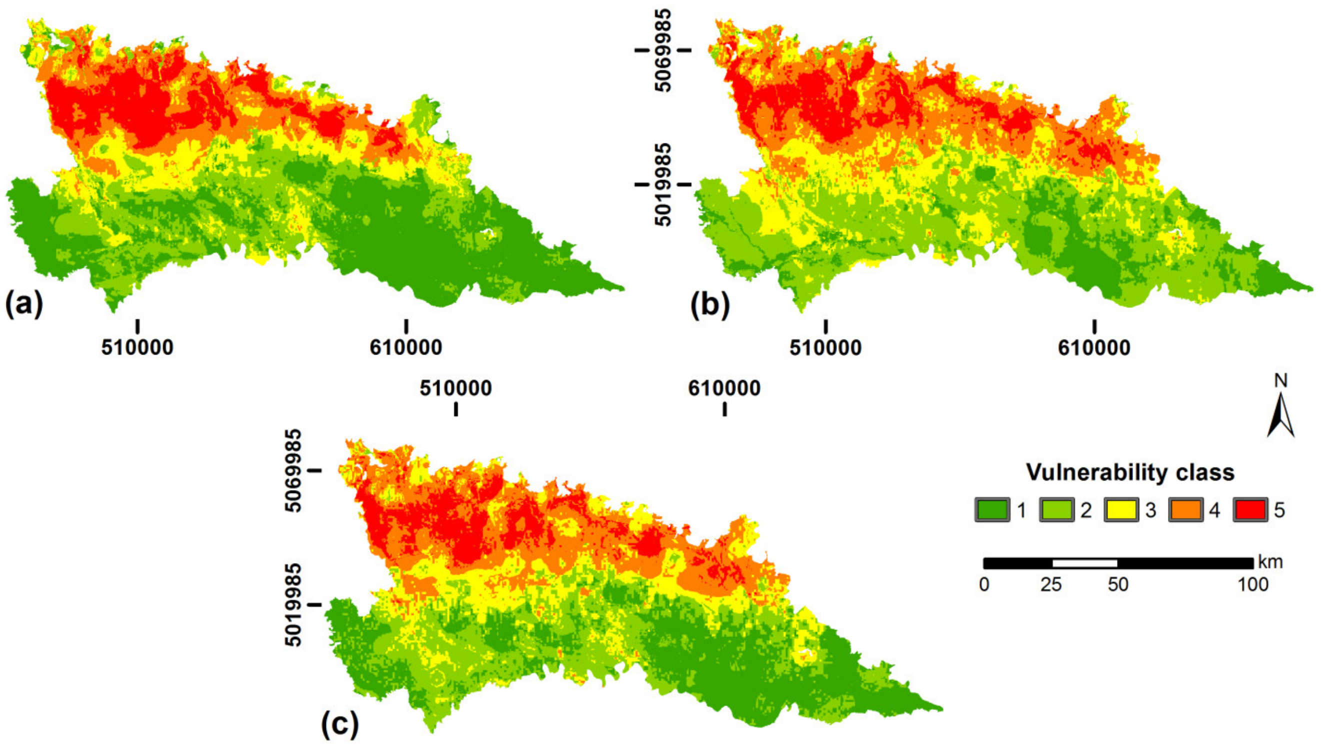


**Fig. 9.3 - Vulnerability maps representing: (a) spatial model (Map W5, Chapter 7); (b) temporal model (Map W2, Chapter 8); (c) spatio-temporal model. Coordinates refer to WGS 1984 – UTM Zone 32 N projection.**

The general quality of each response theme (i.e., post probability map) can be evaluated by the success and predictive rate curves (SRC and PRC, Chung and Fabbri, 1999; Sorichetta et al., 2011), expressed as the area-under-the curve (AUC) values. AUC is a direct measure of the performance of the statistical

approach, and is given by the area under the curve (integral) for cumulated area/cumulated occurrences expressed in percentage, using the training set for the SRC and the control set for the PRC. The calculated AUC values are presented in Table 9.6 showing the quality of the different maps. The high AUC values obtained for the spatio-temporal model, and their similarity with the values obtained for the spatial and temporal models, assert the reliability of this approach in groundwater vulnerability assessment.
Then, the reliability of each classified map was evaluated by considering its overall performance in classifying the occurrences. The average of the response variable of all wells in each vulnerability class has been evaluated, using either the nitrate concentration, or the nitrate concentration trend or the average ranking for the spatial (Chapter 7, Paragraph 7.3.3), temporal (Chapter 8, Paragraph 8.3.3) and spatio-temporal models, respectively. These analyses were carried out using all wells stored in the database.
The evaluation of the average ranking of all wells, $R_{\mathrm{AVG}}$, is expressed as:

$$R_{\mathrm{AVG}} = \frac{\sum_{i=1}^{T_{\mathrm{W}j}} R_{ij}}{T_{\mathrm{W}j}} \tag{9.3}$$

where $R_{ij}$ is the average ranking (5th column, Table 9.3) of well $i$ in the vulnerability class $j$, and $T_{\mathrm{W}j}$ is the total number of wells in the same class $j$. The average should monotonically increase as the degree of vulnerability increases and the central vulnerability class should give a value close to the overall mean value. The three histograms show the expected direct correlation between the average of the response variable and the degree of vulnerability (Fig. 9.4). The spatio-temporal model shows a good performance, with a regression coefficient close to 1 and presents the closest value to the mean of the whole distribution in the central vulnerability class, respect to the other two models.

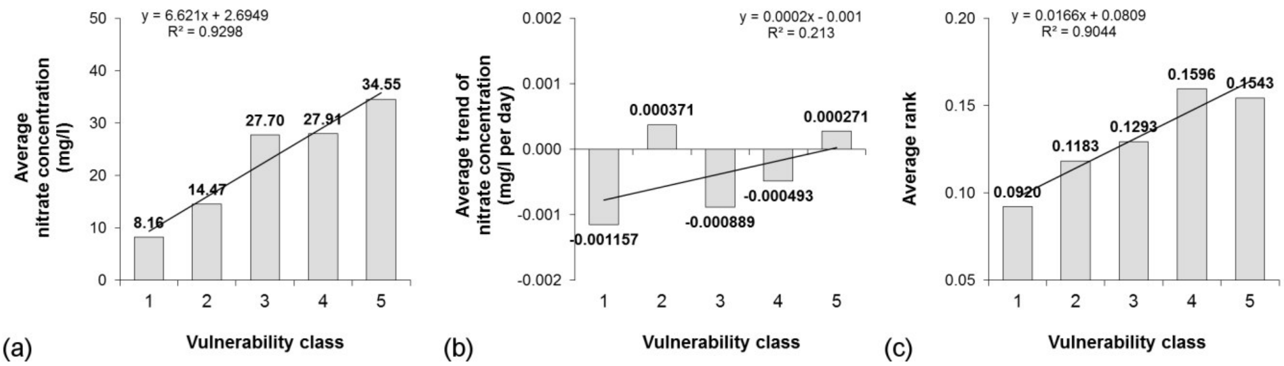


**Fig. 9.4 - Histograms of the average nitrate concentration (a), the average nitrate concentration trend (b) and the average ranking (c) in each vulnerability class of the spatial, temporal and spatio-temporal response theme, respectively. The degree of vulnerability increases from 1 to 5.**

## 9.3.2 Predictive Spatio-Temporal model

The predictive spatio-temporal model considers a hypothetical status of nitrate contamination in groundwater in 2020 and its variation during the period 2011 – 2020, in the Po Plain area in Lombardy Region (Chapter 2, Paragraph 2.1). Two scenarios have been developed: the first one (Scenario 1) considers only a possible evolution of anthropogenic sources of nitrate contamination; the second one (Scenario 2) considers also a possible evolution of one natural factor, which is groundwater depth.

**Scenario 1** considers that the evolution of nitrate contamination and urban nitrate sources (i.e., urban areas) of the period 2011 – 2020 is equal to their evolution related to the decade of 2000s. Natural factors are considered not time-dependent and unchanged in the two decades.
The response variable has been obtained using the approach described in Paragraph 9.2.2. Wells are classified considering the trend in the period 2011 – 2020 and the concentration value calculated for 2020, which depends on the trend. In Scenario 1 the trend of the period 2011 – 2020 is equal to the period 2000 – 2011. This means that the slope of the regression line obtained from the interpolation of concentration data of the period 2000 – 2011 has been kept as trend of the period 2011 – 2020 and used to calculate the nitrate concentration in 2020.
The evidential theme representing urban nitrate sources (i.e., QuikSCAT-DSM) has been obtained using the method described in Paragraph 9.2.3 and applying the formula in Equation 9.2, as:

$$\frac{|\text{Value QuikSCAT DSM}_{2020}|}{\text{Mean of the value QuikSCAT DSM}_{2020}} + \frac{\text{Slope QuikSCAT DSM}_{2011\div2020}}{\text{Mean of the slope QuikSCAT DSM}_{2011\div2020}} \tag{9.4}$$

where the value of QuikSCAT-DSM in 2020 has been calculated using the slope of QuikSCAT-DSM from 2011 to 2020, which is equal to the slope obtained for the period from 2000 to 2009 (Chapter 5, Paragraph 5.1).

**Scenario 2** is an implementation of Scenario 1, where, besides the evolution of nitrate contamination and urban nitrate sources, a possible evolution of one natural factor, which is groundwater depth, has been considered. The evolution of groundwater depth has been evaluated starting from the piezometric levels measured in 2003 and 2014 (Chapter 4, Paragraph 4.2.1). Groundwater depth for the year 2020 has been calculated applying the formula written below:

$$\text{gwd}_{2020} = \text{gwd}_{2003} + 1.5 \times (\text{gwd}_{2014} - \text{gwd}_{2003}) \tag{9.5}$$

where *gwd* is groundwater depth. The formula assumes that groundwater depth varies following a linear regression equation, which considers that the slope of the regression line between 2014 and 2020 is equal to the half of the slope between 2003 and 2014.
The evidential themes used to generate the models are listed in Table 9.7. Soil protective capacity and nitrogen fertilizer load are not statistically or physically significant, and they have not been considered in the analysis.

**Table 9.7 - Combination of evidential themes used to obtain the response themes of the predictive spatio-temporal models and AUC values (QSCAT-DSM [2020] = land use from satellite data calculated for 2020, Slope QSCAT-DSM [2010 ÷ 2020] = land use changes from satellite data calculated for the period 2010 – 2020, gwd [2003] or gwd [2020] = groundwater depth measured in 2003 or calculated for 2020, gwv = groundwater velocity, hcv = hydraulic conductivity of the vadose zone).**

| Predictive model | Combination of evidential themes | AUC value Success Rate | AUC value Prediction Rate |
|---|---|---|---|
| Scenario 1 | QSCAT-DSM [2020] & Slope QSCAT-DSM [2010 ÷ 2020], gwd [2003], gwv, hcv | 74.5% | 53.1% |
| Scenario 2 | QSCAT-DSM [2020] & Slope QSCAT-DSM [2010 ÷ 2020], gwd [2020], gwv, hcv | 75.3% | 53.1% |

The groundwater vulnerability maps, in the form of post-probability maps, obtained through the predictive spatio-temporal model are calibrated and, partially, validated. AUC values of the success rate curves (Table 9.7) are high and consistent with the ones obtained through the other models (spatial, temporal and spatio-temporal models). Instead, AUC values of the predictive rate curves are comparable with the one obtained for the spatio-temporal model, asserting their capability to adequately describe groundwater vulnerability in the study area.
Since the predictive spatio-temporal models are developed hypothesizing a possible evolution of nitrate contamination and nitrate sources of contamination, it is not possible, neither rational, to validate the models through the validation techniques used in the other three cases (Chapter 7, Paragraph 7.3.3; Chapter 8, Paragraph 8.3.3; Chapter 9, Paragraph 9.3.1).

Finally, as described in Paragraph 9.2.4, in order to recognize the critical areas in 2020, given the vulnerable areas in 2011, the maps of criticality have been generated (Fig. 9.5).

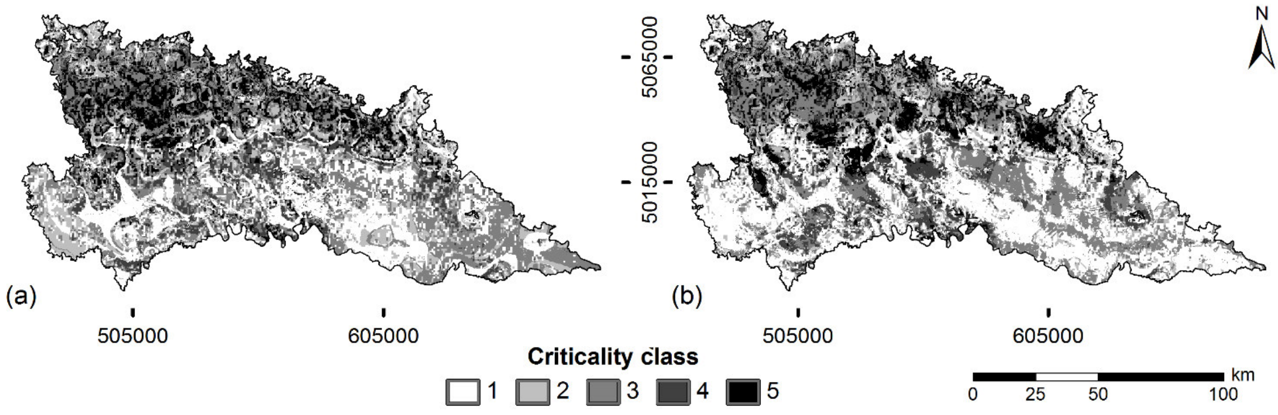


**Fig. 9.5 - Maps of criticality in 2020 according to Scenario 1 (a) and Scenario 2 (b). Coordinates refer to WGS 1984 – UTM Zone 32 N projection.**

## 9.4 Discussion

The development of dynamic and time-dependent groundwater vulnerability approach is a key tool to support sustainable land use practices that preserve groundwater quality in a given hydrogeological context. By determining which natural and anthropogenic factors are most responsible of groundwater deterioration, adequate environmental policies can be decided. The proposed approach for a spatio-temporal vulnerability model proves to be valid in identifying areas where natural and anthropogenic factors are responsible for critical combination of increasing nitrate concentration trends and current nitrate concentration.

The groundwater vulnerability maps obtained through the spatial and temporal models show different classes of vulnerability where, with different degrees, the combination of natural and anthropogenic factors involves either the presence of nitrate contamination or the increasing of nitrate concentrations. Since the two maps have different meanings, it is not possible to directly compare them.

Instead, the groundwater vulnerability map obtained through the spatio-temporal model shows the vulnerable areas due to the presence of nitrate contamination and/or increasing trend of nitrate concentrations. The distribution of the vulnerable areas reflects the distribution of those urban areas that are characterized by the presence of a notable and continuous urban pattern and/or show an increase in their extension or modifications of their urban pattern (e.g., requalification of industrial areas and transformation in residential or green areas).

Moreover, by introducing the time variable in groundwater vulnerability assessment, the proposed approach allows to determine what would happen to groundwater resources if policies are maintained or new ones will be proposed and/or if natural factors are changing under climatic or anthropogenic stresses. In fact, the final calibrated spatio-temporal map can be projected in the future creating prediction scenarios that rely on the observed land use and contamination trends. This allows identifying areas that in the mid-term will be more prone to develop critical contamination situations for a given land use trend and/or given trends of hydrogeological variables.

## 9.5 Conclusions

The inclusion of the time dimension in groundwater vulnerability studies can enable breakthrough advances in mapping hazardous areas on a regional or sub-regional scale, and in assessing the efficacy of land-use planning for groundwater protection:

- The proposed spatio-temporal groundwater vulnerability maps derived through the spatial statistical approach are a reliable tool to combine natural and anthropogenic factors in order to identify areas with critical combination of increasing nitrate concentration trends and current nitrate concentration;
- The introduction of a “map of criticality” offers new perspective in the estimation that future scenarios could have on the quality of groundwater resources in a given area and to drive appropriate land use policies to preserve groundwater quality;
- Through this approach, decision makers can count on high-level guidance on the compatibility between a given activity and a given area thus decreasing the likelihood that new groundwater diffuse contamination situations form and avoiding the deterioration of the existing ones;

- The global result is an improved protection of groundwater quality with clear advantages for the environment and for all the groundwater dependent ecosystems and a general benefit on society, also in terms of sustainable costs.

## References

Chung C.F., Fabbri A.G., 1999. Probabilistic prediction models for landslide hazard mapping. Photogrammetric Engineering and Remote Sensing, vol. 65, n. 12, pp. 1389-1399

European Community, 2006. Directive 2006/118/EC on the protection of groundwater against pollution and deterioration, (Groundwater Directive). OJ L 372, 27 December 2006, pp. 19-31

Kumar P., 2015. Hydrocomplexity: Addressing water security and emergent environmental risks. Water Resources Research, vol. 51, pp. 5827-5838, doi 10.1002/2015WR017342.

Nghiem S.V., Balk D., Rodriguez E., Neumann G., Sorichetta A., Small C., Elvidge C.D., 2009. Observations of urban and suburban environments with global satellite scatterometer data. ISPRS – Journal of Photogrammetry and Remote Sensing, vol. 64, n. 4, pp. 367-380, doi 10.1016/j.isprsjprs.2009.01.004

Sorichetta A., 2011. Groundwater vulnerability assessment using statistical methods. Università degli Studi di Milano, Academic year 2010, 141 pp. http://hdl.handle.net/2434/152913

Sorichetta A., Masetti M., Ballabio C., Sterlacchini S., Beretta G.P., 2011. Reliability of groundwater vulnerability maps obtained through statistical methods. Journal of Environmental Management, vol. 92, n. 4, pp. 1215-1224, doi 10.1016/j.jenvman.2010.12.009

Stillwell W.G., Seaver D.A., Edwards W., 1981. A Comparison of weight approximation techniques in multiattribute utility decision making. Organizational Behavior and Human Performance, vol. 28, n. 1, pp. 62-77

# Chapter 10

# Conclusions

Water crises have been ranked as the most important global risk among ten in terms of impact and the eighth in likelihood, mainly due to the increasing demand that will be required from population growth, intensive land management and economic expansion (World Economic Forum, 2015).

Increasing numbers of contamination sources in developed and developing countries critically threaten groundwater resources and reactive remediation measures can be excessively expensive when groundwater becomes contaminated beyond the required quality standards for safe consumption.

Groundwater vulnerability studies are crucial to understand the cause-effect relationship between groundwater quality and both natural and anthropogenic factors to develop effective groundwater protection plans. Mapping areas where groundwater is most vulnerable to contamination and identifying primary factors influencing the contamination level are imperative to manage and protect groundwater and thus human health.

Many different approaches and methods to produce groundwater vulnerability maps have been developed, since the first attempt by Albinet and Margat in 1970. Although it is not possible to identify an approach which could be the best one for all situations, the final product should always be scientific defensible, meaningful and reliable, to be an effective tool for land use and policy makers (Focazio et al., 2002).

Statistical approaches (e.g., logistic regression, conditional probability) provide useful tools to assess the relative roles of important independent variables or factors controlling vulnerability over various spatial scales, and guarantee quantitative measures of statistical uncertainty (Focazio et al., 2002). In recent years, the reliability of the Weights of Evidence (WofE, Bonham-Carter, 1994) modelling technique in performing meaningful and scientific defensible groundwater vulnerability maps has been proved by various Authors (e.g., Arthur et al., 2007; Masetti et al., 2007, 2008; Sorichetta et al., 2011, 2012, 2013; Uhan et al., 2011).

European Directives require member states, for the protection of groundwater quality, to assess the current groundwater quality status, detect changes or trends in groundwater quality, assess the threat of deterioration and predict future changes in groundwater quality. Such activities would allow to not only identify already highly contaminated areas where expensive remediation measures need to be implemented, but also to detect areas where pro-active interventions need to be planned.

In order to cope with the EU requirements, this study focused on the development of a time-dependent approach, which could take into account both the current groundwater quality status and its changes, assessing groundwater vulnerability to nitrate contamination in the Po Plain area of Lombardy Region, through the WofE technique.

In addition, an innovative dataset to delineate urban areas with satellite scatterometer data (QuikSCAT-DSM; Nghiem et al., 2009), which allows identifying manmade infrastructures or buildings and zones where different rates of urban growth occurred, has been explored. QuikSCAT-DSM dataset would represent urban nitrate sources of contamination. To evaluate its reliability in groundwater vulnerability assessments, QuikSCAT-DSM dataset has been compared with population density, commonly used as a proxy of urban nitrate sources (e.g., Nolan et al., 2002), and land use derived from aerial images (DUSAF; ERSAF, 2014).

Results showed the prevalence of urban sources of contamination (i.e., leakages from the sewage system) respect to agricultural sources (i.e., fertilizers and manures) in influencing the presence of nitrates in groundwater. In addition, introducing the time variable allowed to recognize that, in the study area, increasing nitrate concentrations occur in areas related to urban development or population increase, rather than agricultural environments. These outcomes are strictly related to the simultaneous presence of peculiar geological and hydrogeological factors, whose combination with the anthropogenic activities can mitigate or facilitate nitrate migration from land surface to water table, or through the water body.

QuikSCAT-DSM satellite dataset has proven to be a reliable variable to be used in groundwater vulnerability assessments as a proxy for urban nitrate sources. Moreover, it has the advantages of a worldwide coverage, a continuous data collection and an adequate resolution without spatial gaps. These characteristics, which are not completely covered by population density or land use datasets, allow QuikSCAT-DSM to detect changes in urban areas over a decadal period and different scales.

In addition, the latter result is remarkable for those areas where there are insufficient or inaccurate data for population or land use and their changes, and thus satellite observations of urban change become particularly useful.

This study allowed exploring new fields in groundwater vulnerability assessments. The development of new techniques, which aim to obtain scientific defensible end-products, which could be a useful tool for land use planners, raised the question whether a vulnerability is really assessed. Moreover, introducing the time dimension, new definitions of groundwater vulnerability could be proposed.

In a time-dependent condition, a “zone vulnerable to nitrate contamination” can be defined as an area where the combination of natural and anthropogenic (e.g., growth of urban areas) factors involves a deterioration of groundwater quality.

Whereas, taking into account both the last condition and its evolution, as in the spatio-temporal model, a “zone vulnerable to nitrate contamination” can be defined as an area where the combination of natural and anthropogenic (e.g., extension and growth of urban areas) factors involves both a given absolute level of contamination in the aquifer and a deterioration of groundwater quality.

Creating prediction scenarios leads to a field which has never been explored, where the term “vulnerability” may not be appropriate. Thus, the Author proposes the use of the term “severity” or “criticality” to describe the result of a prediction scenario. This is because “vulnerability” is defined respect to status of its own map (e.g., 2011, decade 2000 – 2009), while “criticality” is defined respect to the status of a previous condition, and describes those areas where the probability that a deterioration of groundwater quality would happen in the future is higher, or lower, respect to the previous conditions.

By introducing the time variable in groundwater vulnerability assessment, the proposed approach allows to determine what could happen to groundwater resources if policies are maintained or new ones will be proposed and/or if natural factors are changing under climatic or anthropogenic stresses. The approach can offer new perspective in the estimation of the effects on groundwater resources due to given land use policies and drive appropriate solutions to preserve groundwater quality.

Through this approach, decision makers can count on high-level guidance on the compatibility between a given activity and a given area thus decreasing the likelihood that new groundwater diffuse contamination situations form and avoiding the deterioration of the existing ones. The global result is an improved protection of groundwater quality with clear advantages for the environment and for all the groundwater dependent ecosystems and a general benefit on society, also in terms of sustainable costs.

New research challenges could focus on:

a) a better comprehension and identification of possible evolutions of the factors influencing groundwater vulnerability (e.g., groundwater depth variations or population growth estimations) to develop different scenarios projected in the future;
b) the application of the time-dependent approach, adopting the Weights of Evidence technique, on other study areas with different geological, hydrological and hydrogeological characteristics and different patterns of anthropogenic activities or land use / land cover, to evaluate the impacts of different conditions on groundwater quality and groundwater vulnerability.

# References

Albinet M., Margat J., 1970. Cartographie de la vulnérabilité à la pollution des nappes d'eau souterraine [Mapping of groundwater vulnerability to pollution], Bulletin BRGM 2éme Sèrie, vol. 3, n. 4, pp. 13-22

Arthur J.D., Wood H.A.R., Baker A.E., Cichon J.R., Raines G.L., 2007. Development and Implementation of a Bayesian-based Aquifer Vulnerability Assessment in Florida. Natural Resources Research, vol. 16, n. 2, pp. 93-107

Bonham-Carter G.F., 1994. Geographic Information Systems for Geoscientists-Modelling with GIS. Pergamon Press

ERSAF - Ente Regionale per i Servizi all'Agricoltura e alle Foreste, 2014. DUSAF (Destinazione d'Uso dei Suoli Agricoli e forestali). http://www.cartografia.regione.lombardia.it/

Focazio M.J., Reilly T.E., Rupert M.G., Helsel D.R., 2002. Assessing Ground-Water Vulnerability to Contamination: Providing Scientifically Defensible Information for Decision Makers. U.S. Geological Survey Circular 1224. ISBN: 0-607-89025-8

Masetti M., Poli S., Sterlacchini S., 2007. The Use of the weights-of-evidence modeling technique to estimate the vulnerability of groundwater to nitrate contamination. Natural Resources Research, vol. 16, n. 2, pp. 109-119, doi 10.1007/s11053-007-9045-6

Masetti M., Poli S., Sterlacchini S., Beretta G.P., Facchi A., 2008. Spatial and statistical assessment of factors influencing nitrate contamination in groundwater. Journal of Environmental Management, vol. 86, n. 1, pp. 272-281, doi 10.1016/j.jenvman.2006.12.023

Nolan B.T., Hitt K.J., Ruddy B.C., 2002. Probability of nitrate contamination of recently recharged groundwaters in the conterminous United States. Environmental Science and Technology, vol. 36, n. 10, pp. 2138-2145, doi 10.1021/es0113854

Nghiem S.V., Balk D., Rodriguez E., Neumann G., Sorichetta A., Small C., Elvidge C.D., 2009. Observations of urban and suburban environments with global satellite scatterometer data. ISPRS – Journal of Photogrammetry and Remote Sensing, vol. 64, n. 4, pp. 367-380, doi 10.1016/j.isprsjprs.2009.01.004

Sorichetta A., Masetti M., Ballabio C., Sterlacchini S., Beretta G.P., 2011. Reliability of groundwater vulnerability maps obtained through statistical methods. Journal of Environmental Management, vol. 92, n. 4, pp. 1215-1224, doi 10.1016/j.jenvman.2010.12.009

Sorichetta A., Masetti M., Ballabio C., Sterlacchini S., 2012. Aquifer nitrate vulnerability assessment using positive and negative weights of evidence methods, Milan, Italy. Computers and Geosciences, vol. 48, pp. 199-210, doi 10.1016/j.cageo.2012.05.021

Sorichetta A., Ballabio C., Masetti M., Robinson G.R. Jr, Sterlacchini S., 2013. A Comparison of Data-Driven Groundwater Vulnerability Assessment Methods. Ground Water, vol. 51, n. 6, pp. 866-879, doi: 10.1111/gwat.12012

Uhan J., Vižintin G., Pezdič J., 2011. Groundwater nitrate vulnerability assessment in alluvial aquifer using process-based models and weights-of-evidence method: Lower Savinja Valley case study (Slovenia). Environmental Earth Sciences, vol. 64, n. 1, pp. 97-105, doi 10.1007/s12665-010-0821-y

World Economic Forum, 2015. The Global Risks Report 2015, 66 pp., Geneva, Switzerland

# Appendix I

# Articles on which the Ph.D. Thesis is based

## Published peer-reviewed journal articles

Stevenazzi S., Masetti M., Nghiem S.V., Sorichetta A. – Groundwater vulnerability maps derived from a time-dependent method using satellite scatterometer data. Hydrogeology Journal, 2015, vol. 23, no. 4, pp. 631-647, doi: 10.1007/s10040-015-1236-3

Stevenazzi S., Masetti M., Nghiem S.V., Sorichetta A. – Use of scatterometer data in groundwater vulnerability assessment. Rendiconti Online della Società Geologica Italiana, 2014, vol. 30, pp. 45-50, doi: 10.3301/ROL.2014.10, ISSN 2035-8008

# Appendix II

# Other scientific activities performed during the Ph.D. studies

## Published peer-reviewed journal articles

Masetti M., Nghiem S.V., Sorichetta A., Stevenazzi S., Fabbri P., Pola M., Filippini M., Brakenridge G.R. – Urbanization affects air and water in Italy's Po Plain. Eos, 2015, vol. 96, no. 21. 15 Nov. 2015, doi: 10.1029/2015EO037575

Masetti M., Pedretti D., Sorichetta A., Stevenazzi S., Bacci F. – Impact of a storm-water infiltration basin on the recharge dynamics in a highly permeable aquifer. Water Resource Management, 2016, vol. 30, n. 1, pp. 149-165, doi: 10.1007/s11269-015-1151-3

## Conference proceedings

Stevenazzi S., Nghiem S.V., Masetti M. – Urban impacts on air quality observed with remote sensing and ground station data from the Po Plain Field Campaign. In: Geoscience and Remote Sensing Symposium (IGARSS), 2015 IEEE International, ISBN: 978-1-4799-7928-8, pp. 73-75, doi: 10.1109/IGARSS.2015.7325700

Masetti M., Nghiem S.V., Sorichetta A., Stevenazzi S., Bonfanti M., Conforto A., Fabbri P., Filippini M., Gargini A., Hall D., Linard C., Pola M., Richter A., Catani F., Paloscia S., Pampaloni P., Santi E. – The Po Plain Experiment (POPLEX) Field Campaign – Effects of urban sprawl on environmental matrices in northern Italy, Rend Online Soc Geol It, 2014, vol. 31, no. 1, p. 531, doi: 10.3301/ROL.2014.140, ISSN 2035-8008

Bacci F., Masetti M., Stevenazzi S. – The effects of an infiltration basin on groundwater: quantitative aspects (River Arno – Lonate Pozzolo – VA). Flowpath 2014, National Meeting on Hydrogeology, Abstract Volume, ISBN 978-88-907553-4-7

Stevenazzi S., Masetti M., Nghiem S.V., Sorichetta A. – Effects of urban changes on groundwater vulnerability. Flowpath 2014, National Meeting on Hydrogeology, Abstract Volume, ISBN 978-88-907553-4-7

## Conference participation

Stevenazzi S.*, Masetti M., Nghiem S.V., Sorichetta A. – New approaches to integrate the time dimension in groundwater vulnerability assessments. (oral presentation) 42° IAH Congress. September 14-18, 2015. Rome – Italy

Stevenazzi S.*, Nghiem S.V., Masetti M. – Urban impacts on air quality observed with remote sensing and ground station data from the Po Plain Field Campaign. (oral presentation) IGARSS 2015 - International Geoscience and Remote Sensing Symposium 2015. July 26-31, 2015 Milan – Italy

Stevenazzi S.*, Masetti M., Nghiem S.V., Sorichetta A. – Effects of urban changes on groundwater vulnerability, a case study in Lombardy (Italy). (oral presentation) 41° IAH Congress. September 13-19, 2014. Marrakech – Morocco

Masetti M., Nghiem S.V., Sorichetta A., Stevenazzi S.*, Bonfanti M., Conforto A., Fabbri P., Filippini M., Gargini A., Hall D., Linard C., Pola M., Richter A., Catani F., Paloscia S., Pampaloni P., Santi E. – The Po Plain Experiment (POPLEX) Field Campaign – Effects of urban sprawl on environmental matrices in northern Italy. (oral presentation) 87° Congresso della Società Geologica Italiana e 90° Congresso della Società Italiana di Mineralogia e Petrologia – The Future of the Italian Geosciences - The Italian Geosciences of the Future. September 10-12, 2014, Milano – Italy

Stevenazzi S.*, Masetti M., Nghiem S.V., Sorichetta A. – Effects of urban changes on groundwater vulnerability. (oral presentation) Flowpath – National Meeting on Hydrogeology, Università degli Studi della Tuscia. June 18-20, 2014. Viterbo (VT) – Italy

Stevenazzi S.*, Masetti M., Nghiem S.V., Sorichetta A. – Use of scatterometer data in groundwater vulnerability assessment. (oral presentation) VIII Convegno Nazionale del Gruppo di Geologia Informatica, Sezione della Società Geologica Italiana (GIT- Geology and Information Technology). June 17-19, 2013. Chiavenna (SO) – Italy

* presenting author